Untangling the interplay between food microstructure mechanical properties macrostructural breakdown and in vitro gastric protein digestion

Dan Liu

Propositions

1. Designing micro- and macrostructure of foods is an effective approach to modify protein digestibility.
   (this thesis)

2. *In vivo* oral processing or realistic oral phase simulation is essential for *in vitro* digestion studies.
   (this thesis)

3. Machine learning accelerates scientific progress.

4. Sacrificing one's personal life is required to become a great scientist.

5. An industry internship completes the PhD training program in applied sciences.

6. The only way to truly integrate into a culture is by speaking its language.

Propositions belonging to the thesis, entitled

Untangling the interplay between food microstructure, mechanical properties, macrostructural breakdown and *in vitro* gastric protein digestion

Dan Liu
Wageningen, 27 February 2025

Untangling the interplay between food microstructure, mechanical properties, macrostructural breakdown and *in vitro* gastric protein digestion

Dan Liu

Thesis committee

Promotor

Prof. Dr Markus Stieger

Personal chair, Human Nutrition and Health

Wageningen University & Research

Co-promotors

Dr Anja E.M. Janssen

Associate professor, Food Process Engineering

Wageningen University & Research

Dr Paul A.M. Smeets

Senior Researcher, Human Nutrition and Health

Wageningen University & Research

Other members

Prof. Dr Lisette de Groot, Wageningen University & Research

Dr Nikkie van der Wielen, Wageningen University & Research

Dr Daniela Freitas, Teagasc, Co. Cork, Ireland

Dr Evan Abrahamse, Danone Nutricia Research, Utrecht, the Netherlands

This research was conducted under the auspices of VLAG Graduate School (Biobased, Biomolecular, Chemical, Food, and Nutrition sciences).

Untangling the interplay between food microstructure, mechanical properties, macrostructural breakdown and *in vitro* gastric protein digestion

Dan Liu

Thesis
submitted in fulfilment of the requirements for the degree of doctor
at Wageningen University
by the authority of the Rector Magnificus,
Prof. Dr C. Kroeze,
in the presence of the
Thesis Committee appointed by the Academic Board
to be defended in public
on Thursday 27 February 2025
at 10.30 a.m. in the Omnia Auditorium

Dan Liu

Untangling the interplay between food microstructure, mechanical properties, macrostructural breakdown and *in vitro* gastric protein digestion
188 pages

PhD thesis, Wageningen University, Wageningen, the Netherlands (2025)
With references, with summary in English

DOI: https://doi.org/10.18174/680298

谨以此书献给我的父亲刘科印先生。

To Liu Keyin, my dad.

Contents

Chapter 1

General introduction

Given the growing global population, limited resources and environmental challenges, it is essential to develop a more efficient and sustainable food system. Various strategies have been explored to address this need, such as promoting resource-efficient food production and reducing food waste. From a nutritional perspective, improving nutrient digestibility can contribute to a more efficient food system (Kraak & Aschemann-Witzel, 2024; Wan et al., 2021). As a key macronutrient in our daily diet, proteins are crucial for growth, maintenance and metabolism of the body (Moughan, 2021). A reduction of animal-based protein foods is desired due to its high demand of land and water and its contribution to greenhouse gas emissions. Meat analogues that attempt to mimic meat have been developed with plant protein sources using various technologies (Imran & Liyan, 2023; Saeed et al., 2023). On the one hand, the nutritional value of meat analogues is challenged by the low quality and digestibility of plant-based proteins due to their unbalanced amino acid profile and the presence of antinutritional factors (Gorissen et al., 2018; Kaur et al., 2022; Sá et al., 2020a; Xie et al., 2022). On the other hand, the introduction of new protein sources and technologies offers great opportunities to engineer food texture and structure, optimizing the sensory and nutritional properties of foods (Baune et al., 2022; Schreuders et al., 2021). Exploring the interactions between food structure and protein digestion is crucial for improving protein digestibility and providing scientific guidance for food design tailored to specific nutrition needs.

1.1 The digestive journey of protein foods in the human body

1.1.1 Oral phase: the first phase of food digestion

Oral processing is inevitable during food consumption and has two main roles. The first is the perception of the texture and flavor of the foods, which contributes to the enjoyment of eating, and is related to the breakdown of foods in the oral cavity during mastication. Secondly, the food is transformed from its initial shape and size into a bolus that is safe to swallow. During oral processing, solid foods are broken down into smaller fragments, increasing the bolus surface area, which aids in nutrient digestion (Chen, 2009; Guo, 2021). Oral processing behavior of chewable foods can be characterized by bite size, chews per bite, chewing rate, etc. It varies across populations based on age, gender, and ethnicity, and

strongly depends on food texture and mechanical, rheological and tribological properties of foods (Aguayo-Mendoza et al., 2019; Ketel et al., 2019). A study on 59 commercial foods reported that foods with less adhesiveness and greater springiness, chewiness and resilience lead to a greater number of chews and more chews per bite (Wee et al., 2018). This chewing behavior together with the mechanical properties of foods influence bolus properties such as size and number of bolus particles (Chen et al., 2024b; Devezeaux de Lavergne et al., 2017; Goh et al., 2021). For different types of foods, such as jellies, carrots, chicken, black beans and breads, prolonged chewing time and increased food hardness result in more and smaller bolus particles (Alpos et al., 2021; Chen et al., 2013; Chen et al., 2021, 2024; Jalabert-Malbos et al., 2007; Pentikäinen et al., 2014). It is evident that before gastric digestion, food structural properties have been significantly altered by mastication. Enzymatic digestion during the oral phase occurs only for carbohydrates, driven by alpha-amylase in saliva. Enzymatic breakdown of proteins does not occur in this phase due to the absence of proteolytic enzymes in saliva (Bornhorst & Singh, 2012). Therefore, the most significant contribution of oral processing to protein digestion is the macrostructural breakdown of foods. Exploring the interplay between food properties, oral macrostructural breakdown and protein digestion is essential for understanding the impact of food properties on protein digestion.

1.1.2 Gastric phase: the first phase of proteolysis

The stomach functions as a container and a processor during food digestion. After the oral phase, the ingested food bolus enters the stomach for further mechanical breakdown and to initiate the enzymatic hydrolysis of protein molecules (Guo et al., 2020; Somaratne et al., 2020a). The disintegration of food particles during gastric digestion is driven by gastric contractions and grinding (Guo et al., 2020). As gastric mixing progresses, pepsins penetrate into bolus particles along with the acidic gastric juice, binding to protein molecules and breaking down the peptide bonds (Capuano & Janssen, 2021). Depending on its composition and texture, as well as corresponding hormonal regulations, the digesta are emptied from the stomach into the duodenum through the pylorus (Hellström et al., 2006; Mackie, 2023). Despite the limited extent of enzymatic protein hydrolysis during the gastric phase, gastric protein digestion is crucial for sufficient proteolysis in the small intestine and for the kinetics of protein digestion and absorption due to its dynamic nature (Abrahamse et al., 2022; Hiolle et al., 2020; Mella et al., 2021; Svook, 1973).

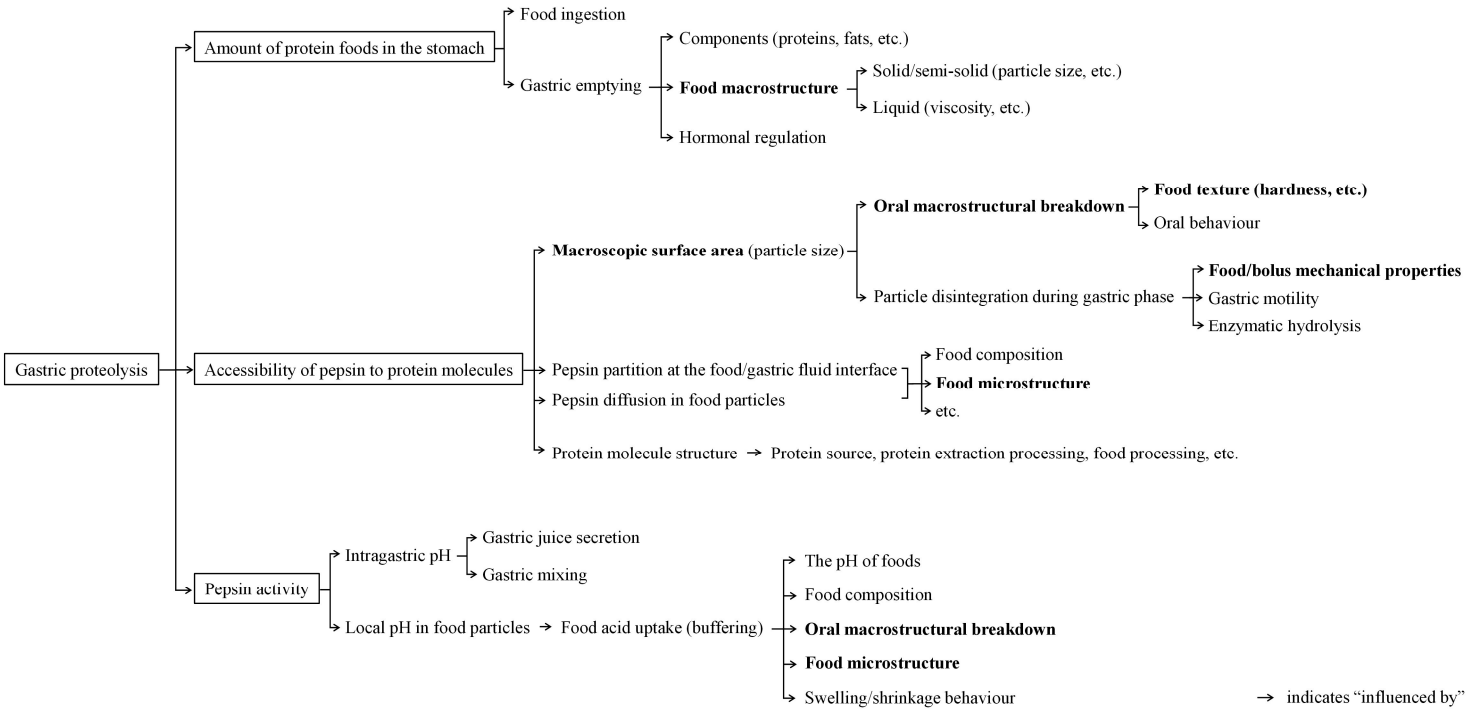

Figure 1.1. *An overview of the factors that influence gastric protein hydrolysis of foods.*

Gastric protein digestion is influenced by multiple interacting factors. Age, medical treatments, and other physiological factors can affect gastric protein digestion (Lee et al., 2023; Waldum et al., 2018). Food-related properties also impact gastric protein hydrolysis. An overview of the factors influencing protein digestion is shown in Figure 1.1. The efficiency of pepsin-driven protein hydrolysis during gastric digestion relies on a) the amount of protein foods in the stomach, b) the accessibility of pepsin to protein molecules and c) the activity of pepsin (Luo et al., 2017, 2019). In addition to the volume of ingested food, the amount of protein foods in the stomach depends on the rate of gastric emptying, which can be affected by energy density, structural changes of gastric content, and is regulated by metabolic responses (Camps et al., 2016; Guo et al., 2015; Mackie, 2023). The accessibility of pepsin to protein molecules, i.e. the ease for pepsin to approach protein molecules, is primarily related to food structure at various scales, ranging from millimeters to the molecular level. Some food properties, such as water absorption capacity influenced by food structure, can affect the acid uptake capacity of food particles in the stomach, which in turn influences gastric protein hydrolysis by altering pepsin activity. It is remarkable that food structure at different length scales influence the gastric protein digestion. Section 1.2 will give a detailed review on the impact of food structure on gastric digestion.

1.1.3 Intestinal phase: subsequent proteolysis and absorption

After gastric emptying, proteolysis continues in the small intestinal phase with the assistance of other digestive fluids and enzymes, such as trypsin, chymotrypsin, and carboxypeptidase. These enzymes further break down the polypeptides into smaller peptides and amino acids. Together with water and other micronutrients, amino acids are eventually absorbed by enterocytes in the ileum, entering the metabolic system (Wu, 2016). The undigested components are fermented in the large intestines and finally excreted from the body.

1.1.4 In vitro models: a window to look closely at food digestion

For food digestion studies, *in* vitro models are widely used as they are simple, efficient and do not involve animals or humans. More importantly, *in vitro* models provide a detailed view of food digestion throughout the gastrointestinal tract, showing food structure changes in

real-time during simulated digestion. This allows for studies on digestion kinetics rather than just end-point analysis (Duijsens et al., 2022). Oral, gastric and small intestinal phases are typically considered in *in vitro* models. Oral processing is mimicked *in vitro* by mincing foods in food processors, texture analyzers or mastication machines with the addition of simulated saliva fluid (SSF) for a few minutes. *In vitro* gastric and small intestinal digestion can be simulated in a static or (semi-) dynamic way depending on the extent of simulation of dynamic changes, such as digestive fluid secretion and passage rates including emptying (Li et al., 2020). These static or dynamic models can be modified to simulate the altered gastrointestinal conditions of specific groups such as infants and the elderly (Lee et al., 2023).

The INFOGEST protocol is a preferred choice for static digestion studies due to its international consensus (Brodkorb et al., 2019; Minekus et al., 2014). This protocol is standardized and harmonized by a group of scientists based on extensive *in vivo* data, allowing for comparison of the results across research groups. The static INFOGEST protocol simulates oral, gastric, and intestinal phases by incubating foods or digesta in corresponding digestive fluids containing enzymes while mixing. There is no artificial control during incubation phases, such as maintaining constant pH or gradually emptying the stomach vessel. A semi-dynamic INFOGEST protocol builds on the static version by incorporating gradual acidification, enzyme addition, calorie-based gastric emptying, and corresponding parallel intestinal digestion (Mulet-Cabero et al., 2020a).

Regarding dynamic digestion models, various systems have been developed such as TNO gastrointestinal model (TIM), Human Gastric Simulator (HGS) and NEar-Real Digestive Track (NERDT) (Blanquet et al., 2003; Chen et al., 2016; Kong & Singh, 2010; Li et al., 2020). These models vary in simulating digestive fluid secretion and gastric motility. The HGS consists solely of the gastric phase, using a latex chamber to mimic the stomach and rollers to simulate peristalsis. Gastric fluid is secreted at a dynamic rate, with gastric emptying regulated by a mesh bag with a 1.5 mm pore size within the chamber (Kong & Singh, 2010). The TIM system mimics the gastrointestinal tract with a set of glass jackets with flexible inner wall, where peristalsis is simulated by applying controlled pressure on the water between the inner and glass walls. Digestive fluid secretion is controlled by a computer program, and absorption during the small intestinal phase is simulated by removing water and hydrolysates through hollow fiber membrane units (Blanquet et al., 2003). A dialysis

system is equipped in TIM-2, enabling the simulation of microbial digestion in the large intestinal phase (Kortman et al., 2016). The NERDT specially replicates the morphology of the stomach including the inner wrinkles by 3D-printing a silicone stomach. The peristalsis in the gastrointestinal tract and digestive fluid secretion can be programmed. Simulated gastric emptying is regulated by the opening of the pyloric valve (Chen et al., 2016; Wang et al., 2019).

The advantages and drawbacks of these models have been systematically and critically reviewed by many researchers (Duijsens et al., 2022; Li et al., 2020; Mackie et al., 2020; Singh, 2024). It is worth noting that all dynamic digestion systems focus on dynamic gastrointestinal digestion, completely omitting the simulation of the oral phase. Static models such as INFOGEST protocols roughly mimic the oral phase by mincing when applicable. Moreover, the choice between static or dynamic *in vitro* digestion models can affect results due to the impact of pH changes, particle size reduction and gastric residence time on nutrient digestion (Duijsens et al., 2022). For example, using a dynamic gastric digestion system that mimics gastric secretion, peristalsis and gastric emptying remarkably increased the protein hydrolysis degree of whey protein emulsion gels after *in vitro* intestinal digestion compared to a static gastric digestion model (Mella et al., 2021).

In summary, the digestion of protein foods involves both mechanical and chemical breakdown. The mechanical breakdown starts during the oral phase and, to some extent, continues during the gastric phase. The enzymatic hydrolysis of proteins starts during the gastric phase. As the first step of enzymatic protein digestion, gastric protein hydrolysis is strongly influenced by food-related factors (compositions, structures, etc.) and their interactions with physiological factors (gastric fluid secretion, gastric emptying, etc.). In order to optimize and enhance protein digestibility, a better understanding of the impact of food structure and mechanical properties of foods on protein digestion is needed.

1.2 The role of food structure in protein digestion

Food texture describes the sensory properties of food that contribute to mouthfeel during the oral phase, such as hardness, chewiness and cohesiveness, greatly determining the enjoyment

and pleasure of eating (Chen & Rosenthal, 2015). Perceived textural properties result from the interactions between food structure and mastication during oral processing. These structures determine the mechanical properties, i.e., the responses of the structure when force is applied, which influences the chewing behavior, and ultimately, the perception of texture (Fundo & Silva, 2017; Stieger & Van de Velde, 2013).

Food structure is a general term to describe the organization and interactions of different structural elements at different length scales, ranging from nanometers to centimeters (Acevedo-Fani et al., 2022). Food macrostructure (> 1 cm) normally refers to the physical status of foods (liquid, semi-solid or solid). At a millimeter length scale (1 mm - 1 cm), the arrangement of ingredients through different processing methods creates structures, such as the porous structure of sponge cakes and the homogeneous structure of puddings. Zooming in on the structure, food microstructure (~10 μm - 1 mm) refers to the spatial partition of heterogeneous food constituents (Verboven et al., 2017), such as the microscopic phase separation of protein networks and polysaccharides in whey protein/polysaccharide mixed gels (van den Berg et al., 2007). At an even smaller length scale (~100 nm - 10 μm), the assemblages of molecules, such as protein aggregates and oil-in-water emulsions, determine food microstructure. Ultimately, this leads to the molecular structure of individual food molecules, such as proteins and lipids, which can be influenced by their source and processing. Several review articles have highlighted the role of food structure in nutrient digestion, particularly its interactions with gastric digestion, suggesting the potential to modulate nutrient digestion by altering food structure (Guo et al., 2017, 2020; Mulet-Cabero et al., 2020b; Somaratne et al., 2020c). In this section, the impact of food mechanical properties, macroscopic breakdown and microstructure on gastric protein digestion is summarized.

1.2.1 Impact of food texture and mechanical properties on gastric protein digestion

The mechanical properties of foods (such as fracture stress, fracture strain, and Young's modulus) are related to food textural properties, which are typically assessed through sensory tests. Both textural and mechanical properties are connected to the macro- and microstructure

of foods (Day & Golding, 2018). Mechanical properties, such as Young's modulus and instrumentally quantified hardness, have been closely related to gastric protein digestion (Figure 1.1). Model gels are commonly used to demonstrate the impact of textural or mechanical properties on *in vitro* gastric protein digestion because their relatively simple system facilitates manipulation of texture while controlling other variables. In general, protein-based gels with hard texture were more resistant to digestion compared to gels with soft or less stiff texture (Deng et al., 2020; Dong et al., 2022; Guo et al., 2014, 2015). Whey protein gels with higher Young's modulus released less free amino groups in simulated gastric fluid (SGF) during *in vitro* gastric digestion than whey protein gels with lower Young's modulus (Deng et al., 2020). Similarly, harder soy protein gels (tofu made with $CaSO_4$) showed lower amino acid content after *in vitro* gastric digestion than softer soy protein gels (tofu made with glucono-δ-lactone) (Lou et al., 2022). Regarding gastric emptying during dynamic *in vitro* digestion, soft whey protein emulsion gels were emptied faster from an *in vitro* human gastric simulator than hard whey protein emulsion gels, which was attributed to their higher levels of disintegration during gastric digestion (Guo et al., 2015). Although these studies demonstrated that increasing Young's modulus or hardness hindered *in vitro* gastric protein digestion, the interactions between mechanical properties and other structural features, such as microstructure, are missing. The close associations between mechanical properties and food micro- and macrostructure could interact with oral and gastric process, thereby influencing gastric protein digestion.

1.2.2 Impact of oral macrostructural breakdown on gastric protein digestion

Oral structural breakdown of solids foods during mastication is an important phase that precedes gastric digestion, significantly influencing protein digestion by altering the total surface area of food particles and gastric emptying behavior (Figure 1.1). Several studies reported that prolonged chewing increases the degree of hydrolysis during *in vitro* gastric protein digestion, which was attributed to the decrease in particle size and the increase in total particle surface area as chewing time increases (Alpos et al., 2021; Chen et al., 2021). For model gels, decreased particle size and increased total surface area promoted protein hydrolysis during *in vitro* protein digestion (Homer et al., 2021; Mennah-Govela & Bornhorst, 2021; Sicard et al., 2018). Whey protein gel cubes with a side length of 3 mm showed a 1.5 times higher degree of protein hydrolysis after *in vitro* gastric digestion than gel cubes with

a side length of 10 mm, which was attributed to their higher acid uptake capacity (Mennah-Govela & Bornhorst, 2021). In a computer simulation, the protein digestibility index increased by half at the end of the gastric phase when the average particle size of the meat bolus decreased by 90% (Sicard et al., 2018). After simulated oral processing, the boli of whey protein gels with a mean diameter of particles of 1.3 mm exhibited a 3.5 times higher o-phthaldialdehyde (OPA) reactivity after *in vitro* static gastric protein digestion than the boli with a mean diameter of particles of 4.6 mm (Homer et al., 2021). Although macrostructural breakdown consistently facilitates protein digestion, the effect sizes of macrostructural breakdown on protein digestion varies considerable across studies. We hypothesize that macrostructural breakdown interacts with other factors, such as microstructure or mechanical properties, and that the interplay between these properties affects protein digestion.

In addition to the oral macrostructure breakdown, the particle disintegration continues as gastric digestion progresses. Particle size reduction was observed in tofu, whey protein gels and egg white gels during dynamic *in vitro* gastric digestion (Drechsler & Ferrua, 2016; Guo et al., 2015; Lou et al., 2022; Somaratne et al., 2020c). Oral macrostructural breakdown along with particle disintegration during gastric phase considerably reduce the size of fragments and thus accelerate gastric emptying during dynamic *in vitro* digestion (Figure 1.1) (Guo et al., 2015; Mennah-Govela & Bornhorst, 2021). The combined effect of structural breakdown and gastric emptying during dynamic *in vitro* digestion led to an increase in protein hydrolysis of whey protein emulsion gels, but did not influence the gastric protein hydrolysis of cooked quinoa (Mella et al., 2021; Tagle-Freire et al., 2022). This suggest that gastric motility has an impact on the structural breakdown of foods during gastric digestion, but its impact on protein digestion still needs further exploration.

1.2.3 Impact of microstructure on gastric protein digestion

The modification of food microstructure is often studied in colloidal systems aiming to achieve controlled release of bioactive compounds by encapsulation (Luo et al., 2021; Nath et al., 2023; Norton et al., 2015). Research focusing on the influence of microstructure on protein digestion is relatively limited, although some studies have reported the impact of microstructure on *in vitro* gastric protein digestion of protein-based gels (Figure 1.1) (Luo et al., 2017; MacIerzanka et al., 2012; Singh et al., 2014; Zhao et al., 2020). In general,

microstructures that facilitate protein hydrolysis during digestion are described as loose, fine stranded, homogeneous and porous, while microstructures that hinder protein hydrolysis during digestion are often described as dense, aggregated, particulate and coarse. Whey protein gels with fine stranded, homogeneous microstructure (50 μm) showed faster *in vitro* gastric protein digestion than gels with dense aggregated microstructure (Singh et al., 2014). On smaller length scale, whey protein gels with larger micro-pores (with pore size smaller than 1 μm) resulted in more peptides in the gastric juice after *in vitro* gastric digestion than gels with smaller pores, although the former had lower protein content than the latter (Luo et al., 2017). β-lactoglobulin gels with fine stranded networks showed higher degree of proteolysis than gels with coarser particulate networks (with particle size at ~2 μm) during *in vitro* gastric digestion. It is not clear whether the difference in proteolysis of β-lactoglobulin gels was caused by differences in the microstructure or difference in the mechanical properties as the gels with fine stranded networks were less elastic than the other gels (MacIerzanka et al., 2012). The degree of soy protein hydrolysis was higher for porous, homogeneous gels (with a pore size around 10 μm) than for coarser and more aggregated gels although the hardness of the porous, homogenous gels was higher than that of the coarser and more aggregated gels (Zhao et al., 2020). In these studies, gel microstructure was altered alongside changes in other properties such as gel hardness and protein content, so that the independent effect of microstructure of gels on protein digestion could not be quantified. As a result, it is often unclear whether changes in protein digestion are caused by the manipulation of microstructure or changes in other factors. The effect of microstructure on gastric protein digestion still needs to be validated by isolating it from the influence of other properties.

Furthermore, studies exploring the relationship between food microstructure and protein digestion should not be limited to colloidal systems, but should also include foods exhibiting other structural elements. Plant-based meat analogues prepared from textured vegetable proteins (TVPs) are excellent examples. TVPs are food ingredients often used in the preparation of meat analogues to provide meat-like texture (Baune et al., 2022). TVPs are made from protein powder through texturization techniques such as low moisture extrusion. The structural features of TVPs like porosity and wall density vary considerably depending on the conditions applied during the texturization process (Flory & Alavi, 2024; Jeon et al., 2023; Samard et al., 2021; van Esbroeck et al., 2024). However, research on the structure of

TVPs often centers on the formulation and process optimization in order to develop TVPs that better mimic meat texture (Maningat et al., 2022; Oppen et al., 2024; Schreuders et al., 2021). Its potential impact on protein digestion is barely explored, with only a few studies reporting the *in vitro* protein digestibility of TVPs differing in structure (Azzollini et al., 2018; Lin et al., 2022; Wang et al., 2024). Wang et al. (2024) found that low-moisture TVPs made from a 1:1 mix of soybean and pea protein had a denser structure, leading to lower free amino acids in digesta compared to the looser structure of TVPs made from soybean protein concentrate. Azzollini et al. (2018) showed that increasing the wall thickness while decreasing pore size of extruded wheat snacks reduced the *in vitro* protein digestibility. Textured wheat protein's loose, fiber-like structure with large gaps improved *in vitro* protein digestibility, but this effect was neutralized by the addition of sodium tripolyphosphate (Lin et al., 2022, 2023). These studies focused on the protein digestion of the TVP *per se* instead of the foods prepared from TVPs, omitting the potential interaction between TVPs and other ingredients. The impact of the microstructural features of TVPs on protein digestion, especially when present in foods prepared from them, needs to be understood to provide guidelines for the extrusion process optimization of TVPs to promote the nutritional value of meat analogues.

1.3 Thesis aim and outline

The interactions between food structure and gastric protein digestion are complex due to the inextricable correlations between food structures at different length scales and the dynamic nature of oral-to-gastric protein digestion. This process involves both mechanical and chemical breakdown, each of which is influenced by the food structure. Understanding these interactions can provide scientific insights to contribute to the development of nutritious foods.

This thesis aimed to untangle the interplay between food microstructure, mechanical properties, macrostructural breakdown caused by oral processing, and gastric protein digestion using *in vitro* digestion models. A schematic overview of this thesis is shown in Figure 1.2.

In **Chapter 2**, we prepared whey protein isolate (WPI)/polysaccharide mixed gels as model foods to investigate the relative contribution of microstructure, mechanical properties and macrostructure breakdown on the *in vitro* gastric digestion. WPI/κ-carrageenan gels with similar mechanical properties and distinct microstructures, as well as WPI/ι-carrageenan and WPI/pectin gels with same microstructure but a series of Young's modulus were subjected to static *in vitro* gastric protein digestion. These gels were also cut into several smaller gel cubes to standardize macrostructure breakdown.

In **chapter 3**, *in vivo* human mastication was applied to WPI/κ-carrageenan gels differing in microstructure to obtain real boli, in order to quantify the interplay between oral macrostructural breakdown, microstructure and static *in vitro* gastric protein digestion of whey protein gels.

Chapter 4 moves from model foods to more complex foods – textured vegetable proteins (TVPs) and the plant-based meat analogues prepared from them. The impact of structural properties of TVPs on the static *in vitro* gastric protein digestion of TVPs and TVP-based meat analogues patties was investigated by quantitatively correlating the structural properties and protein hydrolysis during digestion.

Chapter 5 explored the *in vitro* gastric protein digestion of two commercial plant-based meat analogue patties differing in Young's modulus and bolus particle size after *in vivo* mastication. The boli of these patties were subjected to static digestion and dynamic digestion which mimics gastric motility. The impact of oral macrostructural breakdown on *in vitro* gastric emptying and dynamic gastric digestion was studied using model plant-based meat analogue patties differing only in the TVP particle size.

Chapter 6 presents the main conclusions with an integrated discussion based on the results reported in chapter 2-5, offering a broader perspective. The potential of manipulating food structure to develop protein foods tailored to specific nutritional needs is discussed, along with recommendations for future research.

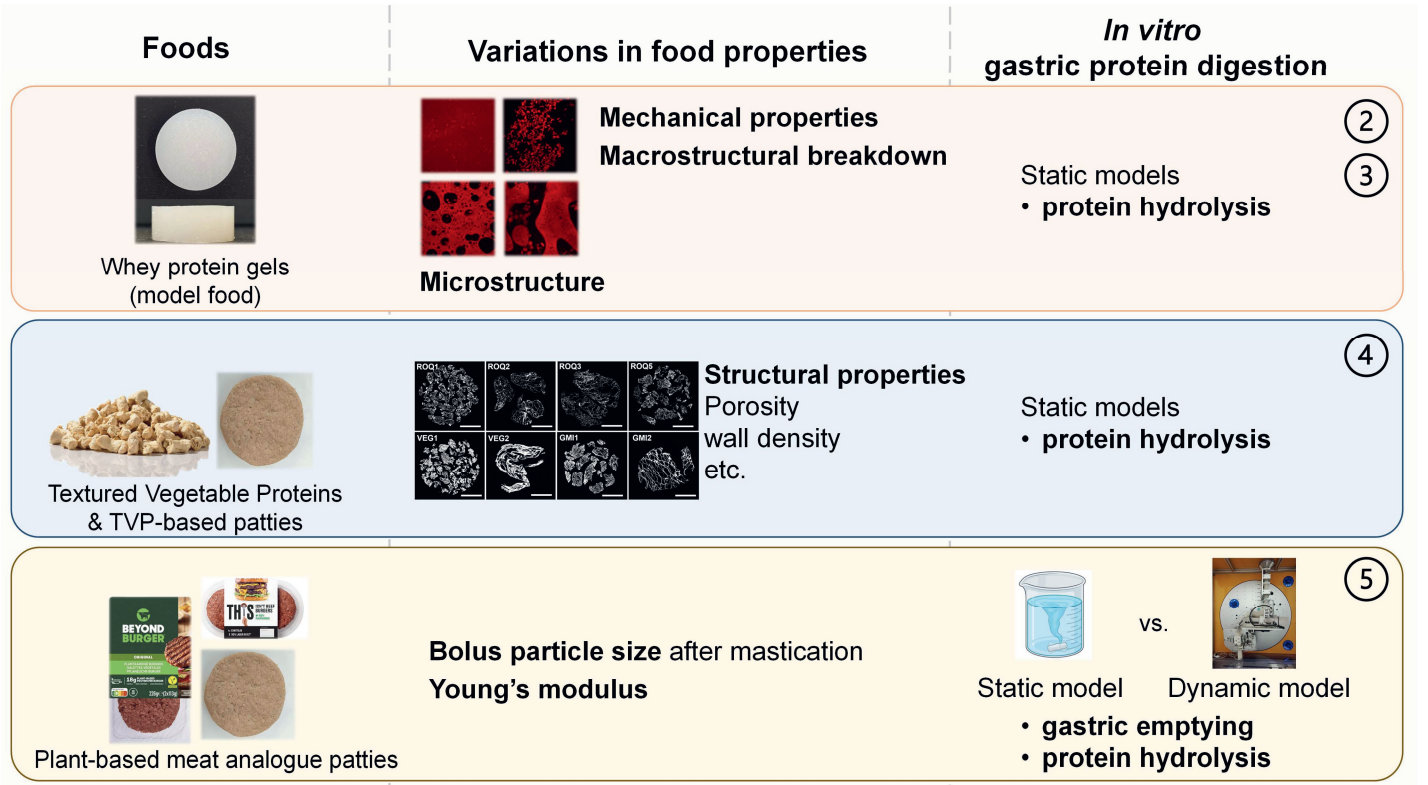

Figure 1.2. *Schematic overview of the framework of this thesis.*

Chapter 2

Interplay between microstructure, mechanical properties, macrostructure breakdown and *in vitro* gastric digestion of whey protein gels

This chapter has been published as:

Liu, D., Janssen, A. E. M., Smeets, P. A. M., & Stieger, M. (2024). Interplay between microstructure, mechanical properties, macrostructure breakdown and *in vitro* gastric digestion of whey protein gels. *Food Hydrocolloids*, *147*, 109352.

https://doi.org/10.1016/j.foodhyd.2023.109352

Abstract

Gastric digestion of proteins is influenced by multiple factors including microstructure, mechanical properties and structure breakdown during mastication. The interplay between these factors affects protein digestion but is underexplored. This study aimed to investigate the contribution of microstructure, mechanical properties and macrostructure breakdown on *in vitro* whey protein gastric digestion. Whey protein isolate (WPI) was mixed with different types of polysaccharides (κ-carrageenan, ι-carrageenan, pectin) at various concentrations to obtain heat- or acid-induced gels with distinct microstructures (homogeneous, coarse stranded, protein continuous and bi-continuous) and Young's moduli (*E*, 19-165 kPa). Structural breakdown during mastication was mimicked crudely by cutting single gel cylinders into several smaller cubes to increase the total surface area by a factor of 2.65. *In vitro* gastric digestion was measured using the INFOGEST 2.0 protocol with minor modifications. Homogeneous heat-induced WPI/κ-carrageenan gels showed the highest digestion rate followed by protein continuous, coarse stranded and bi-continuous heat-induced WPI/κ-carrageenan gels with similar *E*. A 1.47-fold increase in *E* decreased the digestion rate of acid-induced homogeneous WPI/ ι-carrageenan gels by a factor of 0.22. In contrast, a 1.13-1.83-fold increase in *E* barely changed the digestion rate of acid-induced protein continuous WPI/pectin gels. A 2.65-fold increase in total surface area increased the digestion rate of all gels by a factor of 1.35-2.54 depending on microstructure and mechanical properties. We conclude that the microstructure of protein gels affects *in vitro* protein gastric digestion and the impact of Young's modulus on *in vitro* protein gastric digestion depends strongly on the microstructure of protein gels.

2.1. Introduction

Protein is an essential macronutrient in our daily diets. Understanding protein digestion is very important due to the crucial contribution of proteins to tissue and muscle building. Food digestion involves multiple physical and chemical processes. For solid foods, the macroscopic food structure is physically broken down during oral processing by mastication, leading to the formation of a food bolus that is safe enough to be swallowed. Enzymatic digestion of protein food boli starts in the stomach during the gastric phase (Capuano & Janssen, 2021). In the stomach, the bolus is mixed with gastric juice which contains pepsin, hydrochloric acid, salts and organic substances such as mucins, starting the digestion of proteins. Pepsin breaks down peptide bonds within amino acid chains at low pH resulting in the formation of polypeptides which are further hydrolyzed into oligopeptides, tripeptides, dipeptides and free amino acids by trypsin and chymotrypsin, and are ultimately absorbed by transporters in the intestinal epithelium (Capuano & Janssen, 2021; Kong & Singh, 2008b).

Gastric digestion of proteins is influenced by multiple factors including food microstructure, mechanical properties and macrostructure breakdown during oral processing. Protein hydrolysis of soy protein gels was affected by variations of the microstructure. The degree of soy protein hydrolysis was higher for porous, homogeneous gels than for coarser and more aggregated gels although the hardness of the porous, homogenous gels was higher than that of the coarser and more aggregated gels (Zhao et al., 2020). β-lactoglobulin gels with fine stranded networks showed higher degree of proteolysis than gels with coarser particulate networks during *in vitro* gastric digestion. It is not clear whether the difference in proteolysis of β-lactoglobulin gels was caused by differences in the microstructure or difference in the mechanical properties as the gels with fine stranded networks were less elastic than the other gels (Macierzanka et al., 2012). Whey protein gels with dense agglomerates and low gel strength showed slower simulated gastrointestinal digestion than gels with fine stranded homogeneous networks and high gel strength (Singh et al., 2014). Luo et al., (2017) reported that whey protein gels with fine stranded protein networks with smaller pores showed lower amounts of peptides in SGF after *in vitro* gastric digestion than gels with larger pores, although the former was made with higher protein content than the latter. Several studies explored the impact of mechanical properties of protein gels on digestion. Overall, increasing hardness of protein gels decreases gastric digestion. Whey protein gels with higher Young's

modulus released less free amino groups in simulated gastric fluid (SGF) during *in vitro* gastric digestion than whey protein gels with lower Young's modulus (Deng et al., 2020). Soft whey protein emulsion gels were emptied faster from an *in vitro* human gastric simulator than hard whey protein emulsion gels caused by higher levels of disintegration during gastric digestion (Guo et al., 2015). Similarly, harder soy protein gels (tofu made with $CaSO_4$) showed lower amino acid content after *in vitro* gastric digestion than softer soy protein gels (tofu made with glucono-δ-lactone) (Lou et al., 2022).

Gastric digestion of proteins is not only affected by food microstructure and mechanical properties, but also by the macrostructure breakdown during oral processing. Macroscopic structural breakdown of solid foods during mastication typically increases the total surface area of the food bolus that is swallowed, providing a larger surface area for enzymatic protein digestion. For various types of foods such as jellies, carrots and breads, it has been reported that with increased hardness, the number of bolus fragments increases and the size decreases (Chen et al., 2013; Jalabert-Malbos et al., 2007; Pentikäinen et al., 2014) leading to an increase in total surface area (How et al., 2021). Increasing the particle size of whey protein gels by a factor of 3.6 after simulated oral processing decreased the o-phthaldialdehyde (OPA) reactivity by a factor of 0.4 (Homer et al., 2021). In a computer simulation, the protein digestibility index decreased by a factor of 0.5 at the end of the gastric phase when the average particle size of the meat bolus increased 12 times. This model considered particle size, gastric pH and meat buffering capacity as main factors influencing protein gastric digestion (Sicard et al., 2018). Doubling the chewing time led to the formation of more and smaller particles in the boli of chicken and soy protein-based chicken and increased *in vitro* protein hydrolysis by a factor of 1.16 (Chen et al., 2021). Thus, macrostructure breakdown during oral processing plays an important role in *in vitro* gastric protein digestion.

In summary, it has been demonstrated that *in vitro* protein digestion depends on the microstructure, mechanical properties and macrostructure breakdown during oral processing. However, most studies either focused on the effect of mechanical properties on *in vitro* protein digestion without exploring the effect of microstructure on protein digestion (Deng et al., 2020; Lou et al., 2022) or the effect of microstructure on protein digestion was confounded by the effect of mechanical properties on protein digestion (Singh et al., 2014; Luo et al., 2017; Zhao et al., 2020) i.e., microstructure and mechanical properties were varied

simultaneously. Most studies concluded that *in vitro* protein digestion was affected by the combined effects of mechanical properties and microstructure. The independent effects of microstructure and mechanical properties of foods on *in vitro* protein digestion and the interplay between microstructure, mechanical properties, macrostructure breakdown and protein digestion remain underexplored.

The aim of this study was to explore the contribution of microstructure, mechanical properties and macrostructure breakdown on *in vitro* gastric digestion of whey protein gels. The rate and degree of *in vitro* whey protein gastric digestion was compared (a) between WPI/polysaccharide gels differing in microstructure with similar mechanical properties (Young's modulus) and surface area, (b) between WPI/polysaccharide gels differing in mechanical properties (Young's modulus) with same microstructure (homogeneous or protein continuous) and surface area, and (c) between WPI/polysaccharide gels differing in surface area with same mechanical properties (Young's modulus) and same microstructure (homogeneous, coarse stranded, protein continuous and bi-continuous). We hypothesized that there is an interplay between microstructure and mechanical properties of WPI/polysaccharide gels during *in vitro* protein digestion and that increasing the surface area of gels promotes *in vitro* whey protein digestion independent of microstructure and mechanical properties.

2.2. Materials and methods

2.2.1 Materials

Whey Protein Isolate Bipro™ with 97.9% protein content and 1.9% ash was purchased from Davisco Food International, Inc. (Le Sueur, USA). Food grade κ-carrageenan and ι-carrageenan were kindly provided by CP Kelco U.S., Inc. (Atlanta, USA). Food grade glucono-δ-lactone (GDL) was kindly provided by Roquette, Inc. (Lestrem, France). Vanilla extract (Dr. Oetker, NL) and sweetener (AH Zoetjes, NL containing cyclamate and saccharin) were purchased from a local supermarket (Albert Heijn, Wageningen, NL). Pepsin from porcine gastric mucosa, high-methoxyl pectin (HM pectin, 70-75% degree of esterification) and other chemicals were purchased from Sigma-Aldrich (St. Louis, USA).

2.2.2 Preparation of heat-induced WPI/κ-carrageenan gels

Preparation of heat-indued WPI/κ-carrageenan gels was based on Çakir & Foegeding (2011) with minor modifications. κ-carrageenan concentration and ionic strength were varied to obtain different microstructures. The gel formulations are shown in Table 2.1. WPI powder was dissolved in 50 mM, 100 mM and 250 mM NaCl solution and stirred for 17 h at room temperature to obtain a 20.6 w/w% WPI stock solution. The pH of the WPI stock solution was adjusted to 7 by addition of 5M NaOH. κ-carrageenan powder was dissolved in NaCl solutions at twice the final concentration and stirred for 30 min at 90 °C. The κ-carrageenan solutions and WPI stock solution were incubated in a water bath for 15 min at 45 °C. To improve the flavor of the gels for a follow-up study which involved human mastication and sensory evaluation, vanilla extract and sweetener were added to the κ-carrageenan solutions and stirred for 1 min to dissolve. Equal amounts of WPI stock solution and κ-carrageenan solution were mixed while stirring. The pH of the solution was adjusted to 7 by addition of 5M NaOH and the warm solutions were poured into syringes. Syringes containing the warm solutions were covered with aluminum foil while standing straight being immersed in a water bath. Solutions were heated in the water bath for 30 min at 80°C to form gels. Syringes containing the heat-induced WPI/κ-carrageenan gels (pH 7.0) were kept upright at room temperature for at least 1.5 h to cool down. Samples were stored at 4-5°C and removed from the refrigerator 1.5 h before all measurements.

Table 2.1. *Sample name and composition of heat-induced WPI/κ-carrageenan gels differing in microstructure with similar mechanical properties (Young's modulus).*

Sample name	Microstructure	Young's modulus	Ingredients		
		(kPa)	WPI (w/w%)	κ-carrageenan (w/w%)	NaCl (mM)
Homogeneous gel	Homogeneous	19	10.3	0.0	100
Coarse stranded gel	Coarse stranded	19	10.3	0.1	250
Protein continuous gel	Protein continuous	26	10.3	0.2	50
Bi-continuous gel	Bi-continuous	21	10.3	0.3	50

Note: All gels contained 0.88 w/w% vanilla extract and 0.14 w/w% sweetener. Mean of the Young's modulus (Table 2.3) is shown to indicate mechanical properties.

2.2.3 Preparation of acid-induced WPI/polysaccharide gels

To obtain whey protein gels with the same microstructure but different mechanical properties, cold-set acid-induced gels were prepared by adding GDL as acidifier (De Jong & Van De

Velde, 2007; Van den Berg et al., 2007). Whey protein isolate was dissolved in water at 12 w/w% for 2 h at room temperature. The solution was heated in a water bath at 68.5°C for 2.5 h to obtain solutions of whey protein aggregates. HM pectin and ι-carrageenan solutions were mixed with the whey protein aggregate solution to obtain homogeneous gels and protein continuous gels, respectively. The 1 w/w% ι-carrageenan solution was prepared by dissolving ι-carrageenan powder in water at 80°C for 2 h, then storing the solution at room temperature overnight. Before mixing with whey protein solution, ι-carrageenan solution was heated at 80°C for 30 min. HM pectin was dissolved in water at 90°C for 40 min to obtain a 2 w/w% pectin solution. Different amounts of polysaccharide solutions were mixed with the 12 w/w% whey protein aggregate solution to obtain final concentration of 9 w/w% whey protein and ι-carrageenan (0.006 and 0.23 w/w%) or HM pectin (0.05, 0.1, 0.2, 0.3 and 0.4 w/w%) (Table 2.2). All mixtures were stirred at room temperature for 2 h. GDL was added to the solutions at 0.75 w/w% and stirred for 3 min. Solutions were poured into end-closed syringes and sealed with parafilm and stored at room temperature for 48 h to form gels. The final pH of gels was 4.6. Gels were stored at 4-5°C and removed from the refrigerator 1.5 h before all measurements.

Table 2.2. *Sample name and composition of acid-induced WPI/polysaccharide gels differing in mechanical properties (Young's modulus) with homogeneous or protein continuous microstructure.*

Sample name	Microstructure	WPI (w/w%)	GDL (w/w%)	ι-carrageenan (w/w%)	Pectin (w/w%)
WPI/ι-carrageenan gel					
81 kPa	Homogeneous	9	0.75	0.006	/
119 kPa	Homogeneous	9	0.75	0.23	/
WPI/pectin gel					
90 kPa	Protein continuous	9	0.75	/	0.05
102 kPa	Protein continuous	9	0.75	/	0.1
127 kPa	Protein continuous	9	0.75	/	0.2
144 kPa	Protein continuous	9	0.75	/	0.3
165 kPa	Protein continuous	9	0.75	/	0.4

Note: Sample names were given based on the Young's modulus of gels (Table 2.3).

2.2.4 Characterization of microstructure using CSLM

Samples were prepared as described in section 2.2.2 and 2.2.3 except that a solution of 0.002% Rhodamine B was added to 10 mL polysaccharide/WPI solutions before heat-induced or acid-induced gelation. Gels were manually cut into slides and placed onto carriers. A Zeiss

LSM 510-META confocal laser scanning microscope (CSLM) equipped with a He-Ne laser was used. All images were recorded at room temperature. The excitation wavelength was 543 nm, and the emission wavelength was 580 nm. The Zeiss Plan-Apochromat 63x/1.4 oil immersion objective was used to observe microstructure inside gels. Images were snapped when a representative structure was found after widely scanning through the gels. Images were collected with a resolution of 1024 x1024 pixels and size of 179 x 179 μm or 184 μm x 184 μm.

2.2.5 Cutting of gels and characterization of mechanical properties

After preparation gels were pushed out of the syringes and cut into cylinders of 10 mm height and 26 mm diameter (total surface area 1880 mm^2) with a slicer equipped with steel-wires. To crudely mimic the macrostructure breakdown during oral processing, these gel cylinders were manually cut with a knife into 31-35, small cubes of around 5 x 5 x 5 mm (total surface area 4650-5300 mm^2, Supplementary Figure 2.1). Uniaxial compression tests were performed on the gel cylinders (10 mm height, 26 mm diameter) using a Texture Analyzer (Instron Corp. 5564, USA) equipped with a load cell of 2000 N. Uniaxial compression tests were performed at a compression speed of 1 mm/s to 90% of initial height. The Young's modulus (E, kPa) was extracted from the initial slope of the true Hencky's stress-strain curves within the strain region of 0.05-0.15. Measurements were repeated on eight cylinders per sample and each sample was replicated three times yielding 24 measurements per sample.

2.2.6 In vitro gastric protein digestion

In vitro gastric protein digestion was performed according to the INFOGEST 2.0 protocol with minor modifications (Brodkorb et al., 2019). *In vitro* gastric digestion experiments were carried out in triplicates. About 5 g of gel sample either as one cylinder (10 mm height, 26 mm diameter, total surface area 1880 mm^2) or many, small cubes (31-35 cubes of 5 x 5 x 5mm, total surface area 4650-5300 mm^2) were immersed into 30 mL simulated gastric fluid (SGF, containing 25 mmol/L $NaHCO_3$, 47.2 mmol/L NaCl and 2000 U/mL pepsin, pH = 2) for 3 h at 37°C under continuous gentle stirring. The pH of SGF was kept constant at 2 by titrating 1 M HCl solution using an automated titrator. Small aliquots of gastric juice (100-

300 µL) were taken once per hour. Gastric juice samples were diluted with water and heated at 90°C for 5 min while mixing using a pre-heated Eppendorf thermomixer to inactivate pepsin (Deng et al., 2020).

Free amino group concentration in gastric juice were determined using the OPA method (Nielsen et al., 2001). Briefly, 10 µL sample solutions were added into 96-plate wells containing 200 µL OPA reagent and mixed by shaking for 3 min. The absorption of mixed solutions was determined by using a microplate photometer (Thermo Scientific 357, USA) at 340 nm. Serine standard solutions (0-200 mg/mL) were used to obtain a standard calibration curve using Milli-Q water as blank. *In vitro* gastric digestion data were average over the triplicate measures. The rate of free amino groups released into gastric juice during the first 2 h was taken as digestion rate. The mean of free amino groups concentration in gastric juice after 2 h digestion was taken as final free amino group concentration.

To explore and compare the effects of microstructure, mechanical properties and total surface area on *in vitro* protein digestion, relative changes in digestion rate and final free amino group concentration caused by modifications of the microstructure, Young's modulus or total surface area between gels were calculated as

$$\text{Relative change} = \frac{\text{v}(sample)}{\text{v}(reference)} \quad (1)$$

with v(*sample*) referring to the value of the digestion rate or value of the final free amino group concentration of a gel sample and v(*reference*) referring to the value of the digestion rate or value of the final free amino group concentration of a reference gel. For example, to estimate the magnitude of the effect of increasing the total surface area from 1880 mm^2 to 5300 mm^2 of a gel with a given microstructure and Young's modulus, the relative change in digestion rate was obtained as Relative change = Digestion rate (gel with 5300mm^2) / Digestion rate (gel with 1880 mm^2).

To compare the relative impact of microstructure and total surface area on *in vitro* protein digestion, the relative changes in digestion rate between heterogeneous WPI/κ-carrageenan gels (protein continuous, coarse stranded and bi-continuous) with 1880 mm^2 and 4850-5300 mm^2 surface area were calculated to estimate the magnitude of the effect of total surface area. Relative changes in digestion rate between heterogeneous WPI/κ-carrageenan gels and

homogeneous WPI/κ-carrageenan gels with 1880 mm^2 surface area were calculated to estimate the effect of microstructure. To compare the relative impact of Young's modulus and total surface area, relative changes in digestion rate between WPI/ι-carrageenan gels with same Young's modulus (119 kPa) but differing in total surface area (1880 mm^2 and 4850 mm^2) were calculated to show the effect of increasing in surface area. Relative changes in digestion rate between WPI/ι-carrageenan gels with same surface area (1880 mm^2) but differing in Young's modulus (81 kPa and 119 kPa) were calculated to show the individual effect of Young's modulus. To compare the relative impact of Young's modulus and microstructure, relative changes in digestion rate between homogeneous WPI/ι-carrageenan gels and protein continuous WPI/pectin gels but similar Young's modulus (119 kPa and 127 kPa) were calculated to estimate the magnitude of the effect of microstructure.

2.2.7 Statistical data analysis

Young's modulus was analyzed using one-way analysis of variance (ANOVA) followed by post hoc comparison (Tukey's HSD) using SPSS statistics software (IBM SPSS Statistics Version 28, IBM Corp). Data were expressed as means ± standard deviation. A level of significance of $p < 0.05$ was chosen. *In vitro* gastric digestion data were averaged over triplicate measures and reported as means ± standard deviation.

2.3. Results and Discussion

2.3.1 Microstructure and mechanical properties of mixed WPI/polysaccharide gels

2.3.1.1 Heat-induced WPI/κ-carrageenan gels differing in microstructure with similar Young's modulus

Four distinct microstructures were obtained in heat-induced WPI/κ-carrageenan gels (Table 2.3). According to the degree of microphase separation between the polysaccharide-rich and protein-rich phase and connectivity of both phases, these microstructures were classified as "homogeneous" which showed no microphase separation; "coarse stranded" which showed an isotropic, coarse stranded protein network distributed through the κ-carrageenan phase; "protein continuous" which showed a connected protein network with unconnected spherical

κ-carrageenan rich phase pores and "bi-continuous" which showed both connected protein network and connected κ-carrageenan rich phase. Microphase separation was attributed to electrostatic repulsion between whey protein aggregates and κ-carrageenan because both were negatively charged at pH 7 (Çakir & Foegeding, 2011; De Jong & Van De Velde, 2007; Foegeding et al., 2017). Compared to protein continuous microstructures, increasing κ-carrageenan concentration from 0.2 to 0.3 w/w% enabled the connection of the κ-carrageenan rich phase which led to the formation of bi-continuous microstructures. Depletion interactions between κ-carrageenan chains and whey protein aggregates contributed to microphase separation as well (Çakir & Foegeding, 2011; Croguennoc, Nicolai, Durand & Clark, 2001). In case of coarse stranded microstructures, the high ion strength (250 mM NaCl) increased the incompatibility between protein aggregates and κ-carrageenan thus a particulate protein network was formed (Çakir & Foegeding, 2011).

Despite having distinct microstructures, these four heat-induced WPI/κ-carrageenan gels showed similar Young's modulus (Table 2.3) ranging from 19 to 26 kPa. There were no significant differences in Young's modulus ($p > 0.05$) between the homogeneous, coarse stranded and bi-continuous WPI/κ-carrageenan gels. While the protein continuous WPI/κ-carrageenan gel had a significantly ($p < 0.05$) higher Young's modulus than the three other WPI/κ-carrageenan gels, the difference was small (< 7 kPa). All gels were elastic, soft and self-supporting. These four gels displayed distinct microstructures while having similar Young's modulus enabling the investigation of the effect of microstructure on *in vitro* gastric digestion of heat-induced WPI/κ-carrageenan gels independent from the effect of mechanical properties (Young's modulus) on digestion.

2.3.1.2 Acid-induced homogeneous WPI/ι-carrageenan gels differing in Young's modulus with same microstructure

Both WPI/ι-carrageenan gels displayed homogeneous microstructures (Table 2.3). This is in agreement with previous studies (De Jong & Van De Velde, 2007) that suggested low ι-carrageenan concentrations have no effect on the microstructure of WPI gels. By increasing the amount of ι-carrageenan from 0.006 to 0.23 w/w%, the Young's modulus increased significantly ($p < 0.05$) from 81 to 119 kPa (Table 2.3). De Jong & Van De Velde (2007) also observed an increase of Young's modulus in WPI/ι-carrageenan gel with increasing ι-carrageenan concentration. As both ι-carrageenan and whey protein aggregates carry counter

ions, the difference in osmotic pressure was high so that microphase separation was inhibited (De Jong & Van De Velde, 2007). These two gels differed in Young's modulus while displaying the same microstructure (homogeneous) enabling the investigation of the effect of Young's modulus on protein digestion in homogenous gels.

2.3.1.3 Acid-induced protein continuous WPI/pectin gels differing in Young's modulus with same microstructure

Table 2.3 shows the microstructure of acid-induced WPI/pectin gels. The microstructure of all gels was characterized by a connected protein network with spherical, pore-like, pectin rich inclusions. With increasing pectin concentration from 0.05 to 0.4 w/w%, the number and size of pectin pores increased in the protein continuous network. This finding is consistent with that previously reported by Van den Berg et al. (2007). The Young's modulus of the five protein continuous gels ranged from 90-165 kPa (Table 2.3) and differed significantly ($p < 0.05$) between all acid-induced protein continuous WPI/pectin gels. This set of five gels differed in Young's modulus while displaying the same microstructure (protein continuous) enabling the investigation of the effect of Young's modulus on protein digestion in protein continuous gels.

Table 2.3. *Microstructure and Young's modulus of mixed WPI/polysaccharide gels.*

Sample	Young's modulus (kPa)	Microstructure
Heat-induced WPI/κ-carrageenan gel		
Homogeneous gel	19 ± 2[b]	Homogeneous 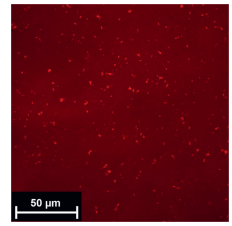
Coarse stranded gel	19 ±1[b]	Coarse stranded 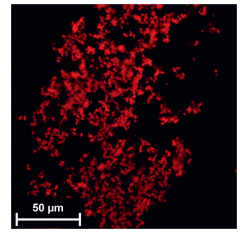

Table 2.3. *Microstructure and Young's modulus of mixed WPI/polysaccharide gels. (continued)*

Sample	**Young's modulus** (kPa)	**Microstructure**
Protein continuous gel	26 ± 1[a]	Protein continuous 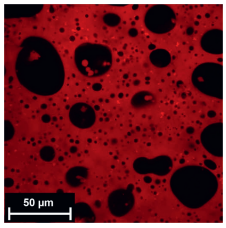
Bi-continuous gel	21 ± 1[b]	Bi-continuous 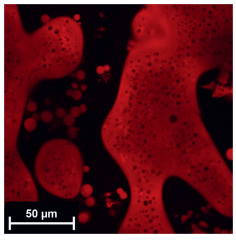
Acid-induced WPI/ι-carrageenan gel		
81 kPa	81 ± 4[b]	Homogeneous 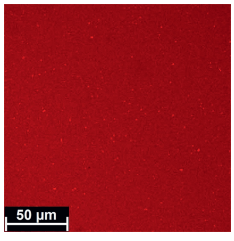
119 kPa	119 ± 7[a]	Homogeneous 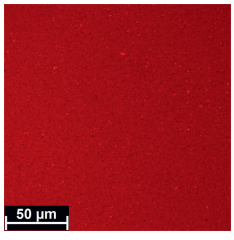
Acid-induced WPI/pectin gel		
90 kPa	90 ± 4[e]	Protein continuous 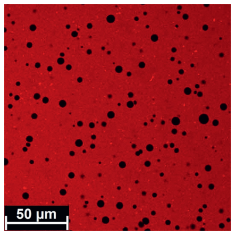

Table 2.3. *Microstructure and Young's modulus of mixed WPI/polysaccharide gels. (continued)*

Sample	Young's modulus (kPa)	Microstructure	
102 kPa	102 ± 4[d]	Protein continuous	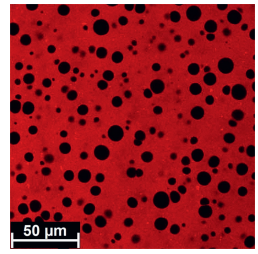
127 kPa	127 ± 5[c]	Protein continuous	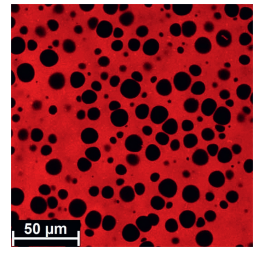
144 kPa	144 ± 5[b]	Protein continuous	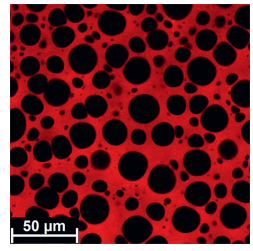
165 kPa	165 ± 6[a]	Protein continuous	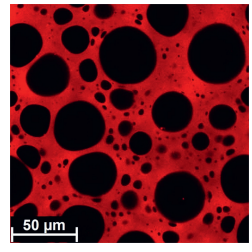

Note: Data (mean ± SD, n=24) with different superscript letters in same column within subsections are significantly different ($p < 0.05$). The scale bars correspond to 50 µm. The red areas represent the protein-rich phase, and the black areas represent the polysaccharide-rich phase. The composition of heat-induced gels is summarized in Table 2.1 and the composition of acid-induced WPI/ι-carrageenan gels and acid-induced WPI/pectin gels in Table 2.2.

2.3.2 Effect of microstructure on in vitro gastric protein digestion

Heat-induced WPI/κ-carrageenan gels (surface area 1880 mm^2) with distinct microstructures but similar Young's modulus and same protein concentration were used to investigate the effect of microstructure on gastric protein digestion independent from an effect of Young's modulus (mechanical properties). The free amino group concentration in gastric juice during digestion of the WPI/κ-carrageenan gels is shown in Figure 2.1. The free amino group concentration differed between gels with different microstructures. Homogeneous gels showed the highest digestion rate (5.61 $mmol \cdot L^{-1}/h$) and final free amino group concentration (11.26 mmol/L) after 2 h digestion (Table 2.4). Bi-continuous gels showed the lowest digestion rate (2.74 $mmol \cdot L^{-1}/h$) and final free amino group concentration (5.74 mmol/L) after 2 h digestion (Table 2.4). The digestion rate and final free amino group concentration after 2 h digestion of the coarse stranded and protein continuous gels (Table 2.4) were comparable and smaller than for the homogeneous gels but larger than for the bi-continuous gels. These findings indicate that the microstructure of WPI/κ-carrageenan gels effects *in vitro* gastric digestion independent of the Young's modulus (mechanical properties). The homogeneous microstructure benefited proteolysis the most compared to the heterogeneous microstructures (protein continuous, coarse stranded and bi-continuous).

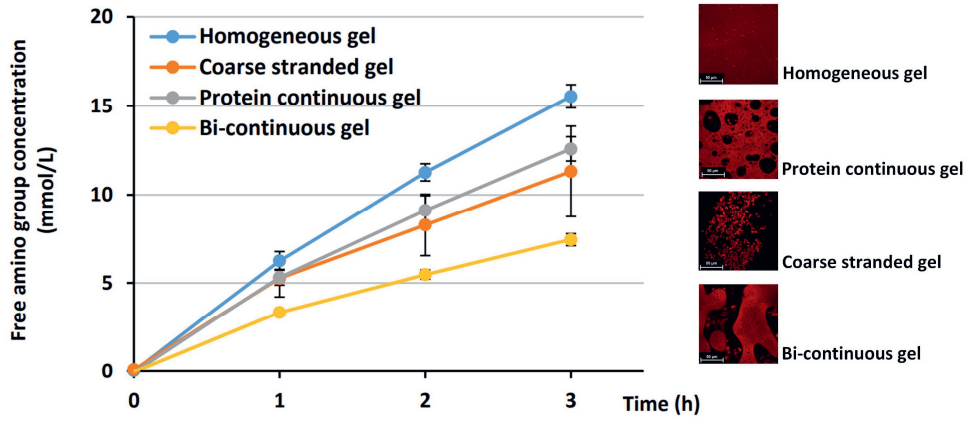

Figure 2.1. *Free amino group concentration during in vitro gastric digestion of heat-induced mixed WPI/κ-carrageenan gels (surface area 1880 mm^2) with different microstructures and similar Young's modulus. Error bars denote standard deviation. The red areas represent the protein-rich phase, and the black areas represent the polysaccharide-rich phase. The scale bars correspond to 50 μm.*

These results can be explained by four mechanisms. Firstly, the dense aggregates in the protein-rich phase of heterogeneous gels might have hindered the proteolysis compared to the loose aggregates in the protein-rich phase of homogeneous gels. This explanation is supported by the study of Singh et al. (2014) who found that whey protein gels with large stranded, heterogeneous microstructures were digested slower than whey protein gels with fine stranded, homogeneous microstructures. They attributed this finding to the denser aggregates of large stranded heterogeneous whey protein gels compared to that of fine stranded homogeneous gels. Secondly, it is reasonable to speculate that in our study more protein molecules were exposed to pepsin at the surface of the homogeneous WPI/ κ-carrageenan gels than the heterogeneous WPI/ κ-carrageenan gels within the same surface area. The penetration of pepsin into the whey protein gels can be limited to the first 2 mm from the gel surface during *in vitro* gastric digestion (Deng et.al., 2020; Luo et al., 2017). This means that proteolysis mainly takes place close to the gel surface during the first hours of *in vitro* protein digestion. For the homogeneous WPI/ κ-carrageenan gels, protein molecules were evenly dispersed at the surface, while for the heterogeneous WPI/ κ-carrageenan gels, protein molecules were congregated in different locations surrounded by the κ-carrageenan rich phase. Fewer whey protein molecules per unit area might have led to lower proteolysis per unit area for the heterogeneous WPI/ κ-carrageenan gels compared to the homogeneous WPI/κ-carrageenan gels. Compared to bi-continuous WPI/ κ-carrageenan gels, coarse stranded WPI/ κ-carrageenan gels showed a less connected protein phase, i.e., fewer whey protein molecules per unit area at the gel surface but higher free amino acids during *in vitro* gastric digestion. This could be attributed to the rougher surface of coarse stranded gels compared to other heat-induced gels (Supplementary Figure 2.2). For the small particles escaped from the rough surface, coarse stranded microstructure together with small particles might have facilitated the pepsin migration within the protein network leading to faster and more release of free amino acids to SGF. The third possible explanation could be differences in acid uptake rate and partition coefficient of pepsin between the whey protein gel surface and the SGF. Deng et al. (2020) found higher concentrations of green fluorescent protein which was used to represent pepsin at the surface of whey protein gels with higher swelling ratios. The digestion rate and acid uptake increased with increasing swelling ratio (Deng et al., 2020). We speculate that the gel microstructure of mixed WPI/ κ-carrageenan gels is highly related to water migration, acid uptake and pepsin penetration during *in vitro* gastric digestion. The fourth explanation is a potential inhibiting effect of the κ-carrageenan

on whey protein digestion, although the concentration of κ-carrageenan used in our study was very low (0.0-0.3 w/w%). Previous studies of milk and whey protein dispersions reported that the addition of 0.5-1.0% alginate decreased the digestion of milk and whey protein by a factor of 0.33-0.63 (Borreani et al., 2016; Markussen et al., 2021).

Table 2.4. *Digestion rate and final free amino group concentration of mixed WPI/polysaccharide gels (surface area 1880 mm^2) after 2 h in vitro gastric digestion. Data are shown as mean ± SD (n = 3).*

Sample	Digestion rate (mmol·L^{-1}/h)	Final free amino group concentration (mmol/L)
Heat-induced WPI/κ-carrageenan gel		
Homogeneous gel	5.61 ± 0.21	11.26 ± 0.48
Protein continuous gel	4.57 ± 0.42	9.12 ± 0.83
Coarse stranded gel	4.08 ± 0.86	8.29 ± 1.74
Bi-continuous gel	2.74 ± 0.19	5.47 ± 0.27
Acid-induced WPI/ι-carrageenan gel		
81 kPa	7.03 ± 0.04	14.07 ± 0.08
119 kPa	1.57 ± 0.09	3.12 ± 0.16
Acid-induced WPI/pectin gel		
90 kPa	6.33 ± 0.17	12.64 ± 0.32
102 kPa	7.01 ± 0.10	14.11 ± 0.18
127 kPa	6.70 ± 0.18	13.29 ± 0.53
144 kPa	6.58 ± 0.04	13.05 ± 0.27
165 kPa	7.09 ± 0.18	14.09 ± 0.24

2.3.3 Effect of Young's modulus on in vitro gastric protein digestion of homogenous and protein continuous mixed WPI/polysaccharide gels

2.3.3.1 Acid-induced homogeneous WPI/ι-carrageenan gels

Acid-induced homogeneous WPI/ι-carrageenan gels differing in Young's modulus (Table 2.3) with same protein concentration (9 w/w%), same microstructure and same total surface area (1880 mm^2) were used to study the effect of Young's modulus on whey protein gastric digestion independent of microstructure. Stiff WPI/ι-carrageenan gels (119 kPa) showed lower free amino group concentrations in gastric juice than less stiff WPI/ι-carrageenan gels (81 kPa) during *in vitro* gastric digestion (Figure 2.2). After 2 h digestion, the final free amino group concentrations were 14.1 mmol/L for less stiff WPI/ι-carrageenan gels (81 kPa) and

3.1 mmol/L for stiffer WPI/ι-carrageenan gels (81 kPa) (Table 2.4). The digestion rate of the less stiff WPI/ι-carrageenan gel (81 kPa) was 4 times higher than that of the stiffer WPI/ι-carrageenan gel (7.03 vs. 1.57 mmol·L^{-1}/h). This demonstrates that whey protein digestion of homogeneous WPI/ι-carrageenan gels can be increased by decreasing the stiffness (decreasing the Young's modulus). These results support evidence from previous studies which suggested that whey protein gels with high Young's modulus inhibited protein hydrolysis (Deng et al., 2020; Guo et al., 2014; Homer et al., 2021).

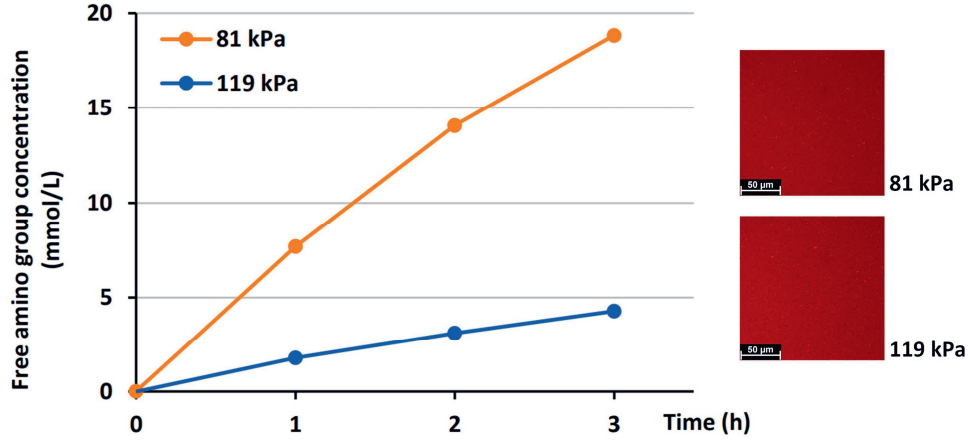

Figure 2.2. *Free amino group concentration during in vitro gastric digestion of acid-induced WPI/ι-carrageenan gels with homogeneous microstructure and different Young's modulus. Error bars are too small to be seen. Only the protein-rich phase is visible in red in CLSM images. The scale bars correspond to 50 µm.*

2.3.3.2 Acid-induced protein continuous WPI/pectin gels

Similar free amino group concentration profiles (Figure 2.3) during *in vitro* gastric digestion are observed for acid-induced protein continuous WPI/pectin gels differing in Young's modulus with same protein concentration (9 w/w%) and same total surface area (1880 mm^2). Increasing the Young's modulus of protein continuous WPI/pectin gels by a factor of 1.83 from 90 to 165 kPa only slightly varied the digestion rate by a factor of 1.12 (Table 2.4). These findings suggest that the Young's modulus showed only a very limited effect on *in vitro* gastric digestion of WPI/pectin gels with protein continuous microstructure. This outcome is in contrast to the results of homogeneous acid-induced WPI/ι-carrageenan gels (section 2.3.3.1; Figure 2.2) where a 1.47-fold increase in Young's modulus from 81 to 119 kPa decreased the digestion rate by a factor of 0.22 from 7.03 to 1.57 mmol·L^{-1}/h. These

findings show that the effect of the Young's modulus on protein gastric digestion depends strongly on the microstructure of the whey protein gel. Previous studies suggested that increasing Young's modulus inhibited proteolysis during *in vitro* protein gastric digestion by limiting the concentration of pepsin at the gel surface (Deng et al., 2020; Guo et al., 2014; Homer et al., 2021). However, in the present work, the pore size of protein continuous WPI/pectin gels increased with increasing Young's modulus (Table 2.3). This might accelerate pepsin diffusion and acid migration from the gel surface inside the gel. We speculate that the combined effect of Young's modulus and pore size led to similar digestion rates and free amino group concentration during *in vitro* gastric digestion of acid-induced protein continuous WPI/pectin gels.

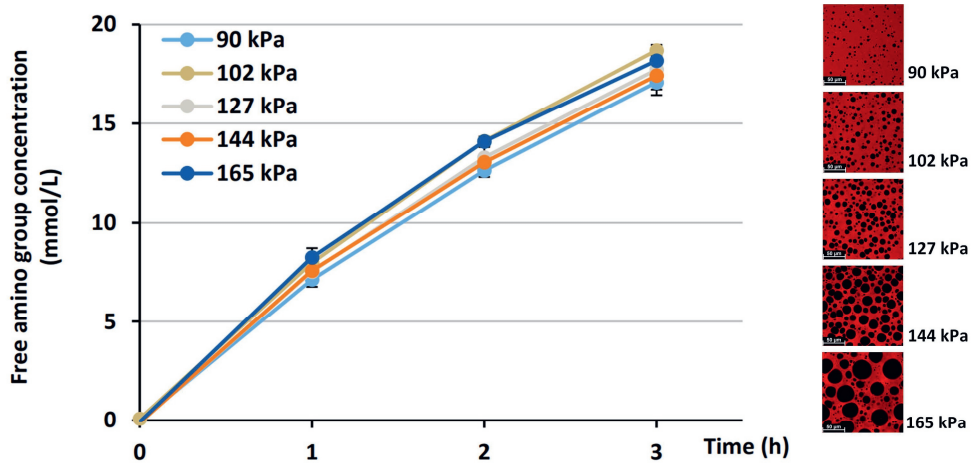

Figure 2.3. *Free amino group concentration during in vitro gastric digestion of acid-induced WPI/pectin gels with protein continuous microstructure and different Young's modulus. Error bars denote standard deviation (n=3). In the CLSM images, red areas represent the protein-rich phase, and black areas represent the polysaccharide-rich phase. The scale bars correspond to 50 μm.*

The acid-induced protein continuous WPI/pectin gels with Young's modulus of 127 kPa showed 4.27-fold higher digestion rate (6.70 mmol·L^{-1}/h) compared with the acid-induced homogeneous WPI/ι-carrageenan gels with comparable Young's modulus (119 kPa) (1.57 mmol·L^{-1}/h) (Table 2.4). This is inconsistent with the results obtained from heat-induced WPI/κ-carrageenan gels. The protein continuous microstructure increased the whey protein digestion rate of acid-induced WPI/pectin gels, while it decreased that of heat-induced WPI/κ-carrageenan gels. This might be related to the pH, whey protein concentration and polysaccharide type of the mixed gels. Protein concentration and initial pH are main factors

affecting gel buffering capacity and degree of protein hydrolysis (Luo et al., 2018; Mennah-Govela et al., 2019; Mennah-Govela & Bornhorst, 2021). In our work, acid-induced WPI/polysaccharide gels had 9 w/w% WPI and pH of 4.6, while heat-induced WPI/κ-carrageenan gels had 10.3 w/w% WPI and pH of 7. Moreover, the type of polysaccharide (κ-carrageenan, ι-carrageenan, pectin) might influence whey protein gastric digestion, especially in the protein continuous and bi-continuous gels where the polysaccharide rich phase was concentrated due to microphase separation.

2.3.4 Effect of surface area on in vitro gastric protein digestion of mixed WPI/polysaccharide gels

The free amino group concentration in gastric juice during *in vitro* gastric digestion of WPI/polysaccharide gels increased over time and was always higher for all gels with total surface area of 4650-5300 mm^2 compared to 1880 mm^2 (Figure 2.4; heat-induced WPI/κ-carrageenan bi-continuous gels and acid-induced WPI/pectin protein continuous gels are shown exemplary). Increasing the total surface area by a factor of 2.65 from 1880 mm^2 to 4650-5300 mm^2 increased the digestion rate to different extents depending on the microstructure of heat-induced mixed WPI/polysaccharide gels (Supplementary Table 2.1). For gels with similar Young's modulus, increasing the total surface area of homogeneous, protein continuous and coarse stranded WPI/κ-carrageenan gels by a factor of 2.66-2.82 increased digestion rate by a factor of 1.75-1.98, while increasing the total surface area of bi-continuous WPI/κ-carrageenan gels by a factor of 2.58 led to a 2.54-fold increase in digestion rate. For acid-induced homogeneous WPI/ι-carrageenan gels, a similar increase in total surface area (2.64-fold and 2.58-fold) led to higher increase (2.35-fold) in the digestion rate of gels with Young's modulus of 81 kPa compared to the increase (1.55-fold) in digestion rate of gels with Young's modulus of 119 kPa (Supplementary Table 2.1). An explanation can be that the digestion degree of acid-induced WPI/ι-carrageenan gel with Young's modulus of 81 kPa after cutting was limited by the protein content, since the free amino group concentration barely increased during the last hour of digestion (22.02 mmol/L after 2 h and 22.82 mmol/L after 3 h). Similar results were observed for final free amino group concentration. These findings are consistent with those of Mennah-Govela & Bornhorst (2021) who demonstrated that the degree of whey protein hydrolysis and free amino group

concentration were higher in smaller gel cubes compared to larger gel cubes after *in vitro* dynamic gastric digestion.

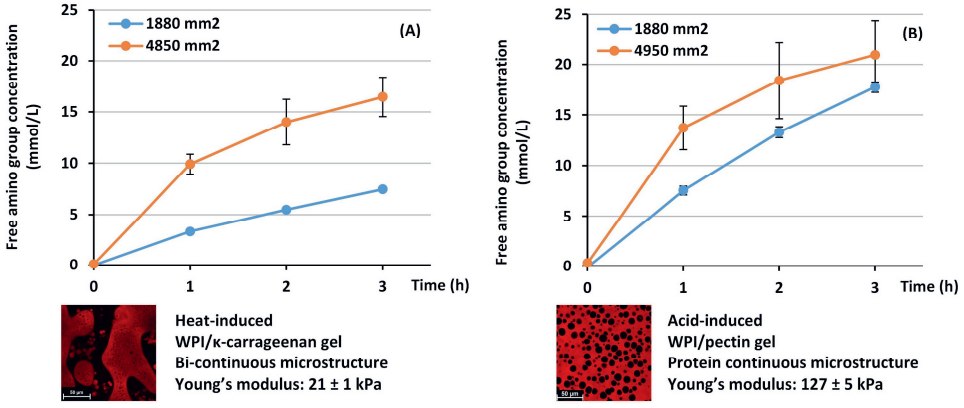

Figure 2.4. *Free amino group concentration during in vitro gastric digestion of mixed WPI/polysaccharide gels (A) with total surface area of 1880 mm² and 4850 mm² for WPI/κ-carrageenan gels and (B) with total surface area of 1880 mm² and 4950 mm² for WPI/pectin gels. Error bars denote standard deviation (n=3). In the CLSM images, red areas represent protein-rich phase and black areas represent polysaccharide-rich phase. The scale bars correspond to 50 µm.*

The digestion rate and final free amino group concentration of heat-induced WPI/κ-carrageenan gels were divided by the initial total surface area to exclude the influence of total surface area on protein digestion (Table 2.5). The digestion rate per mm² decreased by a factor of 0.65-0.69 for homogeneous, protein continuous gels and coarse stranded WPI/κ-carrageenan gels. These findings are consistent with those of Mennah-Govela & Bornhorst (2021) who reported higher whey protein hydrolysis per unit area for larger gel cubes (side length of 10.3 mm) compared to smaller gel cubes (side length of 3.1 mm). A possible explanation for this might be the low initial buffering capacity of larger gel cubes with smaller total surface area. The smaller the particle size of the protein gels, the higher the buffering capacity (Mennah-Govela et al., 2019; Mennah-Govela et al., 2020a). A high buffering capacity results in an elevated pH, thereby reducing the protein hydrolysis per unit area (Luo et al., 2018; Mennah-Govela & Bornhorst, 2021). However, the digestion rate and final free amino group concentration per mm² did not change considerably for bi-continuous WPI/κ-carrageenan gels (0.93-fold change in digestion rate per mm² and 0.99-fold change in final concentration per mm²). This result may be explained by the high connectivity of both the WPI and κ-carrageenan rich phase caused by electrostatic repulsion between negatively

charged protein aggregates and κ-carrageenan polymers at pH 7 (Çakir & Foegeding, 2011; Foegeding et al., 2017). This lead to the formation of a relatively open microstructure which might have facilitated acid uptake and accelerated local pH decrease (low buffering capacity). Therefore, the potential increase of buffering capacity caused by the increase of total surface area might have been counteracted by a potential decrease of buffering capacity caused by the bi-continuous microstructure. Further studies related to the effect of microstructure on acid uptake ability of WPI gels are needed.

Table 2.5. *Digestion rate per mm² and final free amino group concentration per mm² of heat-induced WPI/κ-carrageenan gels differing in microstructure with similar Young's modulus.*

	Digestion rate/surface area ($\mu mol \cdot L^{-1} \cdot h^{-1}/mm^2$)			Final free amino group concentration/surface area ($\mu mol \cdot L^{-1}/mm^2$)		
	Single, large cylinder (1880 mm^2)	Several, small cubes (4850-5300 mm^2)	Relative change*	Single, large cylinder (1880 mm^2)	Several, small cubes (4850-5300 mm^2)	Relative change*
Homogeneous gel	2.99 ± 0.11	1.94 ± 0.04	0.65	5.99 ± 0.25	3.84 ± 0.27	0.64
Protein continuous gel	2.43 ± 0.22	1.67 ± 0.07	0.69	4.85 ± 0.44	3.46 ± 0.24	0.71
Coarse stranded gel	2.17 ± 0.46	1.45 ± 0.05	0.67	4.41 ± 0.93	3.17 ± 0.13	0.72
Bi-continuous gel	1.46 ± 0.10	1.35 ± 0.09	0.93	2.91 ± 0.14	2.89 ± 0.49	0.99

*Note: The results are expressed as mean ± SD (n = 3). *:Relative change was calculated based on equation 1 (section 2.2.6). Data from several, small cubes with total surface area of 4850-5300 mm² were taken as samples; data from single, large cylinder with total surface area of 1880 mm² were taken as reference.*

2.3.5 Interplay between microstructure, mechanical properties, macrostructure breakdown and in vitro gastric digestion of mixed WPI/polysaccharide gels

To compare the relative impact of microstructure and total surface area on *in vitro* protein digestion, heat-induced WPI/κ-carrageenan gels were considered as these gels differed in microstructure while displaying similar Young's modulus (19-26 kPa). For all heterogeneous gels, the relative change in digestion rate caused by increasing the surface area from 1880 mm^2 to 4850-5300 mm^2 was larger than the relative change caused by changing the microstructure from heterogeneous (protein continuous, coarse stranded and bi-continuous) to homogeneous (Table 2.6). Similar results were obtained for final free amino group concentration (Table 2.6). These findings demonstrate that increasing the surface area by a factor of 2.62 had a stronger effect on whey protein hydrolysis of WPI/κ-carrageenan gels during gastric digestion than changing the microstructure from heterogeneous (protein

continuous, coarse stranded and bi-continuous) to homogeneous. We speculate that *in vitro* gastric digestion of whey protein gels may be influenced more by the gel surface area than the gel microstructure.

To compare the relative impact of Young's modulus and total surface area on whey protein gastric digestion, acid-induced homogeneous WPI/ι-carrageenan gels differing in Young's modulus (81 and 119 kPa) were considered. The relative change in digestion rate (4.48-fold) caused by a 0.68-fold decrease in Young's modulus was more pronounced than the relative change in digestion rate (2.35-fold) caused by a 2.58-fold increase in the surface area (Table 2.6). Similar results were obtained for final free amino group concentration (Table 2.6). These findings suggest that *in vitro* gastric digestion of whey protein gels may be influenced more by the Young's modulus of the gels than the gel surface area.

To compare the relative impact of Young's modulus and microstructure on whey protein gastric digestion, acid-induced homogeneous WPI/ι-carrageenan gels and acid-induced WPI/pectin gels were considered. The digestion rate of acid-induced WPI/polysaccharide gels increased by a factor of 4.27 caused by changing the microstructure from homogeneous to protein continuous and by a factor of 4.48 caused by a 0.67-fold decrease in Young's modulus (Table 2.6). Similar results were obtained for final free amino group concentration (Table 2.6). This suggests that for acid-indued mixed WPI/polysaccharide gels, changing the microstructure from homogeneous to protein continuous caused similar changes in *in vitro* whey protein gastric digestion compared to decreasing the Young's modulus by a factor of 0.67.

These comparisons of the relative impact of microstructure, mechanical properties and surface area on *in vitro* digestion provide an indication of the effect size of these modifications. However, we stress that these comparisons cannot be generalized, as the relative impact on *in vitro* digestion depends strongly on the magnitude of the modification that is applied. For example, if the gel surface area would have been changed by a factor of 10 instead of 2.65, the effect of surface area on *in vitro* protein digestion would probably have been larger and might have exceeded the effect of Young's modulus on *in vitro* protein digestion. Further studies are needed to obtain generalizable conclusions about the relative impact of microstructure, mechanical properties and surface area on *in vitro* protein digestion.

Table 2.6. *Relative changes in digestion rate and final free amino group concentration of mixed WPI/polysaccharide gels during 2h in vitro gastric digestion.*

Reference	Sample	Relative change*	
		Digestion rate	Final free amino group concentration
Microstructure vs. surface area			
Protein continuous gel (1880 mm^2)	Homogeneous gel (1880 mm^2)	1.23	1.23
	Protein continuous gel (5300 mm^2)	1.98	2.01
Coarse stranded gel (1880 mm^2)	Homogeneous gel (1880 mm^2)	1.38	1.36
	Coarse stranded gel (5000 mm^2)	1.83	1.91
Bi-continuous gel (1880 mm^2)	Homogeneous gel (1880 mm^2)	2.05	2.06
	Bi-continuous gel (4850 mm^2)	2.54	2.56
Young's modulus vs. surface area			
119 kPa gel (1880 mm^2)	81 kPa gel (1880 mm^2)	4.48	4.51
	119 kPa gel (4850 mm^2)	2.35	2.38
Young's modulus vs. microstructure			
119 kPa gel (homogeneous)	81 kPa gel (homogeneous)	4.48	4.51
	127 kPa gel (protein continuous)	4.27	4.26

**: Relative change was calculated based on equation 1 (section 2.2.6).*

Moreover, the interaction between food mechanical properties and oral breakdown should be considered. It has been reported for various types of foods including gels that the harder the foods, the smaller the bolus particle size and the higher the bolus particle number (Chen et al., 2013; Jalabert-Malbos et al., 2007; Pentikäinen et al., 2014), so the larger the total bolus surface area (Goh et al., 2021; How et al., 2021). Therefore, mechanical properties such as Young's modulus could indirectly affect protein gastric digestion by influencing the total surface area of the bolus when oral processing is involved. Further studies should include oral breakdown when it comes to the effect of mechanical properties on solid food gastric digestion.

2.4. Conclusions

This study investigated the contribution of microstructure, mechanical properties and macrostructure breakdown on *in vitro* gastric digestibility of whey protein gels. Homogeneous microstructure of mixed WPI/κ-carrageenan gels increased whey protein proteolysis the most followed by protein continuous, coarse stranded and bi-continuous microstructures. The effect of Young's modulus on whey protein hydrolysis of acid-induced gels strongly depends on gel microstructure. Increasing the total surface area facilitated *in vitro* gastric digestion of whey protein gels depending on microstructure. Increasing the surface area by a factor of 2.62 had a stronger effect on whey protein hydrolysis of WPI/κ-carrageenan gels during gastric digestion than changing the microstructure. The mixed WPI/polysaccharide gels provided a practical system to investigate the interplay between microstructure, mechanical properties, macrostructural breakdown and *in vitro* whey protein gastric digestion. The effect of microstructure and its interplay with Young's modulus and total surface area emphasized the importance of the microstructure on whey protein gastric digestion. Further studies should focus on exploring the mechanisms by which the microstructure affects gastric proteolysis, especially the effect of microphase-separated heterogeneous structures on gel buffering capacity, swelling behavior and partition coefficient of pepsin between the gel surface and the SGF. Moreover, the influence of *in vivo* oral processing on *in vitro* protein digestion should be considered in future studies.

2.5 Supplementary material

Supplementary Table 2.1. *Effect of increasing the total surface area on digestion rate and final free amino group concentration of mixed WPI/polysaccharide gels during in vitro gastric digestion. Data are shown as mean ± SD (n = 3).*

Sample	Total surface area (mm^2)		Digestion rate ($mmol \cdot L^{-1}/h$)		Final free amino group concentration (mmol/L)	
		Relative change*		Relative change*		Relative change*
Heat-induced WPI/κ-carrageenan gel						
Homogeneous gel	1880		5.61 ± 0.21		11.26 ± 0.48	
	5200	2.77	9.79 ± 1.15	1.75	19.99 ± 2.25	1.78
Coarse stranded gel	1880		4.08 ± 0.86		8.29 ± 1.74	
	5000	2.66	7.47 ± 0.71	1.83	15.87 ± 1.39	1.91
Protein continuous gel	1880		4.57 ± 0.42		9.12 ± 0.83	
	5300	2.82	9.06 ± 0.57	1.98	18.32 ± 1.06	2.01
Bi-continuous gel	1880		2.74 ± 0.19		5.47 ± 0.27	
	4850	2.58	6.96 ± 1.05	2.54	14.00 ± 2.21	2.56
Acid-induced WPI/ι-carrageenan gel						
81 kPa	1880		7.03 ± 0.04		14.07 ± 0.08	
	4900	2.61	10.88 ± 1.29	1.55	22.03 ± 2.65	1.57
119 kPa	1880		1.57 ± 0.09		3.12 ± 0.16	
	4850	2.58	3.69 ± 0.39	2.35	7.41 ± 0.86	2.38
Acid-induced WPI/pectin gel						
90 kPa	1880		6.33 ± 0.17		12.64 ± 0.32	
	4650	2.47	9.75 ± 1.49	1.54	19.86 ± 2.86	1.57
102 kPa	1880		7.01 ± 0.10		14.11 ± 0.18	
	5050	2.69	9.98 ± 1.05	1.42	20.17 ± 2.26	1.43
127 kPa	1880		6.70 ± 0.18		13.29 ± 0.53	
	4950	2.63	9.04 ± 1.91	1.35	18.39 ± 3.77	1.38
144 kPa	1880		6.58 ± 0.04		13.05 ± 0.27	
	4900	2.61	9.36 ± 1.95	1.42	19.08 ± 3.85	1.46
165 kPa	1880		7.09 ± 0.18		14.09 ± 0.24	
	5050	2.69	10.04 ± 0.30	1.42	20.45 ± 0.54	1.45

**: Relative change was calculated based on equation 1 (section 2.2.6). Data from gels with total surface area of 4850-5300 mm^2 were taken as samples; data from gels with total surface area of 1880 mm^2 were taken as references.*

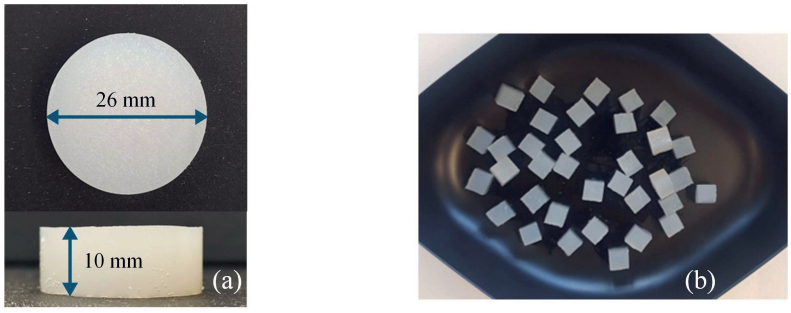

Supplementary Figure 2.1. *Appearance of WPI/polysaccharide gels (heat-induced WPI/κ-carrageenan gel with 10.3 w/w% whey protein isolate, 0.2 w/w% κ-carrageenan and 50 mM NaCl). (a) Single gel cylinder with surface area of 1880 mm^2 and (b) 35 gel cubes (5x5x5 mm) with total surface area of 5250 mm^2.*

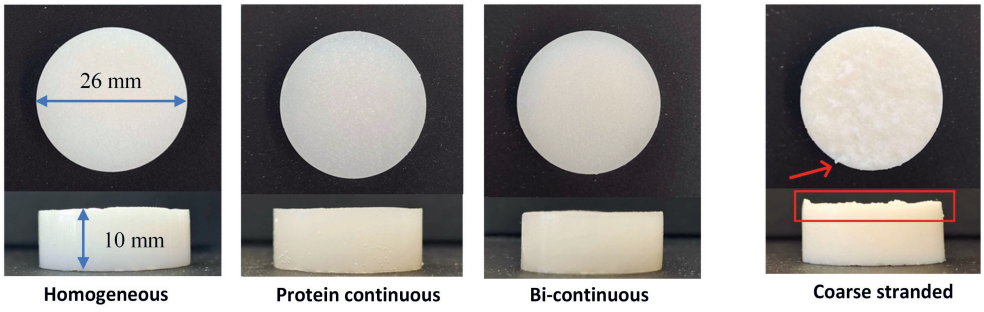

Supplementary Figure 2.2. *Appearance of heat-induced WPI/κ-carrageenan gels with total surface area of 1880 mm^2 and homogeneous, protein continuous, bi-continuous and coarse stranded microstructure. The red arrow and rectangular frame highlight the rough surface area of the coarse stranded WPI/κ-carrageenan gel.*

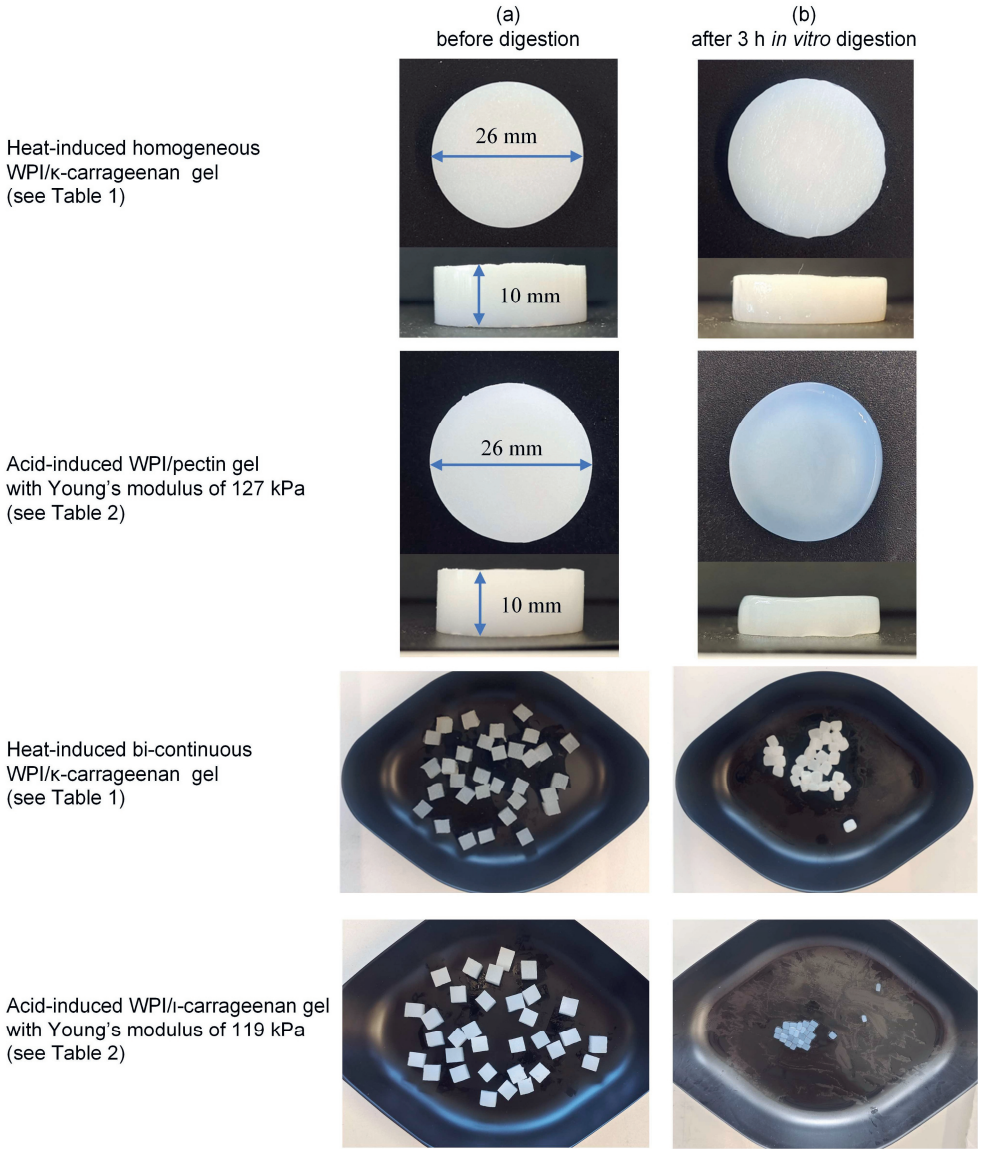

Supplementary Figure 2.3. *Appearance of different WPI/polysaccharide gels (a) before and (b) after 3 h in vitro gastric digestion.*

Chapter 3

Impact of microstructure of whey protein gels on *in vitro* gastric protein digestion is sustained after oral structural breakdown by mastication

This chapter has been published as:

Liu, D., Janssen, A. E. M., Smeets, P. A. M., & Stieger, M. (2025). Impact of microstructure of whey protein gels on *in vitro* gastric protein digestion is sustained after oral structural breakdown by mastication. *Food Hydrocolloids*, *159*, 110619.

https://doi.org/10.1016/j.foodhyd.2024.110619

Abstract

Gastric protein digestion can be influenced by food micro- and macrostructure. Understanding the interplay between microstructure and macrostructural breakdown during oral processing is crucial to enhance the nutritional value of protein-rich foods. This study compared the *in vitro* gastric protein digestion of whey protein gels differing in microstructure before and after mastication. Whey protein isolate was mixed with κ-carrageenan to obtain heat-induced gels differing in microstructure (homogeneous, coarse stranded, protein continuous, bi-continuous). Gel boli were collected from 14 participants. The number, size and total surface area of bolus fragments were determined. *In vitro* gastric protein digestion was quantified following the INFOGEST 2.0 protocol with minor modifications. Before mastication, coarse stranded gels showed the highest digestion rate (1.07 mmol·L^{-1}·g dry $matter^{-1}$/h), while homogeneous, protein continuous and bi-continuous gels showed lower and similar digestion rates (0.82-0.87 mmol·L^{-1}·g dry $matter^{-1}$/h). After mastication, the total surface area of coarse stranded gels increased 7.9-fold leading to a 1.9-fold increase in digestion rate. In contrast, a 3.4-fold increase in total surface area of bi-continuous gels caused a 2.8-fold increase in digestion rate. The total surface area of homogeneous and protein continuous gels increased 3.1- to 3.6-fold upon mastication resulting in a 1.7- to 1.9-fold increase in digestion rate. The increase in protein hydrolysis did not correlate with the degree of structural breakdown after mastication across gels differing in microstructure. We conclude that the impact of microstructure of whey protein gels on *in vitro* gastric protein digestion is sustained after oral structural breakdown by mastication.

3.1. Introduction

Proteins play an essential role in human diets due to their contribution to muscle synthesis and maintenance of health. Solid protein foods first undergo the oral phase upon mastication where they are broken down into particles and lubricated by saliva to form swallowable boli. Food boli then pass through the esophagus to reach the stomach where the first step of proteolysis happens (Capuano & Janssen, 2021). The acidic gastric juice in the stomach facilitates the hydrolyzation of the peptide bonds within protein molecules by pepsins, resulting in the formation of polypeptides. These polypeptides are hydrolyzed further in the small intestine by trypsin and chymotrypsin into oligopeptides, tripeptides, dipeptides and free amino acids (Capuano & Janssen, 2021; Kong & Singh, 2008b).

Gastric protein digestion is influenced by multiple factors including the mechanical properties and microstructure of the food. For example, protein-based gels with hard texture were more resistant to digestion compared to gels with soft or less stiff texture (Deng et al., 2020; Dong et al., 2022; Guo et al., 2014, 2015). Whey protein gels with higher Young's modulus showed lower concentrations of free amino groups during *in vitro* gastric digestion compared to whey protein gels with lower Young's modulus (Deng et al., 2020; Dong et al., 2022). Soft whey protein emulsion gels disintegrated faster and displayed faster *in vitro* gastric emptying than hard whey protein emulsion gels (Guo et al., 2014, 2015). Moreover, several studies demonstrated that the microstructure of protein gels influences their gastric protein digestion. Dense agglomerates were observed in whey protein gels when shear was applied during gelation. These clusters sterically hindered the pepsin diffusion from simulated gastric fluid (SGF) into gel particles, resulting in the slowing down of *in vitro* gastric protein digestion of whey protein gels (Singh et al., 2014). Additionally, the degree of soy protein hydrolysis was higher for porous, homogeneous gels than for coarser and more aggregated gels, although the hardness of the porous, homogenous gels was higher than that of the coarser and more aggregated gels (Zhao et al., 2020). We previously explored the independent effects of mechanical properties and microstructure on gastric protein digestion using mixed WPI/polysaccharide gels (Chapter 2). For gels with similar Young's modulus, homogeneous gels were digested faster than protein continuous, coarse stranded and bi-continuous gels. For gels with homogeneous microstructure, an increase in Young's modulus hindered the free amino group release during *in vitro* gastric digestion, whereas for gels with

protein continuous microstructure, an increase in Young's modulus did not influence *in vitro* gastric protein digestion. This suggests that the impact of mechanical properties (Young's modulus) on *in vitro* protein gastric digestion depends strongly on the microstructure of protein gels. The effect of mechanical properties and microstructure on the *in vitro* gastric digestion of protein gels were closely related to the acid uptake and pepsin partitioning between the gel matrix and gastric juice (Deng et al., 2020; Luo et al., 2019). Whey protein gels with lower Young's modulus and greater swelling exhibited increased acid uptake and simulated pepsin (green fluorescent protein) concentration within the gel surface, leading to enhanced protein hydrolysis (Deng et al., 2020). A loose microstructure may facilitate greater acid uptake and easier pepsin penetration (Luo et al., 2017; Mennah-Govela et al., 2020b; Singh et al., 2014).

Gastric protein digestion is not only affected by mechanical properties and food microstructure but also by the structural breakdown of the food during oral processing. Doubling the chewing time of chicken and plant-based chicken analogues increased the degree of protein hydrolysis during *in vitro* gastric protein digestion, which was attributed to the formation of more and smaller bolus particles after chewing longer (Chen et al., 2021). Similar results were observed for black beans, with higher peptide release during *in vitro* gastric digestion in black beans that were chewed longer (Alpos et al., 2021). The influence of chewing time on protein hydrolysis can be explained by the increase in total surface area derived from macrostructural breakdown during mastication. Whey protein gel cubes with 72% smaller specific surface area showed 36% lower degree of protein hydrolysis after *in vitro* gastric digestion (Mennah-Govela & Bornhorst, 2021). Similarly, a 2.7-fold increase in total surface area of mixed WPI/polysaccharide gels caused by manually cutting increased the *in vitro* gastric protein digestion rate by a factor of 1.4-2.5, depending on the gel microstructure and mechanical properties (Chapter 2).

Oral processing behavior is influenced by food texture and food mechanical properties (Aguayo-Mendoza et al., 2019; Gonzalez-Estanol et al., 2022). Studies with model foods demonstrated that Young's modulus, fracture toughness and fracture stress were positively correlated with the number of chews and chewing duration (Çakir et al., 2012; Guo, 2021; Lasschuijt et al., 2017; Luo et al., 2020). A study on 59 commercial foods reported that foods with less adhesiveness and greater springiness, chewiness and resilience generated a greater

number of chews and more chews per bite (Wee et al., 2018). These studies demonstrate the influence of food mechanical properties on oral behavior, which consequently affects the bolus properties such as the total surface area of bolus particles, resulting in the variations in *in vitro* gastric digestion (Chen et al., 2021; Guo, 2021).

To summarize, gastric protein digestion can be influenced directly by the microstructure and mechanical properties of foods. Gastric protein digestion can be influenced indirectly by oral processing behaviour, where prolonged mastication leads to increased protein hydrolysis due to enhanced macrostructural breakdown. While the interactions between food texture, oral processing behavior and gastric protein digestion have been well-investigated, little is known about how microstructure, oral structural breakdown, and *in vitro* protein digestion interact. The impact of food microstructure on gastric protein digestion might be reduced or even diminished when foods are macroscopically broken down after mastication. Gastric protein digestion of thoroughly broken-down foods might be driven mainly by the total surface area of the bolus fragments rather than the food microstructure, since surface area might be the main factor determining enzymatic digestion. Mechanistic insights into the impact of mastication and food microstructure on protein digestion of model foods may serve to inform the development of protein foods for specific target groups and the improvement of the nutritional value of novel protein foods.

This study builds on our previous study investigating the interplay between microstructure, macrostructure breakdown and *in vitro* gastric digestion of whey protein gels. In our previous study, the macrostructure breakdown of gels was mimicked *in vitro* by manually cutting gel cylinders into serval small gel cubes. The extent of macrostructure breakdown caused by *in vitro* cutting was likely to be much smaller than that caused by *in vivo* mastication. In the current study, expectorated boli were collected after human mastication (*in vivo*). The impact of microstructure and mastication on protein digestion was investigated by comparing the *in vitro* gastric protein digestion of whey protein gels differing in microstructure before and after *in vivo* human mastication. We hypothesize that gels with a larger degree of structural breakdown show faster protein digestion after mastication despite differences in microstructure.

3.2. Materials and methods

3.2.1 Materials

Whey Protein Isolate Bipro™ 9500, with 97.9% dry basis protein content and 1.9% dry basis ash, was purchased from Davisco Food International, Inc. (Le Sueur, USA). Food grade κ-carrageenan was kindly provided by CP Kelco U.S., Inc. (Atlanta, USA). Vanilla extract (Dr. Oetker, Amersfoort, NL) and sweetener containing cyclamate and saccharin (AH Zoetjes, Zaandam, NL) were purchased from a local supermarket (Albert Heijn B. V., Zaandam, NL). Pepsin from porcine gastric mucosa, ovalbumin from chicken egg white and other chemicals were purchased from Sigma-Aldrich (St. Louis, USA).

3.2.2 Preparation of mixed WPI/κ-carrageenan gels

Heat-induced mixed WPI/κ-carrageenan gels were prepared following the method described previously (Chapter 2). The composition of all gels is shown in Table 3.1. Briefly, WPI powder was dissolved in 50 mM, 100 mM and 250 mM NaCl solution to obtain 20.6 w/w% WPI stock solutions. κ-carrageenan was dissolved in NaCl solutions at twice the final concentration and stirred for 30 min at 90°C. Equal amounts of WPI stock solution and κ-carrageenan solution were mixed while stirring. The pH of the mixtures was adjusted to 7. Vanilla extract and sweetener were added to improve the flavor of the gels to make them palatable. Gel solutions were poured into 50 mL syringes at room temperature. Syringes (room temperature) were placed in a pre-heated water bath and heated at 80°C for 30 min. Syringes containing gelled samples were stored at 4-5°C and removed from the refrigerator 1.5 h before all measurements. Gels were cut perpendicularly to the axis of the syringe with a slicer, to obtain gel cylinders with a height of 10 mm and a diameter of 26 mm. The appearance of gel cylinders is shown in Supplementary Figure 3.1.

Table 3.1. *Composition of mixed WPI/κ-carrageenan gels differing in microstructure.*

Sample	Ingredients				
	WPI (w/w%)	κ-carrageenan (w/w%)	NaCl (mM)	Vanilla extract (w/w%)	Sweetener (w/w%)
Homogeneous gel	10.3	0.0	100	0.88	0.14
Coarse stranded gel	10.3	0.1	250	0.88	0.14
Protein continuous gel	10.3	0.2	50	0.88	0.14
Bi-continuous gel	10.3	0.3	50	0.88	0.14

Note: The water content of gels was around 88 %.

3.2.3 Characterization of mixed WPI/κ-carrageenan gel properties

3.2.3.1 Microstructure

The microstructure of the gels was examined using confocal laser scanning microscope (CLSM) as described previously (Chapter 2). Mixed gel solutions were prepared as described in section 3.2.2 but 0.002% Rhodamine B solution was added to the solutions before heating. Gels were sliced after setting and placed onto a STELLARIS 5 Cryo Confocal Light Microscope equipped with a white light laser and a LAS X Coral Cryo Software (Leica Microsystems B.V., Netherlands). The microstructure of the gels was observed through a 63x/1.40 oil objective with an emission wavelength at 580 nm and an excitation wavelength at 535 nm. Multiple images were collected across the sample. Images were captured at a resolution of 1024 × 1024 pixels and dimensions of 184 × 184 μm.

3.2.3.2 Mechanical properties

The Young's modulus and fracture stress of gels were determined through uniaxial compression tests using a Texture Analyzer (Instron Corp. 68TM-5, USA) equipped with a load cell of 2000 N, as described in Chapter 2. Gel cylinders were compressed to 90% of the initial height at a speed of 1 mm/s. Young's modulus (kPa) was determined by analyzing the initial slope of the true Hencky's stress-strain curves within the strain interval of 0.05-0.15. Fracture stress (kPa) was determined by identifying the stress corresponding to the first peak of the stress-strain curves. Measurements were repeated across four gel batches and multiple replicates were performed for each sample resulting in 17 measurements per sample.

3.2.3.3 Partition coefficient of simulated pepsin at gel-simulated gastric fluid interface

The partition coefficient of simulated pepsin at the gel-simulated gastric fluid (SGF) interface (simplified as partition coefficient) was determined by adapting the procedure used by Sassi et al., (1996). Ovalbumin was used as the substitute of pepsin to avoid protein hydrolysis during the measurements. Partition coefficients were quantified using the heat-induced mixed WPI/κ-carrageenan gels described in our previous study (Chapter 2). SGF was used as solvent to prepare 30 mL ovalbumin solutions at 0, 1, 2, 3, 4, and 5 mg/mL concentration. For each sample, WPI/κ-carrageenan gels were manually cut into small cubes (5 × 5 × 5 mm). In each ovalbumin solution of varying concentration, approximately 30 cubes with a total weight of 5 to 6 g were soaked for 24 h at 37˚C while being gently stirred. At time 0, 1, 3, 5,

22, 23, and 24 h, 100 µL of solution was pipetted out and stored at 4-5˚C. After 24 h, the liquid was poured into a pre-weighed graduated cylinder to determine the final volume and weight. Initial and final (after 24 h) weight of gel cubes were measured. Ovalbumin concentration (mg/mL) was determined using High Performance Liquid Chromatography (HPLC). Standard ovalbumin solutions at concentrations of 0.125-2 mg/mL were used to create a calibration curve that shows the relationship between peak area and concentration. The amount of ovalbumin (mg) in SGF was calculated by multiplying the volume of SGF by the ovalbumin concentration in SGF. The amount of ovalbumin in gels at equilibrium was calculated by subtracting the ovalbumin amount in SGF at 24 h from the initial ovalbumin amount in SGF (time 0). The amounts of ovalbumin in gels and SGF at 24 h were divided by the masses of gels and SGF at 24 h to obtain the ovalbumin concentrations (mg/g) in gels and in SGF at equilibrium, respectively. The partition coefficient is defined as the ratio of ovalbumin concentration (mg/g) in the gels to the ovalbumin concentration (mg/g) in SGF at equilibrium. Linear regression was performed with the ovalbumin concentration (mg/g) in the gels as dependent variable and the ovalbumin concentration (mg/g) in SGF as independent variable to determine the slope which was taken as the partition coefficient.

3.2.4 Bolus collection of mixed WPI/κ-carrageenan gels

To determine the average natural chewing time and chewing frequency of mixed WPI/κ-carrageenan gels, n=24 healthy adults (16 females and 8 males, age 29±3 y) were recruited. Participants had a healthy dental status (no missing teeth, no mastication problems (self-reported) and no swallowing problems (self-reported)). During the session, participants first familiarized themselves with the flavor and texture of each of the four gels by tasting all samples. Then, participants received two pieces of each gel (duplicate measures) and were asked to chew and swallow one gel piece at a time (6 g, 10 mm in height and 26 mm in diameter). The presentation order of the four gels was randomized over participants. The chewing process was video recorded. The chewing time and number of chews were manually annotated using a behavioral annotation software (ELAN 6.4, Max Planck Institute for Psycholinguistics, The Language Archive, Nijmegen, The Netherlands) following a standard method described before (Heuven et al., 2023). Chewing frequency was calculated by dividing the number of chews by chewing time. After the video recordings, participants were asked to take a new piece of gel into their mouth, masticate it and rate the perceived intensity

of five sensory attributes (hardness, juiciness, chewiness, sweetness, vanilla flavor) for each gel on a scale from 0 to 100 anchored with "not" at 0 and "very" at 100 using a questionnaire. All participants gave written informed consent and were financially rewarded for participation.

The average chewing time and chewing frequency obtained from n=24 adults for each gel were determined. Chewing time and chewing frequency were similar for the four gels (Supplementary Table 3.1) and the average chewing time (15 s) and chewing frequency (1.6 chews/s) across the four gels (n=24; duplicate) were obtained. For the bolus collection, participants (n=14 healthy adults, 10 females and 4 males, age 28±2 y) were instructed to chew the gels for the average natural chewing time (15 s) at a chewing frequency of 1.6 chews/s. The chewing instructions were provided with a video showing a person chewing a piece of gel for 15 s with a frequency at 1.6 chews/s. The video provided a prompt tone every time a chew had to be taken. Before bolus collection, participants were asked to familiarize themselves with the flavor and texture of every sample and practiced the chewing of gels following the video instructions. For bolus collection, participants (n=14) were given a gel piece (6 g) of each sample and asked to chew it. Participants were instructed to expectorate the bolus into a petri dish, rinse their mouth with a sip of water, and spit the water rinse into another petri dish to avoid potential water uptake by bolus particles. The expectorated water rinse was filtered with a sieve and the gel bolus residues were added to the bolus. The boli of 14 participants were pooled in a petri dish and submitted to further measurements within 12 hours.

3.2.5 Characterization of bolus properties of mixed WPI/κ-carrageenan gels

3.2.5.1 Bolus particle number and size

Image analysis was used to determine the bolus particle number and size (Chen et al., 2021). Five portions of bolus fragments were taken from different positions of pooled boli of each sample. For homogeneous, protein continuous and bi-continuous gels, each portion contained around 0.5 g of bolus fragments. For coarse stranded gels, each portion contained around 0.15 g of bolus fragments due to its relatively high number of particles per gram bolus to ensure that bolus particles could be separated manually. Each portion of bolus fragments was placed in a petri dish and separated manually with a spatula after adding some water. The

petri dish was placed on a flatbed scanner (Canon CanoScan 9000 F MarkII), and a high-resolution color image at 600 dpi was captured against a black background. After gently stirring the samples in the petri dish, an additional image of the same petri dish was captured. Both images of the same petri dish were analyzed to determine the number of particles and the area of each particle. The data were averaged to represent the data of this portion of bolus fragments. The data from five portions of each sample were averaged. ImageJ (version 1.52a, National Institute of Health) was used to analyze the acquired images. Each image was converted to an 8-bit image. The brightness/contrast and a black/white threshold were adjusted to obtain a binary image. For each image, the number of bolus particles and the area (mm^2) of each particle were obtained by running the function "Analyze Particles" in ImageJ. The number of bolus particles was normalized per g bolus (-/g bolus). The mean area of bolus particles (mm^2) was quantified as a measure of bolus particle size. Particles with an area smaller than 0.03 mm^2 or with a circularity less than 0.2 were excluded from data analysis to minimize potential noise.

3.2.5.2 Bolus particle size distribution and estimated total surface area

The bolus particle size distribution was calculated from the bolus particle number and particle size. The number of particles with size between 0.03-0.1 mm^2, 0.1-0.2 mm^2, 0.2-0.4 mm^2, 0.4-1 mm^2, 1-5 mm^2, 5-10 mm^2, 10-20 mm^2, and > 20 mm^2 were counted and divided by the total particle number to obtain the percentage of particles for each size range.

The total bolus surface area (mm^2) was estimated from the particle size distribution and particle number as

$$Total\ surface\ area = \sum Particle\ number \times Bolus\ weight \times Particle\ proportion\ (i) \times Mean\ size(i)$$

with *i* referring to each size range (0.03-0.1 mm^2, 0.1-0.2 mm^2, 0.2-0.4 mm^2, 0.4-1 mm^2, 1-5 mm^2, 5-10 mm^2, 10-20 mm^2 , >20 mm^2), and mean size (*i*) referring to the median size in each size class (0.065, 0.15, 0.3, 0.7, 3, 7.5, 15, 30 mm^2). Particle proportion (*i*) refers to the percentage of particles with size in certain range (*i*) and particle number refers to the number of particles per gram bolus. Bolus weight is 6 g which is aligned with the amount of sample used for the digestion experiment.

3.2.5.3 Bolus saliva content

The bolus saliva content of each sample was determined using the method described by van Eck et al., (2019). 1-2 g of the expectorated boli and 1.7-2.1 g of the gel cubes were placed on aluminum dishes, weighed and dried overnight at 105°C in an atmospheric oven (Binder, Germany). The dried bolus fragments and gel cubes were weighed again. The bolus saliva content per gram dry matter was calculated as:

$$Saliva\ content\ (g\ /g\ \ dry\ matter) = \frac{m(wet\ boli) - m(dry\ boli)}{m(dry\ boli)} - \frac{m(wet\ gel) - m(dry\ gel)}{m(dry\ gel)}$$

with m (wet boli) and m (dry boli) referring to the weight of boli before and after drying and m (wet gel) and m (dry gel) referring to the weight of the original gel cubes before and after drying.

3.2.6 Static in vitro gastric protein digestion

3.2.6.1 Protein hydrolysis during in vitro gastric digestion of mixed WPI/κ-carrageenan gels

The static *in vitro* gastric digestion was done following the INFOGEST 2.0 protocol with minor modifications (Brodkorb et al., 2019). About 6 g of expectorated boli or 6 g of gel (10 mm of a 26 mm diameter cylinder) were fully immersed in 30 mL preheated simulated gastric fluid (SGF, containing 25 mmol/L $NaHCO_3$, 47.2 mmol/L NaCl and 2000 U/mL pepsin, pH = 2) at 37˚C for 5 hours while gently mixing. It should be noted that no simulated salivary fluid was added before the intact gels were subjected to *in vitro* gastric protein digestion, as saliva does not cause enzymatic protein hydrolysis during oral phase, and the macrostructure breakdown caused by mastication was considered as the most significant impact of oral processing on protein digestion. After the addition of samples, the pH of gastric juice was measured with a pH meter once per hour. At the same time, 100 µL gastric juice was pipetted out for determination of free amino group concentration. The gastric juice samples were diluted in water and heated at 90˚C for 5 min while mixing in a pre-heated Eppendorf thermomixer to inactivate pepsin (Deng et al., 2020). The digestion of the gel pieces was conducted in duplicate and the digestion of boli was conducted in five replicates.

The free amino group concentration in gastric juice was determined using the o-phthaldialdehyde (OPA) method (Nielsen et al., 2001). Briefly, the mixtures of 10 µL sample

solution and 200 µL OPA reagent in 96-plate wells were shaking for 3 min followed by determining the absorption of mixed solutions at 340 nm in a microplate photometer (Thermo Scientific 357, USA). A calibration curve made with serine standard solutions (0-200 mg/mL) was used to convert the absorption values to free amino group concentrations. Liner regression was performed on free amino group concentrations as a function of digestion time between 1 h and 5 h of digestion time. The slope of the regression equation was taken as digestion rate (mmol·L^{-1}·g dry $matter^{-1}$/h). This digestion time period was used to determine the digestion rate since the increase in free amino group concentration over time was linear during this period. For comparison, we determined the digestion rate by linear regression of the free amino group concentrations as a function of digestion time between 0 h and 5 h of digestion (data not shown). The time range used for the linear regression did not influence the results and conclusions of our study. It should be noted that only the digestion rate values were smaller when the digestion period of 1-5 h was used compared to 0-5 h.

To quantify the effect of oral structural breakdown on total surface area, *in vitro* gastric protein digestion rate and final free amino group concentration of mixed WPI/κ-carrageenan gels, the relative changes were calculated as:

$$\text{Relative change} = \frac{\text{v}(bolus)}{\text{v}(gel)}$$

with v(bolus) referring to the value of the total surface area, digestion rate or final free amino group concentration of the bolus fragment sample and v(gel) referring to the value of the total surface area, digestion rate or final free amino group concentration of the corresponding gel sample.

Size exclusion chromatography was conducted to determine the peptide molecular weight (MW) distribution of hydrolysates in the liquid phase after 5 h of *in vitro* gastric digestion (Luo et al., 2015). Briefly, this was performed with an Ultimate 3000 UHPLC system (Thermo Scientific, Waltham, USA) equipped with a TSKgel G2000SWxl and a TSKgel G3000SWxl column (Tosoh Bioscience LLC, King of Prussia, PA,USA). The flow rate of the eluent fluid (30% Acetonitrile) was 1.5 mL/min and the UV-detector was set at 214 nm. The liquid phase of the digesta after 5 h digestion was centrifuged for 20 min at 14500 rpm before subjecting to analysis and 10 µL sample was injected for one measurement. The MW-retention time calibration curve was made with multiple standard solutions (thyroglobulin,

bovine serum albumin, β-lactoglobulin, α-lactalbumin, aprotinin, bacitracin and phenylalanine). The peptide profile was separated into seven sections: MW> 50 kD, 50-10 kD, 10-4 kD, 4-2 kD, 2-1 kD, 1-0.5 kD and < 0.5 kD. The peptide MW distribution was calculated based on the proportion of the peak area (mAU*min) of each section in the total peak area for each sample. The same procedure was applied to SGF without pepsin as a control measurement.

3.2.6.2 Gel properties under in vitro gastric digestion condition: in absence of pepsin

To determine the gel properties under the *in vitro* gastric digestion condition, including the H^+ uptake, swelling /shrinkage behaviour and potential protein leaking, the same *in vitro* gastric protein digestion experiments as above were conducted in the absence of pepsin. The pH of gastric juice over time was determined to monitor the H^+ uptake by samples. The gel pieces were weighed after 5 h digestion to determine the swelling/shrinkage behaviour. Size exclusion chromatography was conducted to detect the leaked polypeptides in gastric juice from gel matrix after 5 h of incubation in absence of pepsin.

3.2.7 Data analysis

All data were analyzed by one-way analysis of variance (ANOVA), followed by post hoc comparisons using Tukey's HSD test to compare means between the four gels. SPSS statistics software (IBM SPSS Statistics Version 28, IBM Corp) was used for data analysis. Data are presented as means together with standard deviations. The threshold for statistical significance was set at $p = 0.05$.

3.3. Results and Discussion

3.3.1 Mixed WPI/κ-carrageenan gel properties

3.3.1.1 Microstructure and mechanical properties

Mixed WPI/κ-carrageenan gels with different κ-carrageenan concentrations at various ionic strengths showed distinct microstructures (Table 3.2). Homogeneous gels displayed a homogeneous distribution of whey protein with some protein aggregates. Coarse stranded

gels were characterized by a protein network which was connected via coarse strands and surrounded by a κ-carrageenan rich phase. For protein continuous gels, the structure was characterized by irregular shaped κ-carrageenan rich pores which were surrounded by a connected protein rich phase. Bi-continuous gels displayed a two continuous phases rich in whey protein or κ-carrageenan. These microstructures of mixed WPI/κ-carrageenan gels are in agreement with previous studies (Chapter 2; Çakir et al., 2012). For gels with low NaCl concentration (50-100 mM), i.e. homogeneous, protein continuous and bi-continuous gels, the microphase separation was attributed to electrostatic repulsion between whey protein aggregates and κ-carrageenan because both were negatively charged at pH 7 (Çakir & Foegeding, 2011; De Jong & Van De Velde, 2007; Foegeding et al., 2017). For coarse stranded gels, the microphase separation was attributed to increased incompatibility between protein aggregates and κ-carrageenan derived from high ionic strength (250 mM NaCl) (Çakir & Foegeding, 2011; Croguennoc et al., 2001). Compared to the mixed WPI/κ-carrageenan gels reported in our previous study which had the same composition and preparation process (Chapter 2), the gels in the present work displayed the same microstructure but slightly higher Young's moduli (Table 3.2).

Coarse stranded gels had the lowest Young's modulus followed by homogenous gels. Protein continuous and bi-continuous gels displayed similar Young's moduli which were significantly higher than the Young's moduli of the other gels. Coarse stranded and bi-continuous gels showed similar fracture stress which was significantly lower than the fracture stress of homogenous gels and protein continuous gels. Despite these differences in Young's modulus and fracture stress, homogeneous, protein continuous and bi-continuous gels did not differ significantly in sensory hardness, chewiness and juiciness (Supplementary Table 3.1). The coarse stranded gel which had the lowest Young's modulus and fracture stress was perceived as significantly less hard and more juicy compared to the other gels (Supplementary Table 3.1).

3.3.1.2 Partition coefficient of simulated pepsin at gel-SGF interface

The partition coefficients of simulated pepsin (ovalbumin) between the gel and SGF are shown in Table 3.2. Surprisingly, the partition coefficient of the bi-continuous gel was significantly higher than the partition coefficients of the homogeneous, protein continuous and coarse stranded gels which did not differ significantly. This suggests that gels with bi-

continuous microstructure were able to hold more pepsin inside the gel matrix compared to gels with other microstructures. The partition coefficient of solutes between bath solution and gels is negatively related to the size of the solute and the crosslink density of the gel (Van Der Sman, 2018). We assumed that the high partition coefficient of bi-continuous gels was derived from the relatively loose microstructure. The high connectivity of both protein and κ-carrageenan rich phase might have benefited the penetration of ovalbumin from gastric juice into the gel surface and the diffusion of ovalbumin inside the gel matrix.

Table 3.2. *Microstructure, Young's modulus and fracture stress of mixed WPI/κ-carrageenan gels.*

	Homogeneous gel	Coarse stranded gel	Protein continuous gel	Bi-continuous gel
Young's modulus (kPa)	41±2^{b}	28±4^{a}	48±3^{c}	51±4^{c}
Fracture stress (kPa)	59±2^{b}	26±2^{a}	70±6^{c}	28±4^{a}
Microstructure	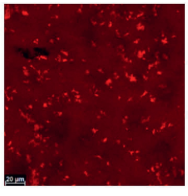	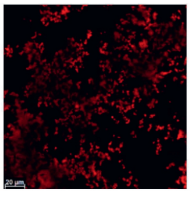	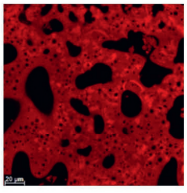	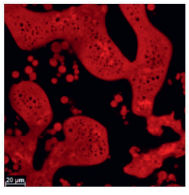
Partition coefficient†*	6.47± 0.54^{a}	5.18± 0.04^{a}	5.50± 0.59^{a}	8.69± 0.20^{b}
Young's modulus (kPa) *	19 ± 2^{b}	19 ±1^{b}	26 ± 1^{a}	21 ± 1^{b}

*Note: Means (mean ± SD, n=17) with different superscript letters in a row are significantly different ($p < 0.05$). The scale bars correspond to 20 μm. The red areas represent the protein-rich phase, and the black areas represent the polysaccharide-rich phase. The composition of mixed WPI/κ-carrageenan gels is summarized in Table 3.1. †The partition coefficient is defined as the ratio of simulated pepsin (ovalbumin) concentration (mg/g) in the gels to the simulated pepsin concentration (mg/g) in simulated gastric juice at equilibrium. *These data were obtained from the heat-induced mixed WPI/κ-carrageenan gels reported in our previous study (Chapter 2).*

3.3.2 Bolus properties of WPI/κ-carrageenan gels after oral processing

After standardized oral processing, coarse stranded gels showed significantly more and smaller bolus particles than homogeneous, bi-continuous and protein continuous gels (Table 3.3). This is attributed to the lower Young's modulus and fracture stress of coarse stranded gels compared to the other gels (Chen et al., 2021; Guo, 2021), which also resulted in lower sensory hardness compared to the other gels. Interestingly, despite the similar mechanical properties and sensory hardness, the bolus properties of homogenous, protein continuous and bi-continuous gels differed considerably. Homogeneous gels showed the most and smallest

bolus particles followed by bi-continuous and protein continuous gels (Table 3.3). These results suggest that in addition to mechanical properties, the microstructure of gels played a role in the bolus properties and oral structural breakdown. Gels with homogeneous microstructure tended to result in a larger degree of structural breakdown during oral processing. Coarse stranded gels showed larger estimated total bolus particle surface area than other gels as expected. Compared to homogeneous, protein continuous and bi-continuous gels, the bolus of coarse stranded gels contained more particles smaller than 0.2 mm^2 and less particles larger than 1 mm^2 (Figure 3.1). These results might be attributed to the specific microstructure of coarse stranded gels which could form micro-cracks and multiple fracture points during oral processing, resulting in a large number of small bolus particles (Stieger & Van de Velde, 2013). It should be noted that the total surface area of bolus particles underestimates the real total bolus particle surface area due to the use of two-dimensional images rather than three-dimensional measurements.

Coarse stranded gels showed the highest saliva content after mastication, while the other gels showed similar saliva content (Table 3.3). This could be related to the larger estimated total surface area of the bolus of coarse stranded gels compared to that of others. It has been reported that saliva uptake is positively related to the total surface area of bolus (Choy et al., 2021; Liu et al., 2017). There was no significant difference in saliva content of the bolus between homogeneous, protein continuous and bi-continuous gels. This suggests that the gel microstructure had no effect on the saliva uptake of whey protein gels during oral processing.

Table 3.3. *Bolus properties of mixed WPI/polysaccharide gels after oral processing (pooled bolus of 14 participants measured in n=5 replicates).*

	Homogeneous	Coarse stranded	Protein continuous	Bi-continuous
Bolus particle number (-/g bolus)	904 ± 182^{b}	5210 ± 382^{c}	324 ± 45^{a}	605 ± 107^{ab}
Bolus particle mean size (mm^2)	1.22 ± 0.20^{b}	0.38 ± 0.03^{a}	2.84 ± 0.22^{d}	1.64 ± 0.30^{c}
Estimated total bolus particle surface area (mm^2)*	6700 ± 1200^{a}	15000 ± 1500^{b}	5900 ± 1000^{a}	6400 ± 800^{a}
Bolus saliva content (g/g dry matter)	2.2 ± 0.2^{a}	3.5 ± 0.5^{b}	2.4 ± 0.3^{a}	2.4 ± 0.3^{a}

Note: Data (mean ± SD) with different superscript letters in a row are significantly different ($p < 0.05$).
**The total bolus particle surface area of 6 g boli.*

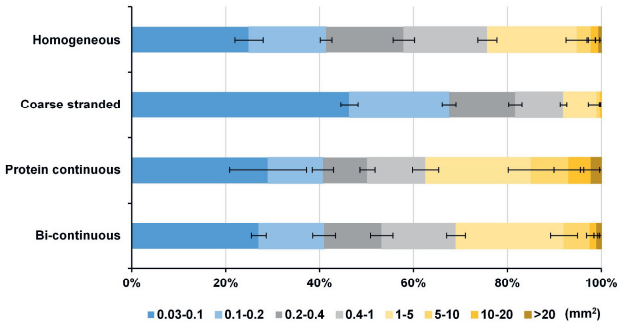

Figure 3.1. *Particle size distribution of bolus fragments of WPI/κ-carrageenan gels after oral processing. Error bars denote standard deviation (pooled bolus of n=14 participants measured in five replicates).*

3.3.3 Gel properties during static in vitro gastric digestion in absence of pepsin

3.3.3.1 H^+ uptake

The pH of simulated gastric juice increased over time during the incubation of gels or boli in absence of pepsin (Figure 3.2).

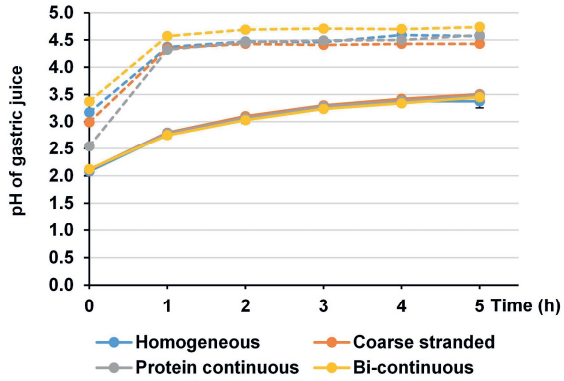

Figure 3.2. *pH value of the simulated gastric juice without pepsin during in vitro gastric digestion of mixed WPI/κ-carrageenan gels differing in mechanical properties and microstructure. Solid lines: before mastication; dotted lines: after mastication. Error bars denote standard deviations, but some bars are too small to be visible. (n = 2 for unmasticated gel, single measurement was performed for boli).*

Both the H^+ uptake of gel particles and the potential leakage of proteins from gels can contribute to the increase in pH of gastric juice during incubation. Given that the amount of proteins leaked from gel matrix was probably limited, the increase in pH shown in Figure 3.2

was mainly attributed to the diffusion of H^+ from gastric juice into the gel matrix. After mastication, for all gels, the pH of gastric juice without pepsin was higher than that of the gels before mastication. This could be explained by the increase in total surface area after mastication, which provides more available surface for acid to diffuse into the gel matrix. Before mastication, no significant difference in the pH was found between the four gels ($p > 0.05$). This result indicates that the acid uptake of un-masticated gels was similar, despite the differences in microstructure. This suggests that microstructure did not affect the acid uptake of whey protein gels, which may be attributed to the small molecular size of H^+. After mastication, bi-continuous gels showed the highest pH of gastric juice during the incubation, although its estimated total surface area was lower than coarse stranded gels (Table 3.3). This finding indicates that oral processing could affect the acid uptake of whey protein gels, which may be related to the great extent of macrostructure breakdown and saliva uptake. Coarse stranded gels contained more saliva after mastication than others (Table 3.3), but it is unclear how the saliva interacts with the microstructure of gels and influences the acid uptake. Further studies are needed to systematically investigate the role of saliva on acid uptake and pepsin diffusion during gastric protein digestion.

3.3.3.2 Whey protein leakage

Peptide size exclusion chromatography profiles of the gastric juice in absence of pepsin indicated potential protein leakage from the gels into the gastric juice. Coarse stranded gels exhibited higher absorbance at retention time 8-12 min (50-10 kDa), suggesting more protein leakage compared to other gels (Figure 3.3a). Analysis of the peptide molecule weight distribution in the gastric juice showed that coarse stranded gels leaked more large polypeptides (> 10 kDa) and correspondingly less small peptides (< 2 kDa) than the other gels (Figure 3.3c). After mastication (Figure 3.3b), there was no difference in absorbance between gels differing in microstructure. Compared to unmasticated gels, the boli of homogeneous, protein continuous and bi-continuous gels showed higher absorbance values at retention time 8-12 min, indicating that mastication induced more protein leakage from homogeneous, protein continuous and bi-continuous gels compared to coarse stranded gels.

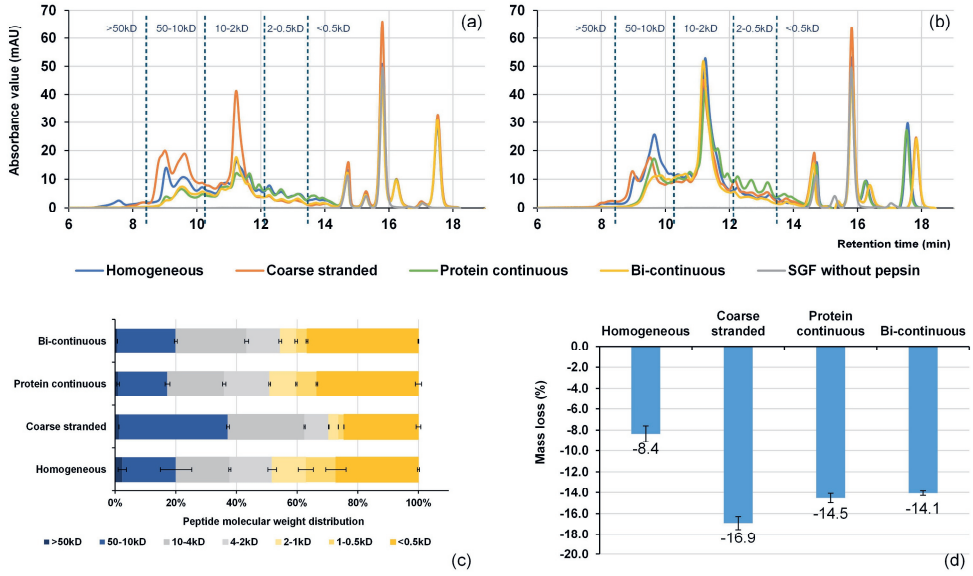

Figure 3.3. *Protein leaking and mass loss of gels digested under control condition (without pepsin) after 5 hours of incubation. The representative peptide size exclusion chromatography map of the gastric juice of (a) unmasticated gels and (b) boli of masticated gels; (c) The peptide molecular weight distribution of the gastric juice of unmasticated gels; (d) Mass loss of unmasticated gels. Error bars denote standard deviation (n = 2).*

3.3.3.3 Shrinkage behavior of gel pieces

Unmasticated WPI/κ-carrageenan gels exhibited mass loss during 5 hours of static *in vitro* gastric digestion without pepsin, demonstrating shrinkage behavior (Figure 3.3d). Gel pieces lost weight to different extents (8.4-16.9 %) after 5 hours of soaking in SGF without pepsin, attributed to factors such as acid transport, protein and κ-carrageenan re-dissolution, and water migration (van der Sman et al., 2020). Due to the relatively small molecular weight of electrolyte ions and the relative low content of κ-carrageenan in gels (0-0.3 wt%), the mass loss of gel pieces likely resulted from whey protein leakage and water loss (shrinkage). Coarse stranded gels showed the largest mass loss among gels, which is consistent with its highest absorbance value shown in Figure 3.3a. The unexpected shrinkage of gels might be related to the pH change over time. WPI hydrogels shrink near the isoelectric point (pI) of WPI (4.9-5.2) due to the low net charge, irrespective of initial pH or buffer strength (Li et al., 2017). Soy protein isolate gels swelled first then shrank at pH=4, explained by the reversal of protein charge when the internal gel pH crosses pI (van der Sman et al., 2020). Due to the change of pH (Figure 3.2) and the high sensitivity of swelling/shrinkage behaviour to pH, the gel pieces in the present study likely swelled at the beginning when the pH of gastric juice

was well below the pI and then shrank when the pH of gastric juice approached the pI. Microstructural differences also affected the extent of gel shrinkage. WPI gels with fixed and rigid microstructures resisted extensive deformation compared to gels with more flexible microstructure (Li et al., 2017). Swelling behaviour of WPI gels influenced the gastric protein digestion by affecting acid uptake and pepsin (Deng et al., 2020). These findings suggest that gel swelling/shrinkage, combined with protein leakage, impacts protein hydrolysis. Further systematic studies on the relationships between microstructure, swelling/shrinkage behaviour, potential protein leaking and gastric protein hydrolysis are needed to better understand the interplay between these factors.

3.3.4 Static in vitro gastric protein digestion of mixed WPI/κ-carrageenan gels differing in microstructure before and after mastication

3.3.4.1 Free amino group concentration and digestion rate

The free amino group concentration in gastric juice during *in vitro* gastric digestion of mixed WPI/κ-carrageenan gels before and after mastication is shown in Figure 3.4. Before mastication, coarse stranded gels showed a higher free amino group concentration during static *in vitro* gastric digestion than the other gels (Figure 3.4a), the highest digestion rate (1.07 $mmol \cdot L^{-1} \cdot g$ dry $matter^{-1}/h$) and the highest free amino group concentration (10.01 $mmol \cdot L^{-1}/g$ dry matter) in the gastric juice after 5 h of *in vitro* digestion (Table 3.4). This result is consistent with the size exclusion chromatography profile where coarse standard gels showed the highest absorbance (Supplementary Figure 3.2a). The higher protein hydrolysis of coarse stranded gels is attributed to the lower Young's modulus of these gels compared to the other gels. Whey protein gels with lower Young's modulus released more free amino group during *in vitro* gastric digestion than those with higher Young's modulus (Deng et al., 2020; Dong et al., 2022), although the influence could be affected by gel microstructure (Chapter 2). The increased leakage of free proteins and polypeptides during the incubation in the SGF could contribute to the faster protein hydrolysis of coarse stranded gels compared to the other gels (Figure 3.3a). The free protein and polypeptide molecules were probably more accessible for pepsins than the proteins trapped in the gel matrix. For homogeneous, protein continuous and bi-continuous gels, the differences in microstructure did not result in significant differences in free amino group concentration in SGF. These gels showed similar

release of free amino groups during digestion (Figure 3.4a). They also showed similar digestion rate (0.82-0.87 mmol·L^{-1}·g dry $matter^{-1}$/h), similar final free amino group concentration in gastric juice (6.58-7.06 mmol·L^{-1}/g dry matter) (Table 3.4) and overlapped peptide size exclusion chromatography profile (Supplementary Figure 3.2a). These results differ from those of our previous study in which homogeneous gels showed the highest *in vitro* gastric protein digestion rate followed by protein continuous, coarse stranded and bi-continuous gels (Chapter 2). This discrepancy can be explained by experimental differences between the studies. In the current study, during the *in vitro* digestion, the pH was not controlled, so that the pH of gastric juice increased from 2 to 4 during the digestion. In contrast, in our previous study the pH during the *in vitro* gastric digestion was kept constant at 2. The higher pH reduced pepsin activity and therefore limited the potential influence of microstructure on protein digestion of mixed WPI/κ-carrageenan gels in the current study.

After oral structural breakdown, all gels showed higher free amino group concentration during static *in vitro* gastric digestion than the corresponding unmasticated gels (Figure 3.4). The increase in total surface area caused by macrostructural breakdown during mastication (Table 3.3 & Table 3.4) led to an increase in free amino group concentration for all gels (Chapter 2). Coarse stranded gels showed higher free amino group concentration than homogeneous and protein continuous gels (Figure 3.4b). This result could be attributed to its significantly larger estimated total surface area (Table 3.3). Unexpectedly, after mastication, bi-continuous gels showed similar free amino group concentration profiles as coarse stranded gels, even though the estimated total surface area of the bolus of bi-continuous gels was smaller than that of coarse stranded gels (Table 3.3). Bi-continuous gels showed higher free amino group concentration than homogeneous and protein continuous gels, although they had similar estimated total surface area. No correlation between bolus particle number per gram bolus and the digestion rate of mixed WPI/κ-carrageenan gels after mastication was observed (Figure 3.5a). No correlation between the mean particle size and the digestion rate of mixed WPI/κ-carrageenan gels after mastication (Figure 3.5b) was found. Total bolus particle surface area did also not correlate with digestion rate of the gels (Figure 3.5c). These results disconfirm our hypothesis that despite the differences in microstructure, gels with larger degree of structural breakdown show faster and more protein digestion of masticated boli. Our results suggest that the degree of oral macrostructural breakdown is not the only determinant of *in vitro* gastric protein digestion of mixed WPI/κ-carrageenan gels. Instead,

the gel microstructure continued to impact *in vitro* gastric protein digestion of mixed WPI/κ-carrageenan gels even after macroscopic structural breakdown during mastication.

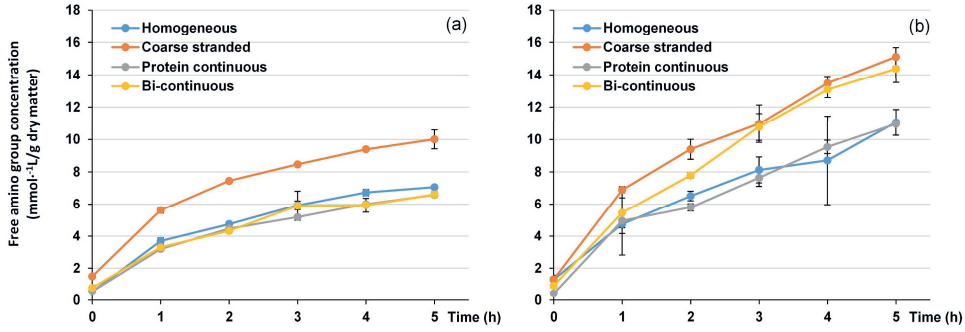

Figure 3.4. *Free amino group concentration during in vitro gastric digestion of mixed WPI/κ-carrageenan gels differing in microstructure. (a) Before mastication and (b) after mastication. Error bars denote standard deviation (n = 2 before mastication and n=5 after mastication).*

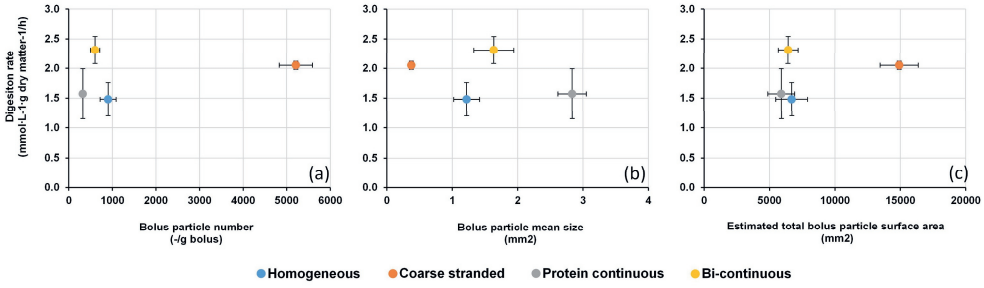

Figure 3.5. *Scatter plots of the digestion rate of mixed WPI/κ-carrageenan gels after mastication against (a) bolus particle number per g bolus, (b) bolus particle mean size and (c) estimated total bolus particle surface area. Error bars indicated the standard deviation (n=5).*

3.3.4.2 Relative changes in structural breakdown and protein hydrolysis of WPI/κ-carrageenan gels after mastication

To further discuss the enhancement of protein digestion of WPI/κ-carrageenan gels after oral processing, the relative changes in estimated total surface area, digestion rate and final free amino group concentration after oral processing are summarized in Table 3.4. Despite the increase in digestion rate and final free amino group concentration after oral processing for all gels, the relative change differed between gels depending on the microstructure. Although coarse stranded gels showed the largest increase in estimated total surface area (7.9-fold) after oral processing, the digestion rate of coarse stranded gels increased only 1.9-fold. In contrast, for bi-continuous gels, a 3.4-fold increase in estimated total surface area led to a

2.8-fold increase in digestion rate after oral processing. Homogeneous and protein continuous gels showed similar increase in estimated total surface area as bi-continuous gels (3.6- and 3.1-fold, respectively), but only 1.7- and 1.9- fold increase in digestion rate after oral processing. For all gels, the relative changes in final free amino group concentration were slightly lower than the corresponding relative changes in digestion rate, but consistent with the digestion rate results, with the bi-continuous gels showing the largest relative change (2.2-fold), while the others exhibited smaller and similar relative changes in final free amino group concentration (1.5- to 1.7-fold). These results highlight further that the increase in protein hydrolysis after mastication does not correlate with the degree of structural breakdown (i.e., total bolus surface area, Figure 3.5c) but depends strongly on the microstructure of the whey protein gels. These results are consistent with the findings reported in our previous study in which the gel pieces were manually cut into several, small cubes to increase the total surface area. Compared to the size of gel cubes (25 mm^2) in our previous study, the bolus particle mean size of gels after mastication (0.38-2.84 mm^2) in the present study was considerably smaller, indicating a much greater macroscopic structural breakdown. These findings suggest that despite the significant macrostructural breakdown, microstructure still impacted the *in vitro* gastric protein digestion of whey protein gels.

Table 3.4. *Effect of oral processing on digestion rate and final free amino group concentration of mixed WPI/polysaccharide gels after 5 h of in vitro gastric digestion.*

		Estimated total surface area (mm^2)		Digestion rate (mmol·L^{-1}·g dry $matter^{-1}$/h)		Final free amino group concentration (mmol·L^{-1}/g dry matter)	
			Relative change		Relative change		Relative change
Homogeneous	Gel	1880		0.87±0.01		$7.06±0.13^{A}$	
	Bolus	$6700±1200^{a}$	3.6	$1.48±0.28^{a}$	1.7	$11.06±0.80^{a}$	1.6
Coarse stranded	Gel	1880		1.07±0.08		$10.01±0.58^{B}$	
	Bolus	$15000±1500^{b}$	7.9	$2.05±0.07^{bc}$	1.9	$15.10±0.57^{b}$	1.5
Protein continuous	Gel	1880		0.83±0.05		$6.58±0.08^{A}$	
	Bolus	$5900±1000^{a}$	3.1	$1.57±0.42^{ab}$	1.9	$10.96±0.06^{a}$	1.7
Bi-continuous	Gel	1880		0.82±0.08		$6.61±0.17^{A}$	
	Bolus	$6400±800^{a}$	3.4	$2.31±0.23^{c}$	2.8	$14.38±0.85^{b}$	2.2

Note: Gel refers to samples before mastication and Bolus refers to samples expectorated after standardized oral processing. Means (mean ± SD, n=2 for gel and n=5 for bolus) with different superscript letters (capital for gel; lowercase for bolus) in the same column are significantly different ($p < 0.05$).

The significantly larger increase in digestion rate and final free amino group concentration of bi-continuous gels than the other gels after mastication can be explained by the larger partition coefficient (Table 3.2) and the slightly higher H^+ uptake (Figure 3.2) of the bi-continuous gels. Gastric protein digestion mainly happens at the gel surface through surface erosion derived by enzymatic hydrolysis which was attributed to the limited penetration depth of pepsin into the gel matrix (Deng et al., 2020; Luo et al., 2017; Somaratne et al., 2020b). The efficiency of proteolysis depends on the availability and activity of pepsin. After mastication, the total surface area of bolus was significantly increased for all gels, providing more available sites for pepsin and speeding up the transport of pepsin from gastric juice into the gels. Compared to un-masticated gels, masticated gels with larger total surface area might need less time to reach the maximum pepsin concentration inside the gel matrix, enhancing the effect of partition coefficient on enzymatic hydrolysis. The higher partition coefficient of bi-continuous gels enabled more pepsin transport towards the gel matrix and hydrolyzing the whey protein. The bi-continuous gel might show lower local pH than the other gels considering the higher H^+ uptake which might have increased the pepsin activity and facilitated protein hydrolysis.

3.3.3.3 pH of gastric juice during digestion

The pH of gastric juice during the digestion of mixed WPI/κ-carrageenan gels before and after oral processing is shown in Figure 3.6. As expected, the pH of gastric juice during static *in vitro* gastric protein digestion increased for all gels. The increase in pH during digestion can be explained by the diffusion of H^+ from acidic gastric juice to the gel matrix and the ionization of amino group released by proteins due to the cleavage of peptide bonds (Deng et al., 2020; Luo et al., 2018). The increased pH of gastric juice over time could in turn inhibit pepsin activity, thus slowing down proteolysis. Therefore, it is observed in Figure 3.4a that the curves of free amino group concentration tend to level off during the digestion of un-masticated gels. However, after mastication, the curves of free amino group concentration show a linear trend after the first hour (Figure 3.4b). Moreover, although the pH of gastric juice during the digestion of boli were obviously higher than that during the digestion of un-masticated gels (Figure 3.6), the boli still showed more free amino groups than the corresponding gels (Figure 3.4). These findings emphasize the impact of macrostructure breakdown caused by mastication on *in vitro* gastric protein digestion. The increased total surface area of gels after mastication could enable more pepsin to penetrate from gastric juice

into the bolus particles simultaneously, promoting protein hydrolysis despite lower pepsin activity. Before mastication, coarse stranded gels showed slightly higher pH of gastric juice after the first hour until the end of digestion compared to other gels. After mastication, the boli of coarse stranded and bi-continuous gels showed slightly higher pH of gastric juice during digestion than that of homogeneous and protein continuous gels. Either before or after mastication, the results of pH during digestion are in accordance with the free amino group concentration results (Figure 3.4). This finding is consistent with previous studies (Deng et al., 2020; Luo et al., 2018) which suggested that the increase in pH of gastric juice caused by protein hydrolysis is proportional to the degree of hydrolysis of whey protein gels. The pH of gastric juice differed at the beginning of the digestion of WPI/κ-carrageenan gels after mastication. Coarse stranded gels showed the highest pH of gastric juice and protein continuous gels showed the lowest pH of gastric juice. This might be attributed to the larger number of smaller bolus particles of coarse stranded gels compared to protein continuous gels (Table 3.2). The more and smaller particles facilitated proteolysis, which releases amino groups resulting in an increase in pH of gastric juice (Luo et al., 2018).

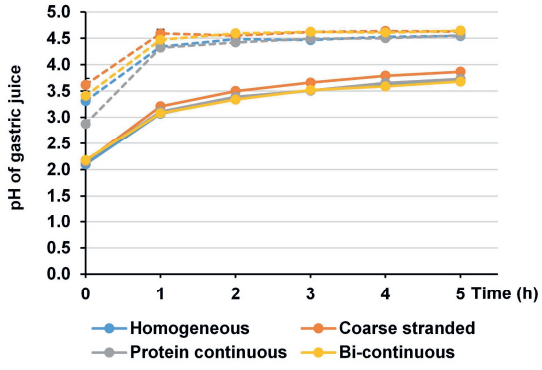

Figure 3.6. *pH value of the simulated gastric juice during in vitro gastric digestion of mixed WPI/κ-carrageenan gels differing in microstructure. Solid line: before mastication; dot line: after mastication. Error bars denote standard deviations, but some bars are too small to be visible. (n = 2 for unmasticated gel, n=5 for boli of masticated gel).*

3.4. Conclusions

This study compared the *in vitro* gastric protein digestion of whey protein gels differing in microstructure before and after mastication. Before mastication, coarse stranded gels showed the highest degree of protein hydrolysis, whereas differences in microstructure between homogeneous, protein continuous and bi-continuous gels did not result in significant differences in degree of protein hydrolysis. This might be attributed to the increase in pH of gastric juice during static *in vitro* gastric digestion, which limited the degree of protein hydrolysis as well as the effect of microstructure on digestion. After mastication, oral structural breakdown caused an increase in total surface area of gel bolus particles for all gels, resulting in an increase in *in vitro* gastric protein digestion of mixed WPI/κ-carrageenan gels. However, the increase in protein hydrolysis after mastication did not correlate with the degree of structural breakdown across gels differing in microstructure. Bi-continuous gels showed a larger increase in protein hydrolysis than coarse stranded gels after mastication although the degree of structural breakdown (increase in total bolus surface area) was smaller. This suggests that the increase in protein hydrolysis depended on both the degree of oral structural breakdown and the initial microstructure of the whey protein gels. We conclude that the impact of microstructure of whey protein gels on *in vitro* gastric protein digestion is sustained after oral structural breakdown by mastication. Further *in vitro* and *in vivo* studies on commercially available foods are needed to validate the effect of microstructure on protein digestion in a more complex context.

3.5 Supplementary material

Supplementary Table 3.1. *Oral processing behaviour and sensory properties (100-unit VAS*) of mixed WPI/polysaccharide gels differing in microstructure.*

	Homogeneous gel	Coarse stranded gel	Protein continuous gel	Bi-continuous gel
Oral behaviour				
Number of chews (-)	24±10^{ab}	19±8^{a}	28±11^{b}	26±10^{b}
Chewing time (s)	14±6	13±6	16±7	16±6
Chewing frequency (-/s)	1.7±0.2^{b}	1.5±0.2^{a}	1.7±0.2^{b}	1.7±0.2^{b}
Sensory properties				
Hardness	37±25^{ab}	21±18^{a}	43±26^{b}	33±23^{ab}
Juiciness	24±17^{a}	54±26^{b}	33±23^{a}	31±21^{a}
Chewiness	41±26	27±21	42±23	40±25
Sweetness	43±18	43±26	52±22	53±22
Vanilla flavor intensity	44±19	40±24	52±28	47±23

*Note: Means (mean ± SD, n=24 in duplicate for oral behaviour, n=24 for sensory properties) with different superscript letters in same row are significantly different ($p < 0.05$). *Visual analog scales.*

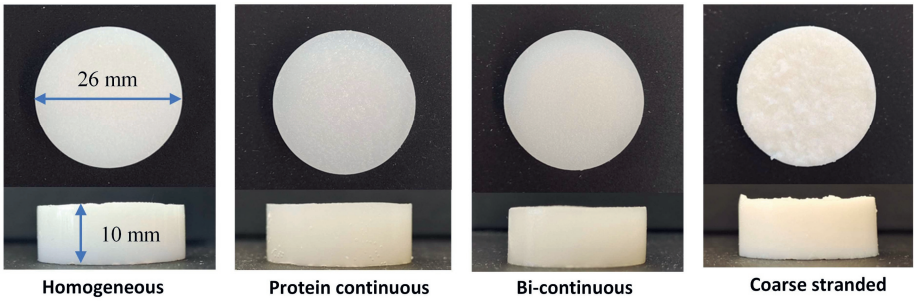

Supplementary Figure 3.1. *Appearance of WPI/κ-carrageenan gels with homogeneous, protein continuous, bi-continuous and coarse stranded microstructure.*

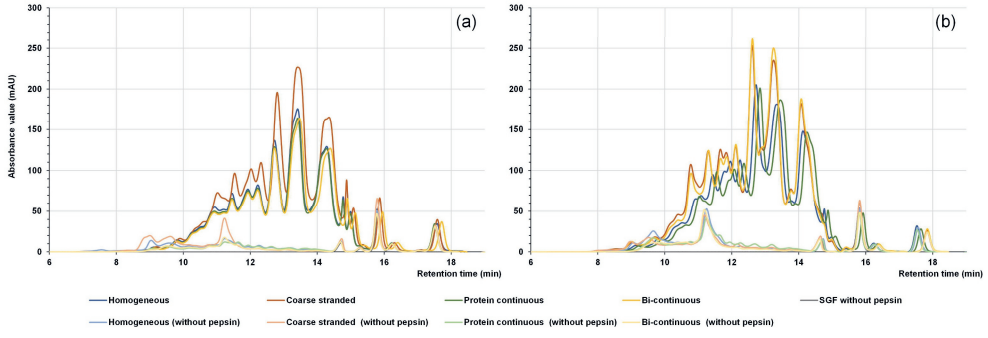

Supplementary Figure 3.2. *The peptide size exclusion chromatography profiles of the simulated gastric fluid of mixed WPI/polysaccharide gels differing in microstructure after 5h in vitro gastric protein digestion. (a) Before mastication and (b) after mastication.*

Chapter 4

Influence of structural properties of textured vegetable proteins on *in vitro* gastric digestion kinetics of plant-based meat analogue patties

This chapter has been published as:

Liu, D., van Esbroeck, T., Janssen, A. E. M., Scholten, E., Smeets, P. A. M., & Stieger, M. (2025). Influence of structural properties of textured vegetable proteins on *in vitro* gastric digestion kinetics of plant-based meat analogue patties. *Food Hydrocolloids*, 162, 111011. https://doi.org/10.1016/j.foodhyd.2024.111011.

Abstract

Textured vegetable proteins (TVPs) differ in structural properties that may affect the protein digestion of TVP-based meat analogues. This study explored the influence of structural properties on *in vitro* gastric protein digestion of TVPs and TVP-based patties. Eight TVPs differing in macroscopic surface area and microstructural properties (porosity, wall density, etc.) were used. As references, TVPs were ground into powders to remove their porous structure. *In vitro* gastric protein digestion was determined following the INFOGEST protocol. Structural properties were correlated with free amino group concentrations at different digestion times. For intact TVPs, surface area ($r = 0.78$) and mean pore size ($r = 0.74$) showed significant positive correlations with free amino group concentrations at 5 min of digestion. These correlations persisted for patties (at 30-120 min for surface area, 5-60 min for mean pore size). For TVP powders, wall density was the main structural feature, which was negatively correlated with free amino group concentrations at 5 min ($r = -0.78$) and 30 min ($r = -0.91$) of digestion. No correlation was found between wall density and protein digestion for intact TVPs and patties. We conclude that pore-related rather than wall-related TVP properties dominated protein digestion of TVPs and patties. Larger macroscopic surface area and larger mean pore size contributed more to accelerating protein hydrolysis during digestion of TVPs and TVP-based patties than smaller wall density. These results suggest that altering TVP microstructure could potentially be a way to enhance protein digestibility of plant-based meat analogues.

4.1. Introduction

Sufficient protein intake in the daily diet is important to maintain and promote human health. Proteins in foods undergo a complex digestion process and are eventually absorbed as free amino acids, which are crucial for protein synthesis and other metabolic processes (Capuano & Janssen, 2021). Nowadays, conventional animal-based proteins are increasingly being replaced by proteins from other sources, especially plants, due to their contribution to greenhouse gas emissions, land and water use, and environmental pollution. Plant-based meat analogues have been developed, with the aim to mimic the texture and flavor of meat or meat products (Baune et al., 2022; Imran & Liyan, 2023), which contributes to the transition towards plant-based dietary patterns. However, plant-based proteins are known to have lower protein quality and digestibility compared to animal-based proteins, due to their unbalanced amino acid profile and the presence of antinutritional factors (Gorissen et al., 2018; Kaur et al., 2022; Sá et al., 2020a; Xie et al., 2022). Understanding and improving protein digestibility recently gained more attention as a result of the development of plant-based meat analogues (Sá et al., 2020a).

After the macroscopic structural breakdown of solid foods during the oral phase, food boli pass through the esophagus to the stomach. The enzymatic digestion of food proteins starts in the stomach. Acidic gastric juice facilitates the hydrolysis of peptide bonds by pepsins, initiating the breakdown of proteins. After gastric digestion, polypeptides are further hydrolyzed by trypsin and chymotrypsin in the small intestine into absorbable, small peptides and free amino acids (Capuano & Janssen, 2021; Kong & Singh, 2008b). Gastric protein digestion is influenced by food micro- and macrostructure (Chapter 2 and 3; Barbé et al., 2013; Zhang et al., 2023a; Zhao et al., 2020). For example, Zhang et al. (2023a) showed that the loose and fragmentary microstructure of myofibrillar protein gels was strengthened by the addition of carboxymethylated cellulose nanofibrils, forming a denser and porous structure. Both the denser structure and harder texture contributed to the decrease in *in vitro* gastric protein hydrolysis (Zhang et al., 2023a). Similar results were observed in soy protein gels. *In vitro* gastric digestion was hindered by modifying the gel microstructure from a coarse and loose structure to a dense ordered porous structure (Zhao et al., 2020). We reported previously that whey protein isolate/polysaccharides mixed gels with similar macrostructures and mechanical properties but differing in microstructure showed differences in protein

digestion (Chapter 2). Mixed gels with a homogeneous microstructure showed a less aggregated protein network, facilitating the proteolysis during *in vitro* gastric protein digestion, whereas gels with a heterogeneous microstructure with an aggregated protein phase showed slower protein digestion (Chapter 2). The impact of macrostructure on gastric protein digestion is attributed to the differences in the total surface area of food and food boli (Chapter 2; Mennah-Govela & Bornhorst, 2021). Large whey protein gel cubes, with a small total surface area, showed lower degree of protein hydrolysis after the *in vitro* gastric digestion than small gel cubes, with a larger total surface area (Mennah-Govela & Bornhorst, 2021). The impact of surface area has also been shown to be related to the specific microstructure of the gels. After cutting a large gel cylinder into many, small cubes, the *in vitro* gastric protein digestion rate of whey protein gels increased the most in gels with a bi-continuous microstructure (2.5-fold) followed by gels with protein continuous (2.0-fold), coarse stranded (1.8-fold) and homogeneous (1.8-fold) microstructure (Chapter 2).

Such differences in micro- and macrostructural properties are also present in textured vegetable proteins (TVPs), which provide meat-like texture in plant-based meat analogues (Baune et al., 2022; van Esbroeck et al., 2024). Extrusion technology is commonly used to produce TVPs (Baune et al., 2022). The shape, particle size, and structural properties, such as porosity, of TVPs can be varied by adjusting the composition and extrusion conditions during production (Brishti et al., 2021; Flory & Alavi, 2024; Jeon et al., 2023; Samard et al., 2019, 2021). The structure of TVPs strongly influences their functional properties and those of TVP-based meat analogues (Flory & Alavi, 2024; Samard et al., 2021; van Esbroeck et al., 2024). Van Esbroeck et al. (2024) characterized the microstructural properties (porosity, mean pore size, mean wall thickness, wall density, apparent density, absolute density, density-based porosity) water absorption capacity (WAC) and water holding capacity (WHC) of 13 commercial TVPs. They found that porosity was positively correlated with the maximum water absorption capacity and the water holding capacity of TVPs (van Esbroeck et al., 2024). In another study, TVPs with a compact structure and smaller internal pores showed higher bulk density and lower water holding capacity (Flory & Alavi, 2024). The structure of TVPs therefore influences the rehydration properties of TVPs, which has been related to the functional and sensory properties of TVP-based patties (Hong et al., 2022; Samard et al., 2021; van Esbroeck et al., 2024).

Although numerous studies have explored the structural properties of TVPs and functional properties of TVP-based patties, the nutritional quality of TVP-based meat analogues remains underexplored (Ishaq et al., 2022). A few studies suggested that the structure of TVPs may affect protein digestion (Azzollini et al., 2018; Lin et al., 2022; Wang et al., 2024). Wang et al. (2024) recently reported that the structure of low moisture TVPs made from soybean and/or pea protein influenced *in vitro* protein digestibility. TVPs made from a 1 : 1 mixture of soybean and pea protein showed a denser and more compact structure, resulting in lower free amino acid concentrations in digesta compared to TVPs made from soybean protein concentrate, which showed a loose and porous structure (Wang et al., 2024). Also the ratio of pore wall thickness to pore size has been shown to be negatively correlated with the *in vitro* protein digestibility for extruded wheat snacks enriched with mealworm powder (Azzollini et al., 2018). For textured wheat protein, the loose, fiber-like structure with large gaps was shown to contribute to higher *in vitro* protein digestibility, although this structure-driven impact could be neutralized by changes in protein molecular interactions after the addition of sodium tripolyphosphate (Lin et al., 2022, 2023). These studies demonstrate that the microstructure of TVPs influences *in vitro* protein digestion of TVPs. Most of these studies used qualitative visual comparisons of microstructure images to characterize the microstructural properties of the TVPs, rather than employing quantitative image analysis to characterize different structural features, such as surface area, porosity, pore size, wall thickness, and wall density. Consequently, there is limited quantitative information available on the relationships between structural properties of TVPs, such as pore size and wall density, and protein digestion of TVPs. Moreover, the studies above investigated the impact of TVP structure on the digestion of TVP itself, which typically needs to be mixed with other ingredients to make meat analogue products and cooked before being consumed and digested. The impact of structural properties of TVPs on the digestion of TVP-based products is not known yet. The interaction between TVPs and other ingredients, as well as the cooking process might affect the protein digestibility of TVP-based meat analogues in addition to the structure of TVPs. A thorough understanding of the impact of TVP structure on protein digestion of TVP-based meat analogues may provide valuable insights for improving the protein digestibility of plant-based meat analogues, benefiting the development of nutritious plant-based protein foods.

This study aims to explore the impact of structural properties (surface area, porosity, mean pore size, mean wall thickness, wall density, apparent density, absolute density, density-based porosity), water absorption and acid absorption of TVPs on the *in vitro* gastric protein digestion of TVPs and TVP-based patties. Eight commercial TVPs differing in structural properties from two protein sources (yellow pea and soybean) were used. The surface area reported in this study refers to the macroscopic surface area of TVPs. Porosity, mean pore size, mean wall thickness, wall density, apparent density, absolute density, density-based porosity represent the microscopic structural properties. As a control, TVPs were ground into fine powders to eliminate the porous structure of TVPs. We hypothesize that a) surface area, porosity, mean pore size, density-based porosity, water absorption capacity and acid absorption positively correlate with protein hydrolysis during *in vitro* gastric digestion of intact TVPs and TVP-based patties and b) mean wall thickness, wall density, apparent density and absolute density negatively correlate with protein hydrolysis during the *in vitro* gastric digestion of intact TVPs and TVP-based patties.

4.2. Materials and methods

4.2.1 Materials

Eight commercially available textured vegetable proteins (TVP) from three suppliers were used. Pea protein TVPs were obtained from Roquette Frères S.A (Lestrem, France). Soy granules (Soja Granulat) and soy strips (Soja Geschnetzeltes) were obtained from Vegafit (Deventer, The Netherlands). Soy Flakes and Soy Chunks XL from the VITATEX® range were kindly provided by GoodMills Innovation GmbH (Hamburg, Germany). The commercial name, supplier, sample code, source, and protein content are summarized in Supplementary Table 4.1. Methylcellulose (MC, viscosity at 2%: 4,000 mPas) was purchased from Sigma Aldrich (St. Louis, MO, USA). Pea protein isolate (PPI) (NUTRALYS® F85M) was obtained from Roquette Frères S.A., (Lestrem, France). Sunflower oil (Reddy, Vandemoortele Nederland BV, Zeewolde, The Netherlands) and sodium chloride were purchased from a local supermarket (Jumbo, Veghel, The Netherlands). Pepsin from porcine gastric mucosa and other chemicals were purchased from Sigma-Aldrich (St. Louis, USA).

4.2.2 Characterization of the structure properties of TVPs

The structural characteristics of TVP pieces have been previously reported by van Esbroeck et.al. (2024). In short, porosity, mean pore size, mean wall thickness and wall density were analyzed using X-ray microtomography (XRT) and image analysis (van Esbroeck et al., 2024). The apparent density, absolute density and density-based porosity were determined using a displacement method. These methods and the results of the characterization have been described in detail by van Esbroeck et al. (2024). The structural characteristics (porosity, mean pore size, mean wall thickness, wall density, apparent density, absolute density, density-based porosity) of the eight commercial TVPs used in this study (ROQ1, ROQ2, ROQ3, ROQ5, VEG1, VEG2, GIM1 and GMI2) are summarized in Table 4.1 and discussed briefly in section 4.3.1.1.

4.2.3 Sample preparation

Each TVP sample was prepared in three forms: powder, intact TVP and patty. Dry TVP particles were blended in a Thermomix (TM5, Vorwerk & Co. KG, Wuppertal, Germany) at high speed followed by sieving with a 2 mm sieve to obtain fine powders. The rationale for blending the dry TVP particles into powders was to remove macroscopic structural characteristics of the TVPs. Powders were rehydrated in water (TVP : water ratio of 1:2 based on weight) for 30 min and stirred every 10 min (VEG2 was rehydrated with 1.5 times its weight). Intact TVPs were rehydrated following the same process as the powders. For samples ROQ1, ROQ5, VEG1 and GMI1, rehydrated TVPs were ready for further analysis. For samples ROQ2, ROQ3, VEG2 and GMI2, rehydrated TVPs were blended in a Thermomix at a speed of 5 for 20 s to slightly reduce their size while maintaining their initial structure. Plant-based meat analogue patties were prepared from the rehydrated TVPs (60 w/w%), sun flower oil (15 w/w%), pea protein isolate (5 w/w%), methylcellulose (2 w/w%), NaCl (0.8 w/w%) and water (17.2 w/w%) following the process described previously by van Esbroeck et al. (2024). Briefly, rehydrated TVPs were first mixed with all dry ingredients for 1 min. Water was then added to the ingredients and mixed for 1 min followed by the addition of oil and mixing for 1 min. The patty batter was mixed for an additional minute and stored in a fridge overnight (4 ˚C). The patty batter was shaped into patties of 100 g using a patty shaper (diameter 70 mm; thickness 20 mm). The patties were placed individually in plastic

cooking bags from which air was removed and cooked for 1 h at 70˚C in a water bath. After cooling down to room temperature, the patties were cut into pieces and the TVP particles were gently separated with a spatula. All samples were freshly prepared and subjected to further analysis within 12 h.

4.2.4 Sample characterization

4.2.4.1 Surface area of TVP powder

Dynamic Vapour Sorption was used to determine the specific surface area of TVP powders (Young et al., 2005). Dry powder (5-10 mg) was placed in a hemispherical metal-coated quartz pan and loaded into a Discovery SA Dynamic Vapour Sorption (DVS) Analyser (TA instruments, New Castle, DA, USA). The Relative Humidity (RH) of the chamber was decreased to 0% within 60 min. Then, the RH was increased from 10% to 90% in 9 steps at constant temperature of 20°C. The criterion for increasing humidity was a weight change of the sample of less than 0.1% for 60 min. The sorption isotherm data were analyzed using TRIOS Software v5.6 (TA instruments, New Castle, DA, USA). The relative sample weight (%) was plotted against the RH. GAB analysis was applied over the range of 10-90% RH to determine the specific surface area (m^2/g). Measurements were performed in duplicate.

4.2.4.2 Surface area of rehydrated TVPs and patties

Two-dimensional image analysis was used to estimate the macroscopic surface area of rehydrated TVPs and patties (Chen et al., 2021). A small amount of sample weighing 1.3-3.0 g was placed in a petri dish (120 × 120 × 17 mm) and pieces were manually separated using a spatula. The dishes were scanned individually on a flatbed scanner (Canon CanoScan 9000 F MarkII) to capture high-resolution color images at 600 dpi against a black background. The captured images were analyzed using ImageJ software (version 1.52a, National Institutes of Health). The images were converted to 8-bit followed by adjusting the brightness/contrast and black/white threshold to generate binary images. The "Analyze Particles" function in ImageJ was used to quantify the surface area (mm^2) of each particle from a top view. The total surface area was then summed and normalized by the sample weight, providing the specific surface area (mm^2/g) of rehydrated TVPs or particles separated from the patty. To reduce noise, particles smaller than the smallest visible particles among each sample or with a circularity below specific levels depending on the particle shape were excluded

(Supplementary Table 4.2). Two measurements were taken for each petri dish and averaged. For each sample, five replicates were taken, and the results were averaged.

4.2.4.3 Water absorption capacity of rehydrated TVPs at pH 2

The water absorption capacity of rehydrated TVPs at pH 2 in simulated gastric fluid (SGF) was determined in duplicate using the method described by van Esbroeck et al. (2024) with modifications. Approximately 20 g of rehydrated TVPs was submerged in 500 mL SGF (containing 25 mmol/L $NaHCO_3$ and 47.2 mmol/L NaCl, pH=2). At time 1, 2, 5, 10, and 20 min, the sample was poured through a sieve with a 2 mm mesh, drained and the obtained TVP was weighed, after which it was put back into the SGF. After 30 min, the samples was again poured through the sieve, after which the TVPs were drained and weighed without putting them back in the SGF. Around 90 g of remaining SGF was transferred to a tray and dried in an oven (Binder MDL 115, Keison products, Chelmsford, UK) at 105˚C to obtain the sample loss on dry matter during the measurement. The initial mass of the sample was corrected by the sample loss and dry matter content of rehydrated TVPs using:

$$corrected\ m_0 = m_0 - \frac{\frac{m_{(after)} \times m_{(SGF)}}{m_{(before)}}}{\text{dry matter content of rehydrated TVPs}} \quad (1)$$

where m_0 is the initial measured mass of sample; $m_{(before)}$ is the weight of SGF before drying; $m_{(after)}$ is the weight of dry matter of the SGF after drying; $m_{(SGF)}$ is the total mass of SGF after 30-min test; dry matter content of rehydrated TVPs is 33% (40% for VEG2).

The water absorption (WA) of rehydrated TVPs at pH 2 was calculated as:

$$WA\ (\%) = \frac{m_{(t)} - correcte\ \ m_0}{corrected\ m_0} \times 100 \quad (2)$$

where $m_{(t)}$ is the measured mass of samples at certain time point. The water absorption capacity (WAC) is defined as the water absorption after 30 min.

4.2.5 In vitro gastric protein digestion of rehydrated TVP powders, rehydrated intact TVPs and patties

The *in vitro* gastric protein digestion was performed following the INFOGEST 2.0 protocol with minor modifications (Brodkorb et al., 2019). Three grams of rehydrated TVP powder, rehydrated TVP or patties were immersed in 30 mL of SGF (containing 25 mmol/L $NaHCO_3$,

47.2 mmol/L NaCl and 2000 U/mL pepsin, pH = 2) for 2 h at 37˚C under continuous gentle stirring. The pH of gastric juice was kept constant at 2 by titrating with a 1 M HCl solution using an automated titrator. The amount of added acid was recorded over time to represent acid consumption (mmol) during digestion. Small amounts (100 µL) of liquid were taken at time 5, 30, 60 and 120 min followed by dilution with SGF without pepsin. The diluted mixtures were heated at 90˚C for 5 min while mixing to deactivate pepsin. After cooling down to room temperature, samples were stored at 4-5˚C for further analysis.

Additionally, all samples were subjected to the *in vitro* gastric protein digestion protocol as described above but in the absence of pepsin (blank digestion) to detect the free amino groups present in gastric juice while only incubating samples under *in vitro* gastric digestion condition. The free amino group concentration at 0 min was determined in addition to that at 5, 30, 60 and 120 min. The amount of added acid during blank digestion was monitored to represent the acid absorption (mmol) of samples under *in vitro* gastric protein digestion condition.

The o-phthaldialdehyde (OPA) method (Nielsen et al., 2001) was applied to quantify the free amino group concentration in gastric juice over time. Briefly, the mixtures of 10 µL sample solution and 200 µL OPA reagent in 96-plate wells were shaken for 3 min in a microplate photometer (Thermo Scientific 357, USA). The absorption of mixed solutions at 340 nm was determined immediately after shaking. A calibration curve made with serine standard solutions (0-200 mg/mL) was used to convert the absorption values to free amino group concentrations. All measurements were done in triplicate. The measured free amino group concentrations in gastric juice during digestion were corrected for the free amino group concentrations present in SGF without pepsin. The corrected free amino group concentrations during digestion is reported in the results section to indicate protein hydrolysis during *in vitro* gastric protein digestion.

4.2.6 Data analysis

The data of surface area, WAC at pH 2, acid consumption during digestion and acid absorption in absence of pepsin were analyzed using one-way analysis of variance (ANOVA) followed by a Tukey's HSD post-hoc test using SPSS statistics software (IBM SPSS Statistics Version 28, IBM Corp). Statistical significance was determined at a threshold of $p = 0.05$.

Results are presented as means with standard deviations. The measured free amino group concentration during blank digestion (in absence of pepsin) was subtracted from the measured free amino group concentration during *in vitro* gastric protein digestion (in presence of pepsin) based on mean values to estimate the free amino groups released as a result of proteolysis. Two-tailed Pearson correlation analysis was performed using SPSS statistics software (IBM SPSS Statistics Version 28, IBM Corp) based on mean values to obtain the correlation coefficients between the structural properties of TVPs (surface area, porosity, mean pore size, mean wall thickness, wall density, apparent density, absolute density, density-based porosity WAC, WAC at pH 2, acid consumption during digestion, acid absorption in absence of pepsin) and the corrected (and measured) free amino group concentrations during digestion. Scatter plots of corrected free amino group concentration during digestion against sample characteristics and linear regressions were obtained by running a Python code in Visual Studio Code (Microsoft Corp.)

4.3. Results and Discussion

4.3.1 Sample characterization

4.3.1.1 Structural properties of TVPs

The two-dimensional image slices of the microstructure of the eight TVPs are shown in Supplementary Figure 4.1 (images are reproduced from van Esbroeck et al., 2024). Table 4.1 summarizes the structural features (porosity, mean pore size, mean wall thickness, wall density, apparent density, absolute density, density-based porosity) of the eight TVPs (reproduced from van Esbroeck et al., 2024). The porosity of TVPs determined by XRT ranged from 27 to 81%, mean pore size from 251 to 4790 µm, mean wall thickness from 108 to 657 µm, wall density from 597 to 1515 $kg \cdot m^{-3}$, and apparent density from 205 to 1042 $kg \cdot m^{-3}$ showing that the TVPs differed substantially in structural features. This can be attributed to the properties of the raw materials and the different extrusion conditions resulting in different expansion ratios and consequently different structures. For some TVPs (ROQ3, GMI1 and GMI2), the XRT-based porosity and density-based porosity deviated considerably from each other, which was related to the wall density of the TVP (van Esbroeck et al., 2024).

Table 4.1. *Characteristics of eight commercial TVPs: XRT-based porosity (Φ_{XRT}), mean pore size (MPS), mean wall thickness (MWT), wall density (ρ_{wall}) as obtained from XRT measurements; apparent density (ρ_{app}), absolute density (ρ_{abs}) and density-based porosity ($\Phi_{density}$) from density measurements.*

TVP type	XRT				Density measurements		
	Φ_{XRT} (%)	MPS (µm)	MWT (µm)	ρ_{wall} (kg·m^{-3})	ρ_{app} (kg·m^{-3})	ρ_{abs} (kg·m^{-3})	$\Phi_{density}$ (%)
ROQ1	63.8 ± 11.6^{cd}	526 ± 138^{ab}	239 ± 5^{abc}	1379 ± 462^{c}	500 ± 51^{def}	1303 ± 4^{b}	60.3 ± 3.9^{bcd}
ROQ2	80.9 ± 1.9^{d}	1921 ± 661^{c}	196 ± 64^{ab}	1298 ± 139^{abc}	248 ± 8^{a}	1298 ± 1^{b}	78.0 ± 0.6^{ef}
ROQ3	65.7 ± 20.8^{cd}	3152 ± 1135^{bc}	108 ± 9^{a}	597 ± 362^{a}	205 ± 8^{a}	1294 ± 4^{b}	81.4 ± 0.7^{f}
ROQ5	57.7 ± 3.0^{bcd}	559 ± 77^{ab}	266 ± 26^{abc}	1036 ± 186^{abc}	438 ± 72^{bcde}	1307 ± 7^{b}	65.8 ± 5.5^{bcdef}
VEG1	27.1 ± 1.4^{a}	251 ± 257^{a}	287 ± 7de	1429 ± 159^{c}	1042 ± 114^{g}	1364 ± 3^{d}	22.8 ± 8.4^{a}
VEG2	32.0 ± 4.7^{a}	2817 ± 629^{d}	657 ± 104^{f}	1515 ± 113^{c}	1031 ± 30^{g}	1375 ± 3^{d}	24.0 ± 2.2^{a}
GMI1	39.8 ± 2.9^{ab}	554 ± 82^{ab}	219 ± 15^{abcd}	973 ± 91^{abc}	586 ± 47^{ef}	1406 ± 9^{e}	58.4 ± 3.4^{bc}
GMI2	64.9 ± 1.7^{cd}	4790 ± 1726^{d}	220 ± 6^{abcd}	888 ± 201^{abc}	312 ± 69^{abc}	1380 ± 1^{d}	77.9 ± 5.0^{ef}

Note: Means are reported with standard deviation. Means sharing superscript letters are not significantly different ($p > 0.05$). Table is adapted from van Esbroeck et al. (2024).

4.3.1.2 Surface area, water absorption and acid absorption of rehydrated TVP powders, rehydrated intact TVPs and patties

For all samples, the surface area of powders was more than four orders of magnitude larger than that of intact TVPs and patties (Table 4.2). The surface area of intact TVPs and patties ranged from 558-1740 mm^2/g and 561-1226 mm^2/g, respectively, whereas the surface area of the TVP powders ranged from 164-231 m^2/g. The water absorption of rehydrated intact TVPs at pH 2 was given at 30 min of incubation (Table 4.2), even though it barely changed anymore after the first minute (Supplementary Figure 4.2). The WAC of dry TVPs at neutral pH reported by van Esbroeck et al. (2024) is also provided. As expected, the WAC of rehydrated TVPs at pH 2 was lower than that of dry TVPs due to their higher water content.

The acid absorption of samples in SGF without pepsin is shown in Table 4.2. The acid absorption of rehydrated TVP powders occurred rapidly during the first 5 min (0.95-1.36 mmol) and then leveled off (Supplementary Figure 4.3a). Compared to TVP powders, the acid absorption of intact TVPs was slower during the first 5 min and showed larger differences among samples (0.60-1.18 mmol). The slower acid absorption during the first 5 min of intact TVPs compared to the TVP powders can be attributed to the presence of a porous structure and the much smaller surface area. The acid absorption at the end of incubation (120 min) are listed in Table 4.2. Patties showed the most difference between 5 and 120 min, indicating a more gradual, i.e. slower, acid absorption than that of powders and TVPs (Supplementary Figure 4.3c). In addition, patties also showed the least acid absorption after 120 min, whereas powder showed the most. The slower and lower acid absorption of patties might be related to the addition of other ingredients to the patty, such as sunflower oil, which might have affected the diffusion of acids to the TVPs.

Table 4.2. *Surface area, water absorption capacity (WAC) after 30 min incubation of dry TVP, WAC at pH 2 after 30 min incubation of rehydrated TVP and acid absorption properties of rehydrated TVP powders, rehydrated TVPs and TVP patties at 5 min and 120 min.*

	Surface area†			**WAC (%)***	**WAC (%) at pH2**	**Acid absorption (mmol) at 5 min without pepsin**			**Acid absorption (mmol) at 120 min without pepsin**		
	powder (m^2/g)	TVP (mm^2/g)	patty (mm^2/g)	dry TVP	TVP	powder	TVP	patty	powder	TVP	patty
ROQ1	231 ± 3^{d}	809 ± 27^{b}	656 ± 25^{a}	397 ± 6^{c}	113 ± 11^{a}	1.10 ± 0.08^{abc}	0.63 ± 0.04^{ab}	0.41 ± 0.16^{ab}	1.18 ± 0.1	1.41 ± 0.55	0.99 ± 0.12^{ab}
ROQ2	183 ± 0^{ab}	1140 ± 97^{de}	837 ± 99^{b}	336 ± 4^{b}	161 ± 27^{ab}	1.10 ± 0.07^{abc}	0.78 ± 0.16^{ab}	0.40 ± 0.21^{ab}	1.18 ± 0.02	1.14 ± 0.1	0.98 ± 0.15^{ab}
ROQ3	223 ± 2^{cd}	1164 ± 51^{e}	1055 ± 54^{d}	709 ± 7^{e}	336 ± 96^{b}	1.12 ± 0.08^{abcd}	0.90 ± 0.05^{bc}	0.60 ± 0.09^{ab}	1.31 ± 0.2	1.20 ± 0.08	1.03 ± 0^{ab}
ROQ5	202 ± 2^{bc}	1040 ± 31^{cd}	900 ± 38^{bc}	488 ± 16^{d}	128 ± 17^{a}	0.95 ± 0.08^{a}	0.75 ± 0.07^{ab}	0.35 ± 0.07^{ab}	1.10 ± 0.14	1.14 ± 0.02	0.89 ± 0.07^{a}
VEG1	167 ± 1^{a}	988 ± 42^{c}	811 ± 49^{b}	401 ± 2^{c}	116 ± 7^{a}	1.33 ± 0.04^{cde}	0.89 ± 0.05^{abc}	0.56 ± 0.03^{ab}	1.38 ± 0.03	1.29 ± 0.06	1.12 ± 0.02^{ab}
VEG2	181 ± 11^{a}	1294 ± 43^{f}	1011 ± 59^{cd}	134 ± 6^{a}	191 ± 63^{ab}	1.34 ± 0.02^{de}	1.12 ± 0.04^{c}	0.83 ± 0.12^{bc}	1.40 ± 0.03	1.52 ± 0.05	1.29 ± 0.12^{b}
GMI1	179 ± 0^{a}	558 ± 16^{a}	561 ± 36^{a}	298 ± 28^{b}	120 ± 12^{a}	1.36 ± 0.04^{e}	0.60 ± 0.08^{a}	0.56 ± 0.02^{ab}	1.37 ± 0.03	1.27 ± 0.07	1.14 ± 0.03^{ab}
GMI2	164 ± 10^{a}	1740 ± 97^{g}	1226 ± 54^{e}	533 ± 3^{d}	247 ± 42^{ab}	1.28 ± 0.04^{bcde}	1.18 ± 0.03^{c}	1.22 ± 0.01^{c}	1.29 ± 0.06	1.31 ± 0.03	1.28 ± 0.01^{b}

*Note: Data (mean ± SD, n = 5 for the surface area of TVP and patty, n = 2 for other measurements) with different superscript letters in a column are significantly different ($p < 0.05$). †The surface areas of dry TVP powders include the microscopic surface area caused by potential nanopores presented in power particles, whereas the surface areas of rehydrated TVPs and patties only represent the macroscopic surface area determined based on 2D images. *data reported by van Esbroeck et al. (2024).*

4.3.2 In vitro gastric protein digestion of rehydrated TVP powders, rehydrated intact TVPs and TVP patties

The corrected free amino group concentrations in gastric juice during *in vitro* gastric protein digestion of rehydrated TVP powders, rehydrated intact TVPs and TVP patties are shown in Figure 4.1. Generally, TVP powders showed higher free amino group concentrations during the first 30 min of *in vitro* gastric protein digestion than intact TVPs and patties, indicating a faster protein hydrolysis at the beginning of digestion for powders compared to TVPs and patties. This was attributed to the much larger surface area (four orders of magnitude) of TVP powders compared to that of TVPs and patties (Table 4.2).

The eight samples were divided into two groups depending on protein source to allow for comparison of the effect of structure on protein hydrolysis independent of protein type. Figure 4.1a-c represent results for yellow pea protein, whereas Figure 4.1d-f shows results for soy protein. For yellow pea, the powders of ROQ2, ROQ3 and ROQ5 displayed similar free amino group concentrations during digestion, while ROQ1 showed the lowest free amino group concentrations (Figure 4.1a). Similar trends were observed for the intact TVPs (Figure 4.1b), although the differences between ROQ1 and other samples were larger. Surprisingly, differences in protein hydrolysis among ROQ2, ROQ3 and ROQ5 were observed in patties, where ROQ3 showed the highest free amino group concentrations during digestion (Figure 4.1c). For soybean samples, GMI1 and GMI2 powders exhibited similar free amino group concentrations during digestion, as did VEG1 and VEG2 except at 60 min. Generally, GMI powders had higher free amino group concentrations than VEG powders (Figure 4.1d). Such a trend was not displayed for the intact rehydrated TVPs, as GMI1 showed the lowest free amino group concentrations instead of the VEG samples, although GMI2 still showed the highest concentrations. VEG1 and VEG2 still displayed a similar evolution of the free amino group concentrations (Figure 4.1e). For patties, the four curves became more separated than the curves of TVP powders and intact TVPs (Figure 4.1f). Specifically, the difference between GMI1 and GMI2 observed for intact TVPs was sustained for patties. Unlike powders and TVPs, VEG2 patties exhibited clearly higher free amino group concentrations than VEG1 patties.

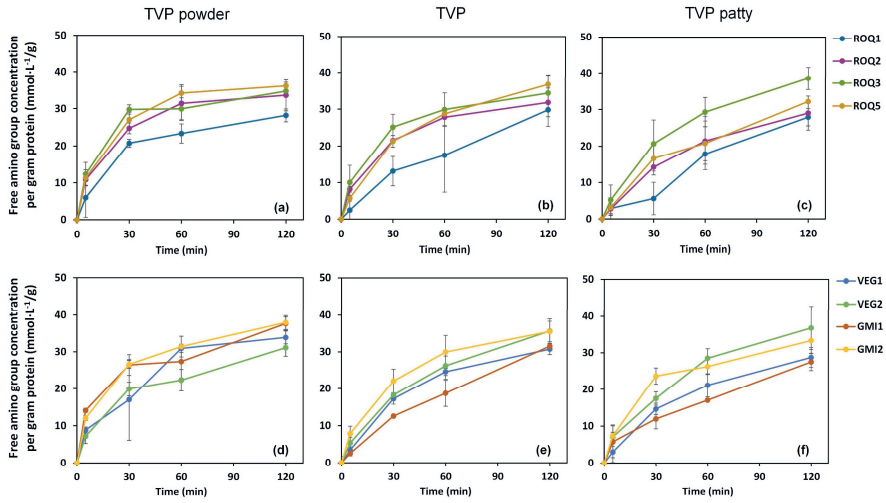

Figure 4.1. *Free amino group concentration per gram protein in gastric juice during in vitro gastric protein digestion of rehydrated TVP powders, TVPs (rehydrated and intact), and TVP patties (corrected for the free amino groups presented in SGF without pepsin). First row: yellow pea; second row: soybean. Error bars denote standard deviations (n = 2).*

The observed differences in protein digestion between TVP powders of the same protein source could be attributed to various reasons, such as differences in composition or extrusion processing techniques applied by different producers (e.g., VEGs and GMIs). It is reported that the digestibility of plant proteins can be affected by fractionation methods, processing conditions and interactions with other components (Del Rio et al., 2022; Sá et al., 2020a). Additionally, differences in wall density between TVP powders (van Esbroeck et al., 2024) potentially affected the protein digestion of powders. For TVPs and patties, the differences in protein hydrolysis could be due to multiple factors, such as surface area, structural properties, water and acid absorption capacity (Deng et al., 2020; Luo et al., 2017, 2018). The impact of these factors on protein hydrolysis during *in vitro* gastric digestion of rehydrated TVP powders, rehydrated intact TVPs and patties is further analyzed and discussed in the following section.

4.3.3 Impact of structural properties, water absorption and acid absorption on in vitro gastric protein digestion of TVP powders, intact TVPs and patties

4.3.3.1 Surface area

For TVP powders, no significant correlations between surface area and protein hydrolysis were observed (Figure 4.2a). This was attributed to the relatively limited variability in surface

area (164-231 m^2/g) between TVP powders. Significant positive correlations between surface area and corrected free amino group concentrations were found during the digestion of rehydrated intact TVPs at 60 min ($p = 0.022$) (Figure 4.2b). This result is consistent with previous studies which reported that an increase in surface area of protein gels strongly promoted *in vitro* gastric protein digestion (Chapter 2; Guo et al., 2015; Markussen et al., 2021). Interestingly, these significant correlations were also found during the digestion of patties at 30 min ($p = 0.002$), 60 min ($p = 0.005$) and 120 min ($p = 0.022$) (Figure 4.2c). This result indicates that the addition of other ingredients and the cooking process during patty preparation did not change the fact that increasing surface area of food particles facilitated protein hydrolysis. It should be mentioned that, for rehydrated intact TVPs and patties, the microscopic surface area provided by pores in the microstructure of TVPs is not considered here, but is discussed in section 4.3.3.2.

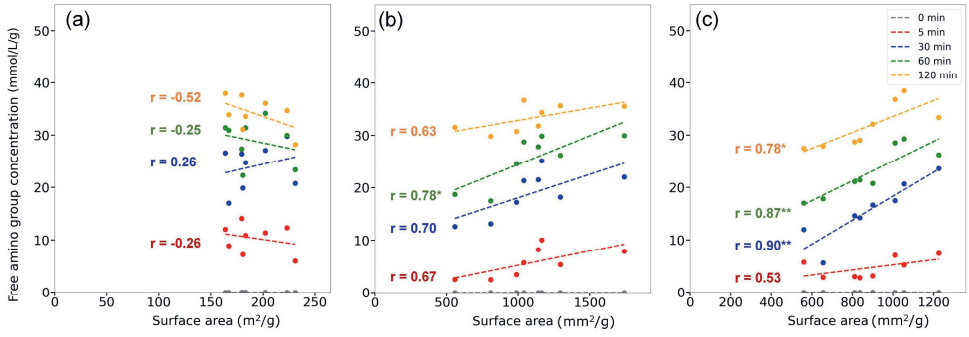

Figure 4.2. *Scatter plots of corrected free amino group concentrations during in vitro gastric protein digestion of (a) rehydrated TVP powders, (b) rehydrated intact TVPs and (c) TVP-based patties against the surface area of TVP powders, rehydrated TVPs and separated particles of TVP-based patties. r refers to the Pearson correlation coefficient. *Correlation is significant at the 0.05 level (2-tailed); **. Correlation is significant at the 0.01 level (2-tailed).*

4.3.3.2 Mean pore size and XRT-based porosity

There were no significant correlations between mean pore size and corrected free amino group concentrations during the digestion of TVP powders (Figure 4.3a). This was expected, as the porous structure of TVPs was removed by milling. For intact TVP, mean pore size was significantly and positively correlated with corrected free amino group concentrations during the digestion, with the highest correlation at 5 min ($p = 0.038$). Such a correlation was also seen for patties for 5 ($p = 0.038$), 30 ($p = 0.019$) and 60 min ($p = 0.016$) (Figure 4.3), where 60 min had the highest correlation.

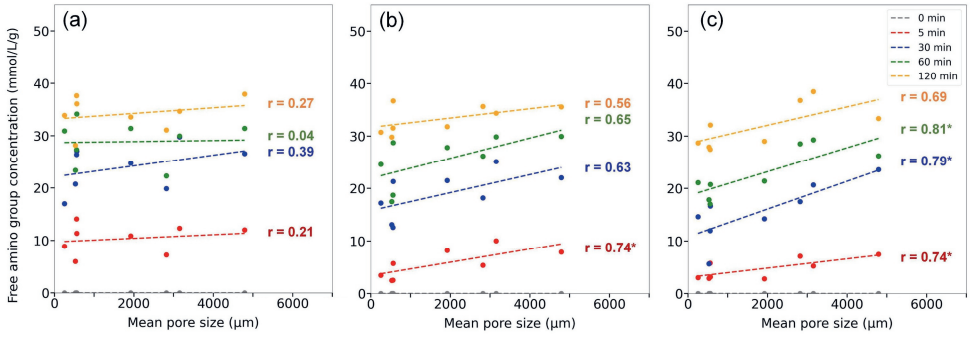

Figure 4.3. *Scatter plots of corrected free amino group concentrations during in vitro gastric protein digestion of (a) rehydrated TVP powders, (b) rehydrated TVPs and (c) TVP-based patties against the mean pore size measured by XRT of dry TVPs. r refers to the Pearson correlation coefficient. *Correlation is significant at the 0.05 level (2-tailed).*

This finding suggests that large pores in TVPs facilitated protein hydrolysis during the *in vitro* gastric digestion of rehydrated intact TVPs, and this impact of pore size on protein digestion persisted in TVP patties. This result is consistent with the result of Azzollini et al. (2018), who reported positive correlations between pore size and the *in vitro* protein and starch digestibility of extruded insect-enriched wheat snacks. It is noted that for TVPs with large mean pore size, they also exhibited large surface area after rehydration (Table 4.2). The significant positive correlations between mean pore size and corrected free amino group concentrations during the digestion of rehydrated TVPs and patties might partly be caused by the correlation between mean pore size and the surface area of rehydrated TVPs. Nevertheless, the impact of mean pore size on protein hydrolysis should not be disregarded. The correlations between structural properties and water or acid absorption shown in Supplementary Table 4.3 provide evidence for this point. Significant positive correlations were found between mean pore size and water absorption capacity of rehydrated TVPs at pH 2 ($r = 0.82$, $p = 0.013$), between mean pore size and acid absorption at 5 min of rehydrated TVPs ($r = 0.81$, $p = 0.014$) and patties ($r = 0.87$, $p = 0.011$), whereas no significant correlations were found between surface area and water absorption or acid absorption except the acid absorption at 5 min of rehydrated TVPs ($r = 0.91$, $p = 0.002$). These results imply that despite its correlation with surface area, large mean pore size could promote the protein hydrolysis of rehydrated TVPs and patties by increasing the water absorption capacity of TVPs at pH 2 and the acid absorption of TVPs and patties. In addition, large pore size could accelerate the diffusion of pepsin in TVP particles. Faster pepsin diffusion was observed in

dairy gels, egg white gels and myofibrillar protein gels with larger pore size, resulting in higher degree of protein hydrolysis (Luo et al., 2017; Somaratne et al., 2020b; Thévenot et al., 2017; Zhang et al., 2023a). For intact TVPs, the positive correlation between mean pore size and protein hydrolysis was significant only at 5 min (Figure 4.3b). This might be attributed to the structure disintegration caused by digestion. The delayed and prolonged impact of pore size on protein hydrolysis during the digestion of patties (Figure 4.3c) might be due to the addition of other ingredients such as sunflower oil, pea protein isolate, and methylcellulose. At the beginning of the digestion (the first 5 min), these ingredients might hinder the penetration and diffusion of pepsin into TVPs, as well as the acid absorption.

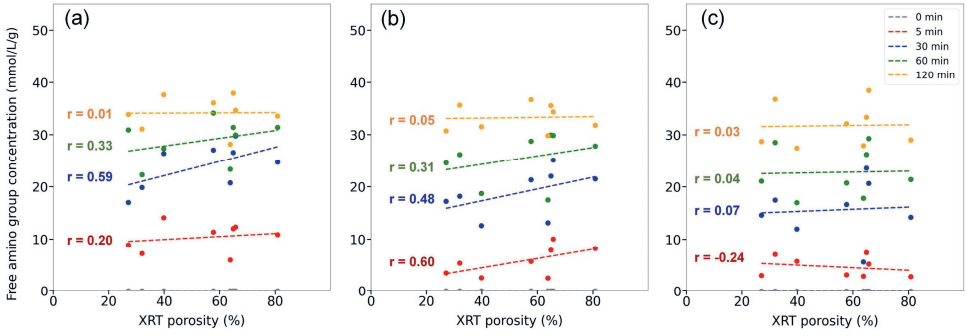

Figure 4.4. *Scatter plots of corrected free amino group concentrations during in vitro gastric protein digestion of (a) rehydrated TVP powders, (b) rehydrated TVPs and (c) TVP-based patties against the porosity measured by XRT of dry TVPs. r refers to the Pearson correlation coefficient.*

Porosity of TVPs measured by XRT did not significantly correlate with corrected free amino concentrations during the *in vitro* gastric digestion of rehydrated TVP powders, rehydrated intact TVPs and patties (Figure 4.4). The determination of XRT-based porosity was volume-based, while the determination of mean pore size was based on the detected distances between each air pixel and the nearest wall (van Esbroeck et al., 2024). Therefore, XRT-based porosity could be influenced by the volume of walls present in TVPs, while mean pore size depends purely on pore size. For example, ROQ1 and ROQ3 had similar XRT-based porosity (64% and 66%), but ROQ1 had a significantly smaller mean pore size (526 µm) than ROQ3 (1921 µm), which is in accordance with the XRT images showing more large pores in ROQ3 than in ROQ1 (Supplementary Figure 4.1). The porosity of TVPs measured by XRT thus contributed less to protein hydrolysis during *in vitro* gastric digestion of rehydrated TVPs and patties. TVP pore size promoted protein digestion more than TVP porosity.

4.3.3.3 Mean wall thickness and wall density

Mean wall thickness was not significantly correlated with the corrected free amino group concentrations (Supplementary Table 4.4), which was attributed to the extremely large mean wall thickness of VEG2 and relatively small variability in mean wall thickness of all other samples (Table 4.1). Wall density was negatively correlated with the corrected free amino group concentrations during the *in vitro* gastric digestion of TVP powders at 5 min ($p = 0.021$) and 30 min ($p = 0.002$) (Figure 4.5a). This could explain the differences in corrected free amino group concentrations among TVP powders (Figure 4.1). Even though TVPs were ground into fine powders, differences in wall density of TVPs might still be present. Higher wall density suggests a more compact and dense protein network, which hinders the diffusion of pepsins in the protein network of TVPs, resulting in less protein hydrolysis. The resistance of a dense protein network to protein hydrolysis was also found in whey protein and myofibrillar protein gels (Chapter 2; Singh et al., 2014; Zhang et al., 2023a). Gels with a heterogeneous microstructure were digested slower than those with a homogeneous microstructure, which was attributed to the dense protein aggregates in the protein-rich phase. However, the negative correlations between wall density and corrected free amino group concentrations were not significant ($p > 0.05$) for intact TVPs and patties (Figure 4.5). This may suggest that, when porous structures are present in the TVPs, pore size, rather than wall density, is the primary structural property determining protein hydrolysis during the digestion of TVPs and TVP-based patties. This could be because pore size contributes to the protein hydrolysis at the microscopic surface of TVPs, whereas wall density affects the diffusion of pepsins inside the walls. Once pepsin reaches the pores, protein hydrolysis starts from the surface of solid materials (walls, in case of TVPs), which was also reported for whey protein gels during *in vitro* gastric protein digestion (Deng et al., 2020; Luo et al., 2017). Furthermore, the disintegration of whey protein gels was shown to be dominated by surface erosion (Guo et al., 2015). The *in vitro* gastric protein digestion of TVPs seemingly followed a similar disintegration mechanism as for the whey protein gels. As discussed before, large pores in TVPs could accelerate the dispersing of pepsin between walls and enhance the absorption of water and acid, boosting the protein hydrolysis and the erosion at the microscopic surface of TVPs (the surface of walls in TVPs). Therefore, wall density, which influences the diffusion of pepsins inside walls rather than the protein hydrolysis at the wall surface, contributed less to the protein digestion of intact TVPs and TVP-based patties than pore size.

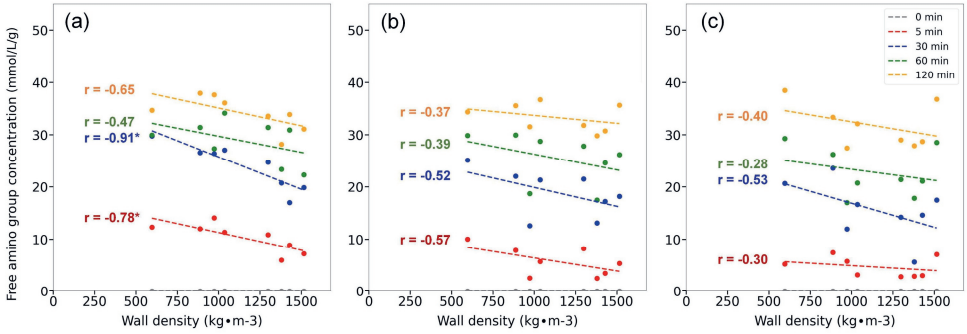

Figure 4.5. *Scatter plots of corrected free amino group concentrations during in vitro gastric protein digestion of (a) rehydrated TVP powders, (b) rehydrated TVPs and (c) TVP-based patties against the wall density of dry TVPs. r refers to the Pearson correlation coefficient. *Correlation is significant at the 0.05 level (2-tailed).*

4.3.3.4 Apparent density, absolute density and density-based porosity

Apparent density, absolute density and density-based porosity were not correlated with the corrected free amino group concentrations during *in vitro* gastric protein digestion of TVPs and patties (Supplementary Table 4.4). However, when VEG1 and VEG2, which had very low density-based porosity and very high apparent density (Table 4.1), were excluded from the data set, significant negative correlations were found between apparent density and the protein hydrolysis of TVPs and patties (Figure 4.6, the top row). Correspondingly, positive correlations were found between density-based porosity and the protein hydrolysis of TVPs and patties (Figure 4.6, the bottom row). The fact that VEG1 and VEG2 were outliers could be attributed to variations in extrusion cooking, which may also have caused the obvious darker color of the TVPs (Supplementary Table 4.1). These high correlations without VEG samples indicate that density-based porosity and apparent density were positively and negatively correlated with protein hydrolysis during the *in vitro* gastric digestion of TVPs and TVP-based patties, respectively. These results are inconsistent with that of Lin et al. (2022, 2023) who reported larger extent of protein digestion during *in vitro* gastrointestinal digestion of textured wheat proteins (TWPs) with larger bulk density. The TWPs tested by Lin et al. displayed fibrous microstructure instead of a porous structure as shown in this study, which might be due to the variation in the moisture content during extrusion. The larger degree of protein digestion of TWPs was attributed to the finer fibers and greater exposure of hydrophobic groups in protein molecules with no explanation about the influence of bulk density (Lin et al., 2022, 2023). In this study, the apparent density of TVPs was positively

correlated with the wall thickness (r = 0.756, p = 0.030) and the wall density (r = 0.708, p = 0.050), and negatively correlated with the porosity measured by XRT (r = -0.920, p = 0.001) and, of course, the density-based porosity (r = -0.997, p < 0.001). Therefore, the impact of apparent density and density-based porosity can be seen as the combined effect of pores and walls of TVPs on protein hydrolysis during the digestion of intact TVPs and TVP-based patties. Regarding the exceptions of VEG1 and VEG2, further studies are needed to explore the impact of compact structures of TVPs on their gastric protein digestion, with consideration of extrusion conditions.

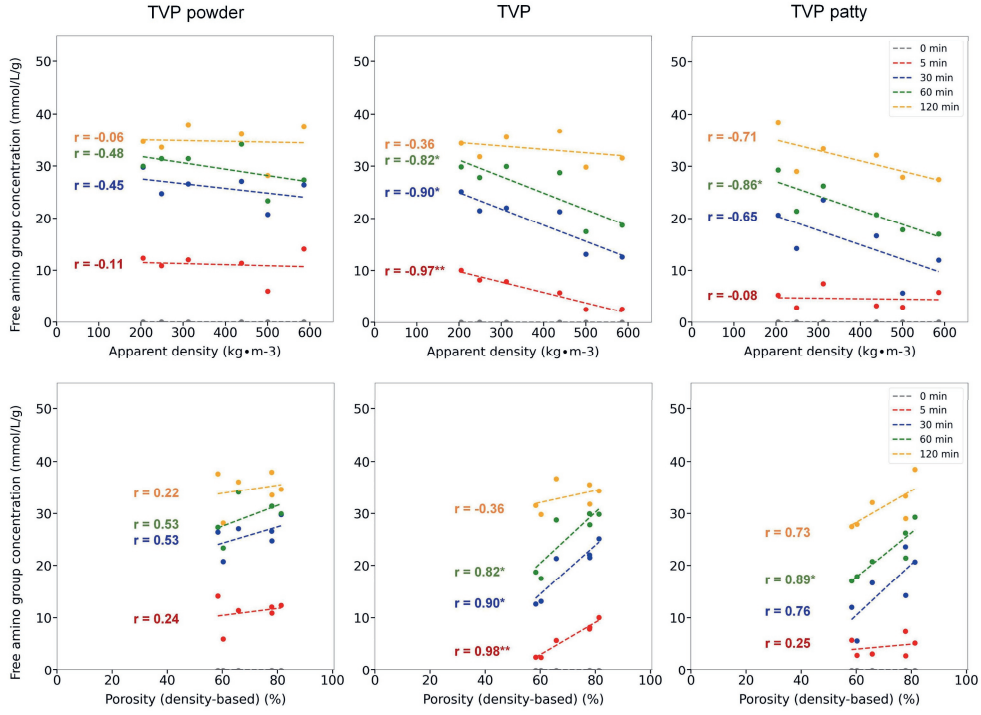

Figure 4.6. *Scatter plots of corrected free amino group concentrations during in vitro gastric protein digestion of rehydrated TVP powders, TVPs (rehydrated and intact), and TVP patties against the apparent density and density-based porosity of dry TVPs. Note: VEG1 and VEG2 are excluded. r refers to the Pearson correlation coefficient. *Correlation is significant at the 0.05 level (2-tailed). **Correlation is significant at the 0.01 level (2-tailed).*

4.3.3.5 Water absorption and acid absorption

As protein hydrolysis is expected to be related to the ease of water and acid uptake by samples during digestion, we evaluated the correlation between water absorption capacity and

corrected free amino group concentrations, as well as between acid absorption (with and without pepsin) and corrected free amino group concentrations (Supplementary Table 4.4).

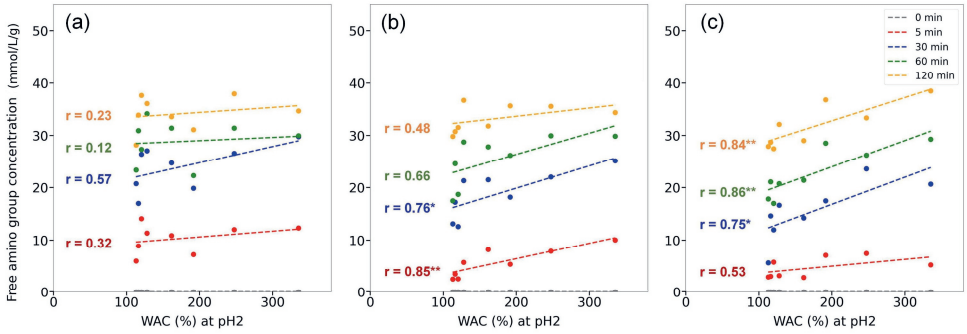

Figure 4.7. *Scatter plots of corrected free amino group concentrations during in vitro gastric protein digestion of (a) rehydrated TVP powders, (b) rehydrated TVPs and (c) TVP-based patties against the water absorption capacity at pH 2 of rehydrated TVP powders, rehydrated TVPs and separated particles of TVP-based patties. r refers to the Pearson correlation coefficient. *Correlation is significant at the 0.05 level (2-tailed); ** Correlation is significant at the 0.01 level (2-tailed).*

The WAC of rehydrated TVPs at pH 2 was positively correlated with the corrected free amino group concentrations during *in vitro* gastric digestion of intact TVPs and patties (Figure 4.7). These results confirm that increasing in WAC of rehydrated TVPs at pH 2 facilitated the protein hydrolysis during *in vitro* gastric digestion of TVPs and TVP-based patties. This is consistent with the results of Deng et al. (2020), who studied the impact of swelling on the *in vitro* gastric protein digestion of whey protein gels. They concluded that swelling, i.e. water absorption, increased the digestion rate of whey protein gels by enhancing acid diffusion and pepsin partitioning at the gel-liquid interface. In our study, we can observe that the impact of WAC at pH 2 in TVPs appeared larger during the first 30 min, whereas in patties, the impact became larger in the period between 30 and 120 min (higher correlations). This was most likely due to the presence of additional ingredients in the patties, such as fat, which might have hindered the accessibility of the porous structure to gastric juice in early stages of digestion. No correlation was found between WAC of dry TVPs at neutral pH and the corrected free amino group concentrations during digestion of TVP powders, TVPs and patties (Supplementary Table 4.4). This result suggests that the typical WAC of dry TVPs in water at neutral pH is less relevant to the digestibility of TVPs during gastric digestion. When the WAC of TVPs is manipulated in order to improve the digestibility of TVPs, WAC should

be determined under digestion conditions (in simulated gastric juice at pH 2 without pepsin) rather than in water at neutral pH.

Regarding acid absorption, positive correlations between acid absorption in the absence of pepsin and corrected free amino group concentrations were found for patties at 5 min of digestion (Supplementary Table 4.4). This indicates that the increased acid absorption capacity of TVP patties facilitated the protein hydrolysis of patties at the beginning of digestion. There were no significant correlations between acid absorption in the absence of pepsin and protein hydrolysis for intact TVPs (Supplementary Table 4.4). The acid consumption during digestion with pepsin also did not significantly correlate with the corrected free amino group concentrations during the digestion of intact TVPs. These results imply that despite the significant positive correlations between mean pore size and acid absorption (Supplementary Table 4.3), the increased acid absorption was not the dominant reason for promoted protein hydrolysis of TVPs with large pores. This finding supports our assumption in section 4.3.3.2 and section 4.3.3.3 that, apart from water and acid absorption, pepsin diffusion within TVP particles could also be affected by TVP structural properties, thereby influencing the protein hydrolysis during TVP digestion. Further studies exploring the impact of structural properties of TVPs on pepsin penetrating and diffusion during the protein digestion of TVP-based meat analogues could gain more insight into this aspect.

4.4. Conclusions

This study evaluated the impact of structural properties of texture vegetable proteins (TVPs) on the *in vitro* gastric protein digestion of TVPs and TVP-based patties in a quantitative way. We hypothesized that a) surface area, porosity, mean pore size and density-based porosity positively correlate with protein hydrolysis during *in vitro* gastric digestion of intact TVPs and TVP-based patties and b) mean wall thickness, wall density, apparent density and absolute density negatively correlate with protein hydrolysis during the *in vitro* gastric digestion of intact TVPs and TVP-based patties. The surface area, which represents the macrostructure of TVPs, and mean pore size, wall density, apparent density, density-based porosity as microscopic structural properties are relevant for the protein hydrolysis during *in vitro* gastric digestion of rehydrated TVPs and TVP-based patties. Other structural properties

including porosity measured by XRT, mean wall thickness and absolute density are less relevant. Increased macroscopic surface area, mean pore size and density-based porosity gave rise to faster protein hydrolysis during digestion of TVPs, whereas increased apparent density of TVPs slowed down protein hydrolysis. These correlations persisted for patties prepared from these TVPs by mixing them with other ingredients and cooking, although correlations were often more pronounced at later stages during digestion. It is worth noting that the negative correlation between wall density and protein hydrolysis was observed only when the porous structure of TVPs was removed. The lack of such correlations for intact TVP and patties suggests that the impact of microscopic structural properties on protein digestion of TVPs and patties was more dominated by pore-related TVP properties rather than wall-related TVP properties. Pores in TVPs influenced water absorption capacity at pH 2 and acid absorption, which influenced the protein digestion of TVPs and TVP-based patties. We suggest that for enhancing protein digestion of TVP-based meat analogues, increasing the pore size of TVPs with a porous structure and decreasing the wall density of TVPs with a compact structure should be considered in addition to increasing macroscopic surface area (i.e. reducing the particle size) of TVPs. Future studies should explore the relationships between structural properties and protein digestion of meat analogues made from TVPs with compact, fibrous microstructure taking extrusion conditions and pepsin diffusion into consideration.

4.5 Supplementary material

Supplementary Table 4.1. *Sample code (1), commercial name (2), supplier (3), source (4), and protein content according to the supplier (5) of the TVPs used in this study.*

TVP information	Picture of TVPs	TVP information	Picture of TVPs
1. ROQ1 2. Roquette Frères S.A 3. NUTRALYS® TP70G 4. Yellow pea 5. 68.8% protein	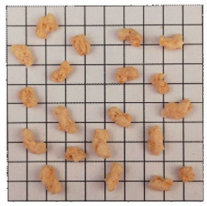	1. VEG1 2. Vegafit 3. Soja Granulat 4. Soybean 5. 63.5% protein	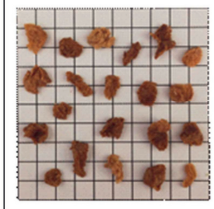
1. ROQ2 2. Roquette Frères S.A 3. NUTRALYS® T70S 4. Yellow pea 5. 68.9% protein		1. VEG2 2. Vegafit 3. Soja Geschnetzeltes 4. Soybean 5. 43.7% protein	
1. ROQ3 2. Roquette Frères S.A 3. NUTRALYS® TP-C 4. Yellow pea 5. 69.4% protein		1. GMI1 2. GoodMills Innovation GmbH 3. VITATEX® Soy Flakes 4. Soybean 5. 50.1% protein	
1. ROQ5 2. Roquette Frères S.A 3. NUTRALYS® TP65M 4. Yellow pea 5. 63.8% protein	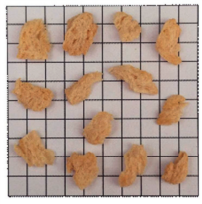	1. GMI2 2. GoodMills Innovation GmbH 3. VITATEX® Soy Chunks XL 4. Soybean 5. 47.9% protein	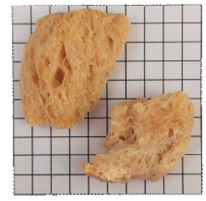

Note: Images are for TVP visualization and each square represents 5 mm. Adapted from Van Esbroeck et al. (2024).

Supplementary Table 4.2. *The setting for image analysis to recognize particles in binary images and exclude noise.*

	Sample	Size	Circularity
Intact rehydrated TVPs	ROQ1	0.04-infinity	0.2-1
	ROQ2	0.3-infinity	0.1-1
	ROQ3	0.05-infinity	0.1-1
	ROQ5	0.3-infinity	0.2-1
	VEG1	0.05-infinity	0.2-1
	VEG2	0.04-infinity	0.15-1
	GMI1	0.3-infinity	0.2-1
	GMI2	0.3-infinity	0.05-1
TVP-based patties	ROQ1	0.04-infinity	0.2-1
	ROQ2	0.03-infinity	0.2-1
	ROQ3	0.05-infinity	0.1-1
	ROQ5	0.05-infinity	0.2-1
	VEG1	0.05-infinity	0.2-1
	VEG2	0.05-infinity	0.15-1
	GMI1	0.05-infinity	0.2-1
	GMI2	0.05-infinity	0.1-1

Note: The minimum threshold of size is depending on the smallest visible particle size and the noise among each sample; the minimum threshold of circularity depended on the shape and the noise among each sample. Example images are shown in the following figure:

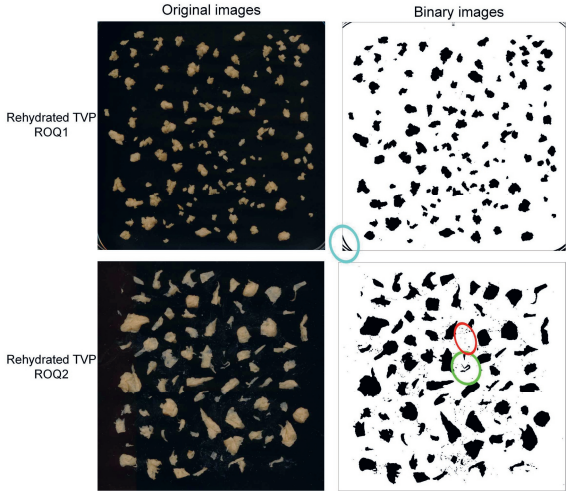

Examples of noise and irregular particle shape in binary images. Black dots in red circle represent noise from background; strip-like particle in green circle represents irregular particles. Strips in blue circle represent light reflection at the edge of petri dish.

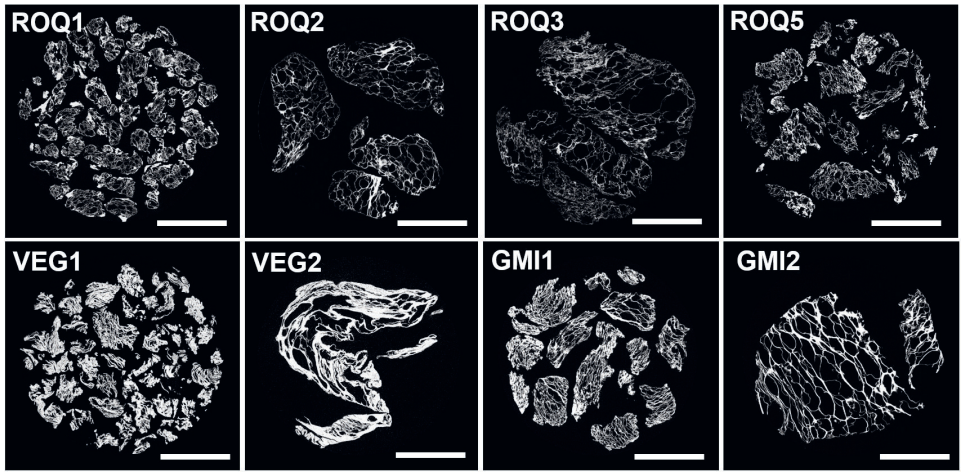

Supplementary Figure 4.1. *Two-dimensional slices of X-ray microtomography images of all eight TVP chunks. The white scale bars represent 10 mm. Bright and black areas represent solid material and air, respectively. Reproduced with permission from Van Esbroeck et al. (2024).*

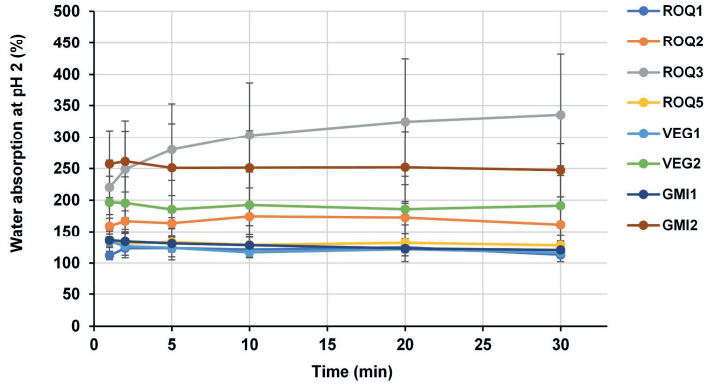

Supplementary Figure 4.2. *The water absorption of rehydrated TVPs at pH 2. Error bars denote standard deviation (n = 2).*

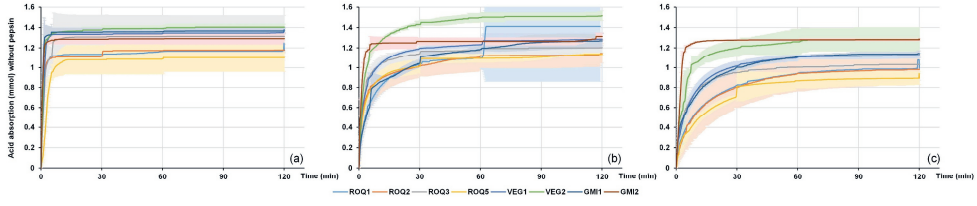

Supplementary Figure 4.3. *The acid absorption of (a) rehydrated TVP powders, (b) rehydrated TVPs and (c)patties under in vitro gastric protein digestion condition in absence of pepsin. Shadows around the lines denote standard deviation (n=2).*

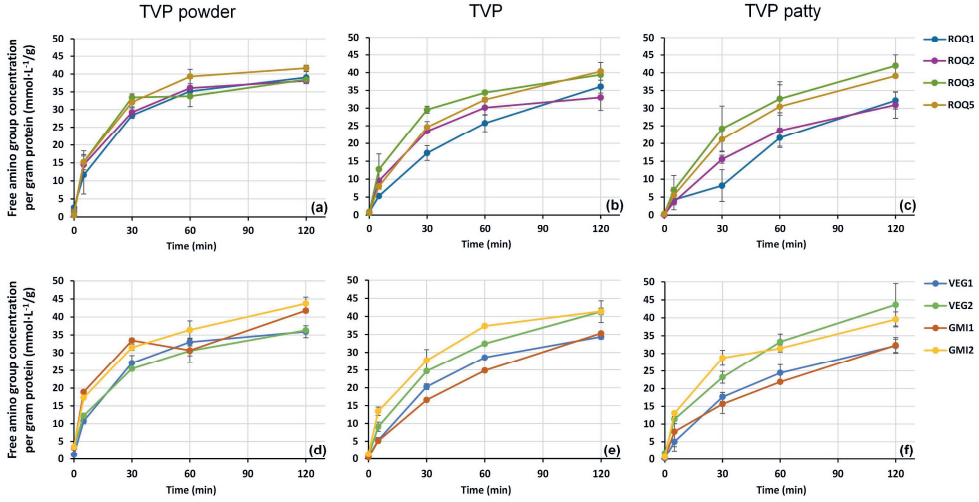

Supplementary Figure 4.4. *The measured free amino group concentration in gastric juice during in vitro gastric protein digestion of TVP powders, TVPs and TVP patties. First row: yellow pea; second row: soybean. Error bars denote standard deviations (n = 2).*

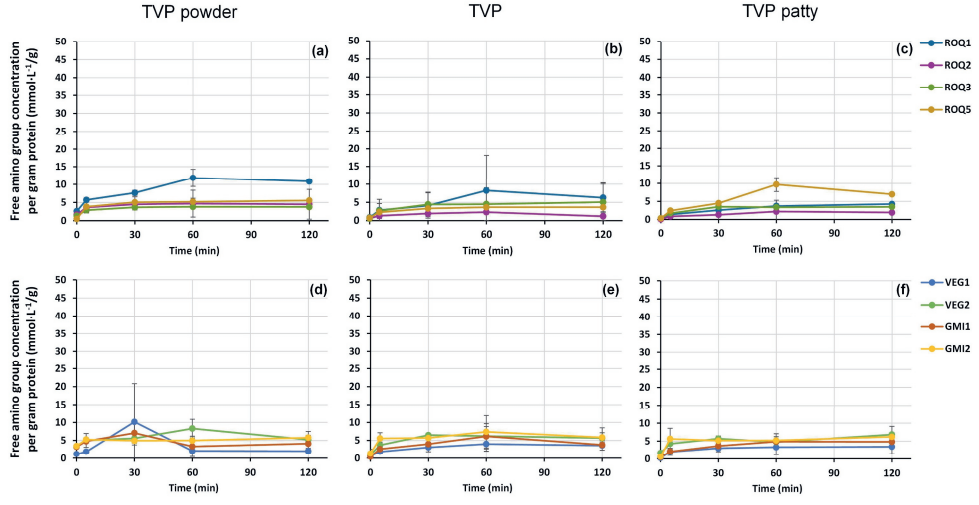

Supplementary Figure 4.5. *The free amino group concentration present in SGF without pepsin during in vitro gastric protein digestion of TVP powders, TVPs and TVP patties. First row: yellow pea; second row: soybean. Error bars denote standard deviations (n = 2).*

Supplementary Table 4.3. *The Pearson correlation coefficients between surface area, structural properties and the water and acid absorptions of rehydrated TVPs and TVP-based patties.*

	WAC (%)	WAC (%) at pH2	Acid absorption (%) at 5 min		Acid absorption (%) at 120 min	
	TVP	TVP	TVP	patty	TVP	patty
surface area	0.39	0.15	**0.91****	0.70	0.10	0.39
Φ_{XRT} (%)	0.48	0.34	-0.13	-0.13	-0.50	-0.48
MPS (µm)	0.28	**0.82***	**0.81***	**0.83***	0.15	0.57
MWT (µm)	**-0.77***	-0.20	0.44	0.25	**0.73***	0.52
ρ_{wall} (kg·m^{-3})	**-0.80***	-0.68	-0.02	-0.19	0.52	0.12
ρ_{app} (kg·m^{-3})	-0.66	-0.46	0.18	0.06	0.62	0.45
ρ_{abs} (kg·m^{-3})	-0.44	-0.40	0.22	0.51	0.49	0.65
$\Phi_{density}$ (%)	0.65	0.46	-0.17	-0.01	-0.61	-0.40

*Note: XRT: X-ray microtomography; MPS: mean pore size; MWT: mean wall thickness; WAC: water absorption capacity of dry TVPs after 30 min incubation in water with neutral pH; WAC at pH 2: water absorption capacity of rehydrated TVPs after 30 min incubation in SGF with pH 2. *Correlation is significant at the 0.05 level (2-tailed); **. Correlation is significant at the 0.01 level (2-tailed).*

Supplementary Table 4.4. *The Pearson correlation coefficients between sample properties and the free amino group concentrations corrected for those in SGF without pepsin during in vitro gastric protein digestion of rehydrated TVP powders, rehydrated TVPs and TVP-based patties.*

	Time 5 min			Time 30 min			Time 60 min			Time 120 min		
	powder	TVP	patty	powder	TVP	patty	powder	TVP	patty	powder	TVP	patty
surface area	-0.26	0.67	0.53	0.26	0.70	**0.90****	-0.25	**0.78***	**0.87****	-0.52	0.63	**0.78***
Φ_{XRT} (%)	0.20	0.60	-0.24	0.59	0.48	0.07	0.33	0.31	0.04	0.01	0.05	0.03
MPS (µm)	0.21	**0.74***	**0.74***	0.39	0.63	**0.79***	0.04	0.65	**0.81***	0.27	0.56	0.69
MWT (µm)	-0.55	-0.28	0.37	-0.57	-0.23	0.01	-0.58	-0.05	0.28	-0.37	0.30	0.27
ρ_{wall} (kg·m^{-3})	**-0.78***	-0.57	-0.30	**-0.91****	-0.52	-0.53	-0.47	-0.39	-0.28	-0.65	-0.37	-0.40
ρ_{app} (kg·m^{-3})	-0.51	-0.62	0.08	**-0.84****	-0.49	-0.20	-0.44	-0.32	-0.04	-0.30	-0.14	-0.10
ρ_{abs} (kg·m^{-3})	0.00	-0.60	0.48	-0.35	-0.53	0.03	-0.20	-0.31	-0.22	0.29	0.08	-0.26
$\Phi_{density}$ (%)	0.55	0.60	-0.03	**0.85****	0.48	0.23	0.45	0.31	0.04	0.36	0.16	0.09
WAC (%)	0.41	0.56	-0.10	0.61	0.61	0.41	0.58	0.45	0.26	0.34	0.19	0.32
WAC (%) at pH2	0.32	**0.85****	0.53	0.57	**0.76***	**0.75***	0.12	0.66	**0.86****	0.23	0.48	**0.84****
Acid absorption (mmol) without pepsin												
at 5 min	0.02	0.50	**0.86****	-0.42	0.54	0.68	-0.41	0.67	0.58	0.15	0.60	0.43
at 120 min	0.05	-0.42	**0.85****	-0.31	-0.48	0.42	-0.40	-0.40	0.44	0.12	-0.08	0.28
Acid consumption (mmol) during digestion												
at 5 min	-0.45	0.47	**0.76***	-0.48	0.54	**0.73***	-0.61	0.53	0.58	-0.47	0.42	0.43
at 120 min	-0.39	-0.07	0.34	-0.48	-0.06	0.30	-0.41	-0.05	0.66	-0.59	0.12	**0.74***

*Note: XRT: X-ray microtomography; MPS: mean pore size; MWT: mean wall thickness; WAC: water absorption capacity of dry TVPs after 30 min incubation in water with neutral pH; WAC at pH 2: water absorption capacity of rehydrated TVPs after 30 min incubation in SGF with pH 2. *Correlation is significant at the 0.05 level (2-tailed); **. Correlation is significant at the 0.01 level (2-tailed)*

Chapter 5

Bolus particle size impacts protein digestion of plant-based meat analogues patties primarily during dynamic *in vitro* gastric digestion

This chapter has been submitted for publication as:

Liu, D., Janssen, A. E. M., Smeets, P. A. M., & Stieger, M. Impact of mechanical and bolus properties on static and dynamic *in vitro* gastric protein digestion of plant-based meat analogues.

Abstract

Increasing food hardness can hinder protein hydrolysis during gastric digestion, but also lead to smaller bolus particles during mastication, which might enhance protein hydrolysis. The conjoint influence of mechanical and bolus properties on gastric motility and protein digestion is underexplored. This study explored the impact of mechanical and bolus properties on static and dynamic *in vitro* gastric protein digestion of plant-based meat analogues (PBMA). Two commercial PBMA patties (Beyond Meat, THIS) were masticated and subjected to static (INFOGEST) and dynamic gastric-emptying-mimicking digestion models (NERDT). THIS patties had a higher Young's modulus than Beyond Meat patties and broke down into smaller particles during mastication. During static digestion, THIS patties had lower free amino group concentrations than Beyond Meat patties, probably due to the higher Young's modulus. In contrast, during dynamic digestion, THIS patties showed more free amino groups in emptied liquid and faster gastric emptying than Beyond Meat patties. To further explore the effect of bolus particle size, three model PBMA patties differing only in bolus particle size were digested using static and dynamic models. During dynamic digestion, patties with small bolus particles (<0.18 mm^2) exhibited more free amino groups than patties with large bolus particles (0.59-0.68 mm^2). The enhanced digestion was attributed to the lower intragastric pH and faster gastric emptying of smaller bolus particles. We conclude that bolus particle size primarily impacts dynamic gastric protein digestion of PBMA patties. Future studies should use dynamic gastric-motility-mimicking models when studying factors sensitive to gastric emptying, and include mastication and bolus characterization before *in vitro* digestion.

5.1. Introduction

Sufficient protein intake is crucial for maintaining body metabolism and function, growth and overall health (Moughan, 2021; Wan et al., 2021). It is especially important in reducing malnutrition among vulnerable populations, such as children, low-income groups and elderly (De Groot, 2016; Jha et al., 2022; Qasrawi et al., 2024). Animal-based protein as primary protein source has been challenged due to its contribution to greenhouse gas emissions, land-water shortage and animal welfare. Alternative protein sources are increasingly explored, including plant-based proteins, insect proteins, fermentation proteins etc. (Aiking & de Boer, 2020; Zhang et al., 2024a). Plant-based proteins are commonly used for the production of plant-based meat analogues (PBMAs), which dominate the meat analogue market (Baune et al., 2022; Singh et al., 2021). However, plant-based proteins are often poorer in protein quality and digestibility compared to animal-based proteins due to the presence of anti-nutrients and unbalanced amino acid composition (Gorissen et al., 2018; Kaur et al., 2022; Sá et al., 2020a; Xie et al., 2022). Therefore, enhancing the protein digestibility of PBMAs to improve their nutritional value is crucial for developing sustainable and nutritious protein-rich foods.

The human body digests protein through a complex process involving mechanical and structural breakdown of food, protein hydrolysis by enzymes, and absorption of peptides and amino acids (Capuano & Janssen, 2021; Stieger & Van de Velde, 2013). The macrostructural breakdown of solid food occurs during the oral phase through mastication, where the food is broken down into smaller particles, increasing its surface area, and mixed with saliva to form a swallowable bolus. The food bolus passes through the esophagus and enters the stomach, where protein hydrolysis is initiated by pepsin in acidic gastric fluid. The hydrolysates and digesta from gastric digestion are delivered to the small intestine by gastric emptying (Mackie, 2023). During the small intestinal phase of digestion, the protein hydrolysates are further broken down into small peptides and amino acids so that they can be absorbed. Gastric protein digestion is a crucial process that converts swallowed food into protein hydrolysates that can be further hydrolyzed and absorbed. A thorough understanding of this process is essential for improving protein digestibility.

Gastric protein digestion is strongly influenced by mechanical and structural food properties and bolus properties. Increasing the hardness or elasticity of protein foods or model gels hindered protein hydrolysis during static *in vitro* gastric digestion (Deng et al., 2020; Dong et al., 2022; Fang et al., 2016; Nyemb et al., 2016; Peh et al., 2024). Whey protein gels with higher Young's modulus showed lower concentrations of free amino groups during static *in vitro* gastric digestion compared to whey protein gels with lower Young's modulus (Deng et al., 2020; Dong et al., 2022). This was ascribed to lower absorption of acid and less partition of pepsin at the gel-gastric juice interface of whey protein gels with higher Young's modulus, which can be affected by gel microstructure (Chapter 2 and 3; Deng et al., 2020). Egg white gels with a rigid texture displayed slower release of soluble peptides than soft egg white gels during static *in vitro* gastrointestinal digestion, which was ascribed to their higher pH and less porous microstructure (Nyemb et al., 2016). Mozzarella cheese which had higher hardness and springiness than camembert cheese exhibited a lower degree of protein hydrolysis during static *in vitro* gastric digestion. This was explained by a slower release of soluble proteins from mozzarella cheese due to its slower disintegration (Fang et al., 2016). Microalgae-modified plant-based fishcake analogues showed decreased protein digestibility after static *in vitro* gastrointestinal digestion when hardness was increased (Peh et al., 2024). These studies consistently show that hard, stiff, brittle foods are more resistant to *in vitro* gastric protein digestion compared to soft, elastic foods.

Increasing the hardness of solid foods can hinder protein hydrolysis by reducing acid and pepsin diffusion during gastric digestion, but can also lead to the formation of more and smaller bolus particles with increased surface area during mastication, which can enhance protein hydrolysis. Several studies demonstrated for a range of solid foods that an increase in hardness results in a greater number of bolus fragments, while their size becomes smaller (Chen et al., 2013; Jalabert-Malbos et al., 2007; Pentikäinen et al., 2014). Boli consisting of more and smaller particles often show a larger degree of protein hydrolysis during *in vitro* gastric digestion (Alpos et al., 2021; Chen et al., 2021; Homer et al., 2021). Harder whey protein gels generated boli with smaller particles after simulated oral processing, exhibiting a higher o-phthaldialdehyde (OPA) reactivity after *in vitro* gastric protein digestion than softer gels which generated boli with larger particles (Homer et al., 2021). More and smaller particles in boli after prolonged mastication of chicken, soy protein based chicken or black beans increased the degree of hydrolysis during static *in vitro* gastric protein digestion (Alpos

et al., 2021; Chen et al., 2021). The enhanced protein hydrolysis during digestion of foods with smaller bolus particle size was ascribed to the increase in total bolus surface area, which facilitates the diffusion of pepsin and acid from gastric fluid into food particles by providing more accessible reaction sites (Chapter 2 and 3). Our previous studies on whey protein gels showed that increasing the total surface area by a factor of 2.6 accelerated protein digestion rate by 1.8 to 2.5 times depending on gel microstructure during static *in vitro* gastric digestion (Chapter 2). After mastication, the boli of whey protein gels with larger total surface area showed a higher pH in the digestive fluid during static *in vitro* gastric protein digestion compared to the gel before mastication (Chapter 3). This suggested greater acid uptake by the bolus particles than by the non-masticated gels, which consequently led to a higher free amino group concentration in the gastric juice after static gastric digestion.

Most of the studies described above applied static *in vitro* gastric digestion models, which focus on the enzymatic protein hydrolysis without considering gastric motility. Food mechanical properties and bolus particle size can interact with gastric motility. During dynamic gastric digestion, food mechanical properties are closely related to bolus particle disintegration caused by gastric grinding (Guo et al., 2015; Kong & Singh, 2008a). Decreasing the hardness of carrots by cooking accelerated the *in vitro* gastric disintegration of carrots (Kong & Singh, 2008a). Foods consisting of small particles are typically emptied faster from the stomach than those with large particles (Holt et al., 1982; Hornby et al., 2021). The interactions between food mechanical properties, bolus particle size, gastric contractions and emptying can influence gastric protein digestion. Using dynamic *in vitro* models that mimic gastric motility can help to account for these interactions while studying the impact of food mechanical properties and bolus particle size on gastric protein digestion.

In summary, increasing the hardness of foods often results in more and smaller bolus particles after mastication, providing a larger total surface area that can facilitate gastric protein digestion. However, increasing food hardness can also make the food more resistant to protein hydrolysis, thereby hindering gastric protein digestion. During dynamic gastric digestion, gastric contractions can breakdown bolus particles in the stomach further depending on their mechanical properties. Small bolus particles can be emptied faster from the stomach than large bolus particles. Little is known about the interplay between the food

mechanical properties, bolus properties and *in vitro* gastric protein digestion, especially during dynamic gastric digestion.

This study aimed to explore the impact of mechanical properties (Young's modulus) and bolus particle size on protein hydrolysis of plant-based meat analogue (PBMA) patties during static and dynamic *in vitro* gastric protein digestion. Two commercial PBMA patties differing in Young's modulus and bolus particle size after *in vivo* mastication were subjected to static and dynamic *in vitro* gastric protein digestion. Moreover, three model PBMA patties prepared from textured soy bean proteins (TVPs) differing only in initial TVP size (large, small and powder) were subjected to static and dynamic *in vitro* gastric protein digestion after *in vivo* mastication. We hypothesized that a) the effect of Young's modulus of commercial PBMAs on protein digestion is more pronounced under static than dynamic *in vitro* digestion conditions, b) the effect of bolus particle size on protein digestion is more pronounced under dynamic than static *in vitro* digestion conditions, and c) smaller particle size of rehydrated TVPs leads to smaller bolus particle size of the PBMA patties after mastication, which accelerates gastric emptying and facilitates protein hydrolysis during dynamic *in vitro* gastric protein digestion.

5.2. Materials and methods

5.2.1 Materials

Two commercial patties (Beyond Meat Plant-based burger, Beyond Meat EU BV, and THIS Plant-based burger, THIS™) were purchased from a local supermarket (Albert Heijn B.V., Zaandam, NL). Both commercial patties are made from textured pea proteins. The protein content of Beyond Meat patties and THIS patties is 16% and 14%, respectively (Supplementary Table 5.1). Textured yellow pea protein (TVP, NUTRALYS® TP-C, containing 70% protein) was obtained from Roquette Frères S.A (Lestrem, France). Methylcellulose (metolose mce-100TS) and pea protein concentrate (NUTRALYS® S85F) were provided by Symrise AG (Holzminden, Germany). Sunflower oil (Reddy, Vandemoortele Nederland BV, Zeewolde, The Netherlands) was purchased from a local supermarket (Jumbo, Veghel, The Netherlands). Pepsin from porcine gastric mucosa and other chemicals were purchased from Sigma-Aldrich (St. Louis, USA).

5.2.2 Sample preparation

5.2.2.1 Commercial PBMA patties

The commercial PBMA patties (Beyond Meat and THIS) were stored in the fridge at 4˚C and left to equilibrate to room temperature before cooking. Commercial PBMA patties were cooked sous-vide in a pre-heated water bath at 70˚C for 1 h for further experiments.

5.2.2.2 Rehydrated TVP particles and model PBMA patties

The process for preparing rehydrated TVPs differing in size and model PBMA patties is shown in Figure 5.1. Dry TVP particles from textured yellow pea protein were sieved through a 10 mm mesh size sieve to separate them into small and large particles. Small, dry TVP particles were blended in a Thermomix (TM5, Vorwerk & Co. KG, Wuppertal, Germany) at speed 5 for 1 min, followed by sieving with a 2 mm mesh size sieve to obtain a fine dry powder. The TVP powder and large TVP particles were rehydrated in water at a TVP:water ratio of 1:2 based on weight for 30 min. The rehydrated large TVPs were blended in a kitchen blender (Magimix CS 5200 XL, Burgundy, France) for 5 s or 15 s to obtain TVPs with a mean particle size of 16 mm^2 and 8 mm^2, respectively.

PBMA patties differing in TVP size were prepared by using rehydrated TVPs differing in particle size (large: 16 mm^2, small: 8 mm^2, powder: < 2 mm^2). Rehydrated TVPs (60 w/w%) were mixed with sunflower oil (15 w/w%), pea protein isolate (5 w/w%), methylcellulose (2 w/w%), NaCl (0.8 w/w%) and water (17.2 w/w%) following the preparation procedure described previously by van Esbroeck et al. (2024) to prepare PBMA patty doughs with large TVPs (L patty), small TVPs (S patty) and powder TVPs (powder patty), respectively. Doughs were stored at 4˚C overnight. The stabilized patty dough was shaped into patties of 100 g with a diameter of 70 mm and a height of around 20 mm using a patty shaper. PBMA patties were cooked sous-vide in a pre-heated water bath at 70˚C for 1 h for further experiments.

5.2.2.3 Bolus collection

All boli used in this study were collected from the same person following a fixed chewing protocol. This procedure was followed to remove inter-individual variability in mastication behavior and to minimize intra-individual variability in mastication behavior and bolus properties. Cooked patties were cut into pieces of 10 g bite size and cooled to room

temperature. Patty pieces (10 g) were chewed individually by the person at a frequency of 1.7 chews/s for 30 chews. This mastication behavior has previously been reported as natural mastication behavior of these patties (Zhang et al., 2024b). An audio signal prompting chews was used to instruct mastication behavior. Boli were expectorated into a petri dish and subjected to further analysis and *in vitro* digestion within 8 h.

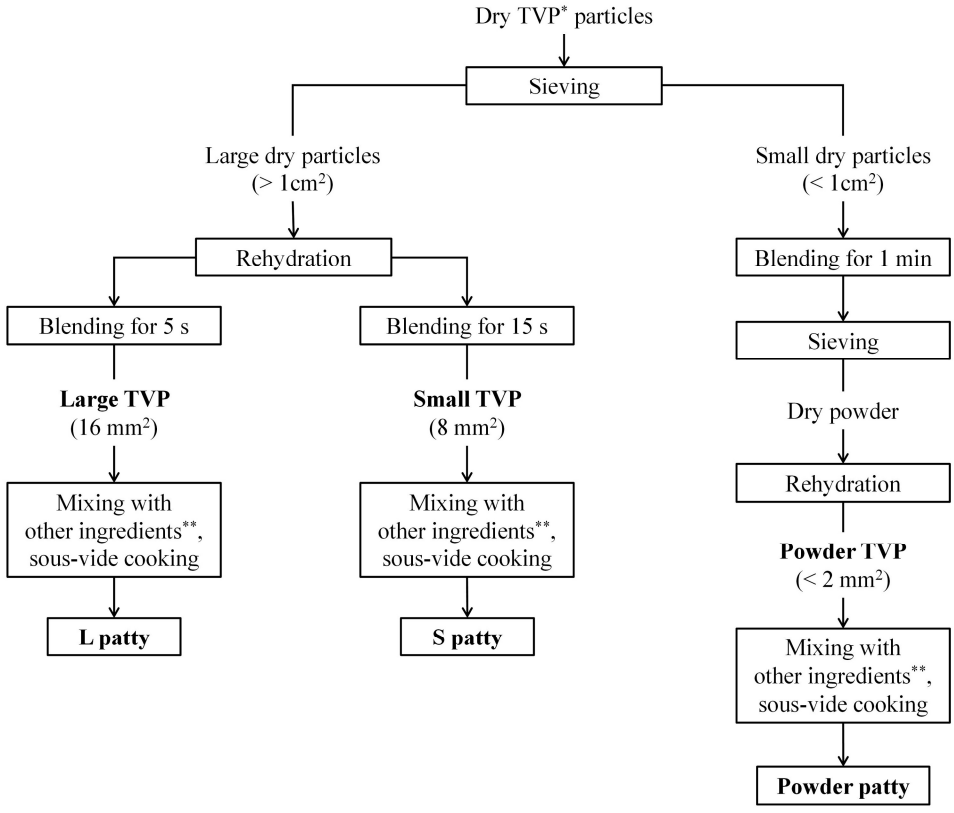

Figure 5.1. *Process for preparing rehydrated TVPs differing in particle size and PBMA patties. *Textured yellow pea protein containing 70% protein. **Oil (15 w/w%), pea protein isolate (5 w/w%), methylcellulose (2 w/w%), NaCl (0.8 w/w%) and water (17.2 w/w%).*

5.2.3 Measurement of the Young's modulus of patties

The cooked patties were cut into cylinders using a sharp cylindrical cutter with a diameter of 30 mm and subjected to a Texture Analyser (TA-XTplusC, Stable Micro Systems Ltd., Godalming, UK) equipped with a 50 kg load cell (van Esbroeck et al., 2024). Uniaxial

compression tests were performed when the internal temperature of patty cylinders was 30°C using a cylindrical probe with a diameter of 75 mm at a trigger force of 0.1 N and a compression speed of 1 mm/s. Compression was stopped when 80% strain was reached, and the probe was returned to the initial height (25 mm). Young's modulus (kPa) was calculated as the initial slope of the true Hencky's stress-strain curves within the strain region of 0.05-0.13. Measurements were performed in six replicates.

5.2.4 Measurement of particle size

Image analysis was used to determine particle size and number of particles per gram for rehydrated TVPs and expectorated patty boli (Chen et al., 2021). For rehydrated TVPs, six portions (around 1.5 g each) of rehydrated TVP particles were sampled. For boli of expectorated patties, six portions (around 0.36 g each) of bolus particles were sampled from three expectorated boli per patty. Each portion of particles was placed on a petri dish (120 × 120 × 17 mm) and gently separated manually using a spatula. Water was added in the petri dish to the patty boli to aid particle separation . The petri dish was placed on a flatbed scanner (Canon CanoScan 9000 F MarkII). A color image with a resolution of 600 dpi was captured against a black background. An additional image was captured for each petri dish after gently stirring the samples in the petri dish. Both images of the same petri dish were analyzed to determine the number of particles per gram and the area of each particle. The data were averaged to represent the data of this portion of particle sample. ImageJ (version 1.52a, National Institute of Health) was employed to analyze the captured images. Binary images were obtained by converting the original images to 8-bit format and adjusting the brightness/contrast and black/white threshold. The function "Analyze Particles" in ImageJ was used to obtain the number of particles and the area (mm^2) of each particle in each image. Particles with an area smaller than 0.03 mm^2 or with a circularity less than 0.1 were excluded from data analysis to remove noise. The number of particles was normalized per g sample (-/g). The mean area of particles (mm^2) was quantified as a measure of particle size. The total surface area per gram bolus (mm^2/g) was determined by summing the area of each particle in a given bolus and dividing it by the mass of the bolus.

5.2.5 In vitro gastric protein digestion

5.2.5.1. Static in vitro gastric protein digestion

Static *in vitro* gastric protein digestion of patties after mastication was performed following the INFOGEST 2.0 protocol with minor modifications (Brodkorb et al., 2019). Three grams of expectorated boli were immersed in 30 mL simulated gastric fluid (SGF, containing 25 mmol/L $NaHCO_3$, 47.2 mmol/L NaCl and 1900 U/mL pepsin, pH = 2) for 2 h of digestion at 37˚C while gently mixing. The pH of the gastric juice was measured immediately after the samples were placed in SGF as the first measurement (0 min) and at 10, 30, 60, 90, 120 min. 200 µL of gastric juice was pipetted out at the same time points with the exception of t=0 min. The collected samples were heated for 5 min in a pre-heated Eppendorf thermomixer at 90°C while mixing. After cooling to room temperature, samples were centrifuged at 14500 rpm for 20 min and stored at 4°C for further analysis. The digestion for each patty was conducted in triplicate.

5.2.5.2 Dynamic in vitro gastric protein digestion

The NEar Real Digestive Track (NERDT, Xiao Dong Pro-health Instrumentation Co. Ltd., Suzhou, China) was used to perform dynamic *in vitro* gastric protein digestion. The NERDT (Supplementary Figure 5.1) simulates the human gastrointestinal tract and focuses on mimicking the gastric morphology, peristalsis and emptying (Chen et al., 2016; Peng et al., 2021; Wang et al., 2019). The dynamic *in vitro* gastric protein digestion protocol was developed based on the protocol previously described by Peng et al., (2021) and the recommended NERDT settings provided by the manufacturer. The environment temperature of the equipment was set at 37˚C. SGF (containing 25 mmol/L $NaHCO_3$, 47.2 mmol/L NaCl and 4000 U/mL pepsin, pH = 2) and 0.5 M HCl were filled into the gastric fluid secretion tube and the acid secretion tube, respectively. Thirty-five mL of SGF were loaded into the stomach to simulate the fasting state. Boli (100 g) expectorated after *in vivo* mastication obtained from human mastication of ten bites of 10 g patties were gently mixed with 250 g water and loaded into the funnel at the top of the NERDT while the clamps of the simulative esophagus were closed. The operation time included the feeding time (3 min) and gastric digestion time (120 min). During the feeding time, the upper clamp of the esophagus was opened for 6 s while the lower clamp of the esophagus was closed, followed by opening of the lower clamp for 6 s while the upper clamp was closed. This procedure was repeated 15

times for 3 min to gradually deliver the entire loaded sample into the stomach. At the same time, the esophagus was shaken by a vibrator at 50 rpm to aid passing of the bolus through the esophagus. After 3 min feeding, the clamps of the esophagus were closed. The rolling-extrusion device of the stomach was set to roll towards the pylorus at 500 mm/min for 8 cm while squeezing the stomach and then rolled back to the initial position at 600 mm/min while releasing the stomach. This procedure was repeated 3 times per min during the operation time (123 min) to mimic gastric peristalsis. SGF and 0.5 M HCl were secreted into the stomach following the program shown in Table 5.1. The pyloric valve remained closed during the feeding time. During the gastric digestion time, the pyloric valve opened 4 mm at a speed of 300 mm/min for 10 s after every three contractions and was then closed at the same speed. The digesta emptied from the pylorus were collected and weighed every 10 min during the digestion time. The pH of the digesta mixture was measured immediately, and then adjusted to above 7 using NaOH, followed by weighing the mixture to determine the amount of added NaOH. The collected digesta were centrifuged at 14000 g for 20 min at 4°C to separate the solid and liquid fraction. The liquid fractions were weighed and stored at 4°C for further analysis. The total gastric content (g) during the near-real dynamic digestion was determined by subtracting the mass of emptied digesta from the current gastric content (including the amount of gastric secretion) at each time point. The amount of emptied solid digesta (g) was determined by subtracting the weight of liquid fraction (corrected for added NaOH) from the weight of the emptied mixture at each time point. The digestion for each patty was conducted in triplicate.

Table 5.1. *Secretion rates of simulated gastric fluid and acid during dynamic in vitro gastric digestion using NERDT.*

Operation time (min)	0-13	13-23	23-33	33-43	43-53	53-63	63-123
SGF* (mL/min)	1.6	2.2	2.6	3	2.6	2.2	2
0.5 M HCl (mL/min)	2	2	2	1	1	0	0

** Simulated gastric juice consists of 25 mmol/L $NaHCO_3$, 47.2 mmol/L NaCl, and 4000 U/mL pepsin at pH 2.*

5.2.5.3 Determination of free amino group concentration

The o-phthaldialdehyde (OPA) method (Nielsen et al., 2001) was used to determine the free amino group concentration (mmol/L) of SGF samples collected during static digestion and that of emptied liquid fraction collected during near-real dynamic digestion. All samples were

diluted tenfold with water, and 10 µL of each diluted sample was mixed with 200 µL OPA reagent in 96-plate wells for 3 min. The absorption of the mixed solutions at 340 nm was measured using a microplate photometer (Thermo Scientific 357, USA) right after mixing. Serine standard solutions (0-200 mg/mL) were used to generate a calibration curve for the concentration of free amino groups. The amount of cumulative emptied free amino groups (mmol) during near-real dynamic digestion was calculated by multiplying the volume of the emptied liquid fraction (corrected for added NaOH and assuming a density of 1 g/mL) by the free amino group concentration at each time point and then accumulating the values.

5.2.6 Statistical data analysis

SPSS statistics software (IBM SPSS Statistics Version 28, IBM Corp) was used for data analysis. All data are reported as means with standard deviations. Independent t-tests were used to compare the Young's modulus and bolus properties between Beyond Meat and THIS patties. Independent t-tests were used to compare the TVP particle properties and bolus properties between PBMA patties prepared from large and small TVPs. One-way analysis of variance (ANOVA) followed by Tukey's HSD test was used to compare the Young's modulus between PBMA patties prepared from large, small and powder TVPs. Differences in free amino group concentration, cumulative emptied free amino groups, total gastric content, cumulative amount of emptied solid and pH during digestion were tested using linear mixed models. Fixed factors were time, treatment and the interactions between time and treatments. Replicates were added as random factor. Bonferroni-corrected post hoc tests were used to compare the differences between treatments at each time point. The threshold for statistical significance was set at $p = 0.05$.

5.3. Results and Discussion

5.3.1 Static and dynamic in vitro gastric protein digestion of commercial PBMA patties

5.3.1.1 Young's modulus and bolus properties after in vivo mastication

Table 5.2 shows that the Young's modulus of Beyond Meat patties was significantly lower ($p = 0.04$) than that of THIS patties. After *in vivo* mastication, Beyond Meat patties had significantly larger bolus particle size ($p = 0.03$) than THIS patties. The number of bolus

particles per gram and the total bolus surface area per gram did not differ significantly between the two patties ($p = 0.23$ and $p=0.77$, respectively). The difference in bolus particle size between Beyond Meat and THIS patties might have been too small to lead to significant difference in total bolus surface area. To summarize, THIS patties were stiffer than the Beyond Meat patties and broke down into smaller bolus particles during *in vivo* mastication. This finding is consistent with previous studies, which reported that increased food hardness resulted in decreased bolus particle size and increased number of bolus particles for other foods such as jellies, carrots and breads (Chen et al., 2013; Jalabert-Malbos et al., 2007; Pematilleke et al., 2020). The reasons for the stiffer texture of THIS compared to Beyond Meat patties are unclear, as little is known about the ingredient properties and production process of these two products. We speculate cautiously that the TVPs used in THIS patties may have a lower water absorption capacity compared to those in Beyond Meat patties, which could contribute to a firmer texture (Hong et al., 2022; Samard et al., 2021).

Table 5.2. *Young's modulus and bolus properties after in vivo mastication of two commercial plant-based meat analogue patties.*

	Young's modulus (kPa)		Bolus particle size (mm^2)		Number of bolus particles (-/g)		Total bolus surface area (mm^2/g)	
	Mean ± SD	p value	Mean ± SD	p value	Mean ± SD	p value	Mean ± SD	p value
Beyond Meat	35 ± 4	0.04	1.05 ± 0.15	0.03	1800 ± 400	0.23	1850 ± 220	0.77
THIS	45 ± 9		0.87 ± 0.11		2200 ± 500		1810 ± 270	

5.3.1.2 Static in vitro gastric protein digestion

The free amino group concentrations during static *in vitro* gastric protein digestion in the liquid phase was significantly higher for Beyond Meat than THIS patties ($p < 0.001$) (Figure 5.2a), although the bolus particles of Beyond Meat patties were larger. This indicates a larger degree of protein digestion for Beyond Meat patties than THIS patties during static *in vitro* gastric digestion. This cannot be explained by the total surface area of bolus for these two patties, as these values were similar (Table 5.2). It is more likely that the lower Young's modulus of Beyond Meat patties contributed to its greater protein hydrolysis. It has been widely reported that decreasing Young's modulus or hardness of foods promotes static *in vitro* gastric protein digestion (Deng et al., 2020; Dong et al., 2022; Fang et al., 2016; Nyemb et al., 2016; Peh et al., 2024).

The pH of gastric juice during static *in vitro* gastric protein digestion of commercial PBMA patties increased immediately after the expectorated boli were immersed in it and leveled off after 30 min (Figure 5.2b). The initial rise in pH could be attributed to several factors, including acid uptake by the patty boli, buffering effect of proteins in PBMA patties and the ionization of amino group released by proteolysis (Deng et al., 2020; Luo et al., 2018). The increased pH could in turn suppress pepsin activity, reducing the proteolysis. However, despite showing consistently a significantly higher pH in the gastric juice than THIS patties ($p < 0.001$) (Figure 5.2b), Beyond Meat patties did not exhibit a slower release of free amino groups compared to THIS patties as indicated by the nearly parallel curves (Figure 5.2a). This indicates that although the pepsin activity during static digestion of Beyond Meat patties might be lower than that of THIS patties, other factors, such as the lower Young's modulus, still ensured competitive proteolysis efficiency over time, resulting in higher free amino group concentrations in the gastric juice.

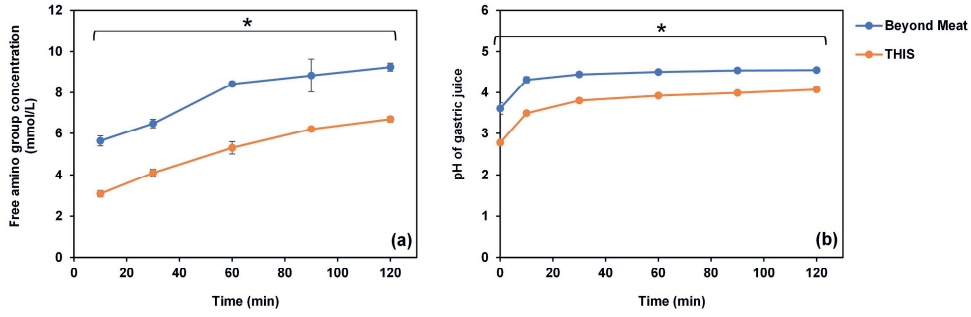

Figure 5.2. *Free amino group concentration (a) and pH (b) of gastric juice during static in vitro gastric protein digestion of two commercial plant-based meat analogue patties (Beyond Meat: blue; THIS: orange) after in vivo mastication. Error bars denote standard deviations (n = 3), but some bars are too small to be visible. The * above the line denotes the main effect of treatment (p < 0.001).*

5.3.1.3 Dynamic in vitro gastric protein digestion

During dynamic *in vitro* gastric protein digestion, THIS patties showed a gradually decreasing total gastric content (Figure 5.3a), reflecting a continuous and progressive gastric emptying process. After 73 min, a quarter of the total gastric content for THIS patties had been emptied. In contrast, the total gastric content of Beyond Meat patties slightly increased until 103 min of digestion time, suggesting that more gastric secretion than gastric emptying occurred during dynamic *in vitro* gastric protein digestion. By the end of digestion (123 min),

a quarter of the total gastric content of the Beyond Meat patties had been emptied, taking almost twice as long as for the THIS patties. THIS patties showed much faster gastric emptying than Beyond Meat patties. Correspondingly, THIS patties exhibited higher cumulative amounts of emptied solid than Beyond Meat patties during dynamic digestion (Figure 5.3b). After 73 min, approximately half of the total solid gastric content had been emptied for THIS patties, while for Beyond Meat patties, it took an additional 40 min (113 min) to empty half of the total solid gastric content. These results indicate that after *in vivo* mastication, the bolus particles of THIS patties emptied faster than those of Beyond Meat patties, indicating that commercially available foods belonging to the same product category can differ considerably in their gastric transit behavior.

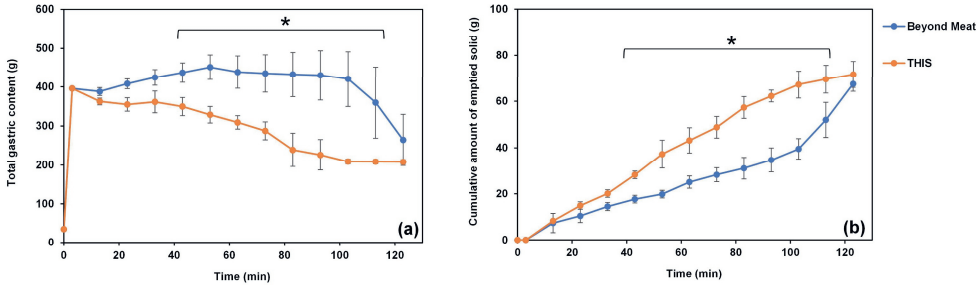

Figure 5.3. *Total gastric content (a) and cumulative amount of emptied solid (b) during dynamic in vitro gastric protein digestion of two commercial plant-based meat analogue patties (100 g, Beyond Meat: blue; THIS: orange) after in vivo mastication. Error bars denote standard deviations (n = 3). Main effect of interactions between treatment and time was found for both total gastric content and cumulative amount of emptied solid ($p < 0.001$). The * above the line denotes significant differences ($p<0.05$) between the two patties at each time point covered by the line.*

Many properties of solid foods can influence gastric emptying including energy density, particle size, etc. (Camps et al., 2017; Mackie, 2023; Ménard et al., 2018; Roelofs et al., 2024). Given that the dynamic system (NERDT) used in this study simulates gastric emptying only based on physical mechanisms without considering metabolic feedback regulations, it was speculated that the small bolus particle size of THIS patties led to faster emptying (Guo et al., 2015; Mennah-Govela & Bornhorst, 2021). The lower Young's modulus of Beyond Meat patties did not appear to affect gastric emptying, although it could potentially accelerate it by increasing the degree of disintegration as gastric contractions progress (Guo et al., 2015). It is noted that neither the THIS patties nor the Beyond Meat patties were completely emptied from the stomach after 120 min of dynamic digestion

(Figure 5.3a). This was due to the upright position and the J-shape of the silicon stomach (Supplementary Figure 5.1). As the gastric content emptied from the stomach, the liquid level dropped and eventually fell below the pylorus, making it difficult for further emptying of gastric contents.

The free amino group concentration in the emptied liquid during dynamic *in vitro* gastric protein digestion of THIS patties was lower than that of Beyond Meat patties during the first 30 min of gastric digestion, and it gradually increased during 33-93 min, surpassing that of Beyond Meat patties after 43 min (Figure 5.4a). THIS patties exhibited significantly larger amount of cumulative free amino groups in the emptied liquid than Beyond Meat patties during 63-113 min of digestion ($p < 0.05$) (Figure 5.4b). These results can be explained by the faster gastric emptying of THIS compared to Beyond Meat patties, likely due to the smaller bolus particle size of THIS patties. Faster gastric emptying of THIS patties resulted in less liquid and food bolus in the stomach during digestion compared to Beyond Meat patties (Figure 5.3a). During the first 53 min, the same amount of acidic gastric fluid was secreted into the stomach for both patties. Consequently, there might be a lower intragastric pH for THIS patties compared to Beyond Meat patties, as indicated by the lower pH of emptied liquid for THIS patties in Figure 5.4c. It is inferred that the pepsin activity during the dynamic digestion of THIS patties was higher than that of Beyond Meat patties, promoting the enzymatic protein hydrolysis and resulting in the faster increase in free amino group concentrations.

These results indicate that the degree of protein digestion during dynamic *in vitro* gastric digestion of THIS patties was larger than that of Beyond Meat patties. This is in sharp contrast to the results obtained from static digestion which showed that THIS patties were less digested than Beyond Meat patties (Figure 5.2a). This highlights that the outcome of *in vitro* gastric protein digestion of PBMA patties is strongly affected by the digestion model which modulates the effect of food properties on protein hydrolysis. In this study, the lower Young's modulus of Beyond Meat patties likely caused a higher degree of protein hydrolysis during static digestion. In contrast, the smaller bolus particle size of THIS patties caused faster gastric emptying and lower intragastric pH which likely led to a higher degree of protein hydrolysis during dynamic digestion. These findings support our hypotheses a) and b) that the effect of Young's modulus on protein digestion is more pronounced under static than

dynamic *in vitro* digestion conditions, while the effect of bolus particle size on protein digestion is more pronounced under dynamic than static *in vitro* digestion conditions. However, we characterized only two properties (Young's modulus and bolus properties after *in vivo* mastication) of the commercial patties. Many other factors such as composition, processing and microstructure can influence *in vitro* gastric protein digestion of PBMAs (Cutroneo et al., 2023; Lv et al., 2024; Peh et al., 2024). These factors are not known for these commercial patties. Therefore, the effect of Young's modulus and bolus particle size of PBMA patties on protein hydrolysis during static and dynamic *in vitro* gastric digestion needs to be examined while controlling for composition and other variations. To achieve this, three model PBMA patties with comparable Young's modulus were prepared from textured yellow pea proteins differing only in particle size (large, small and powder), and subjected to static and dynamic *in vitro* digestion. The results are reported and discussed in section 5.3.2.

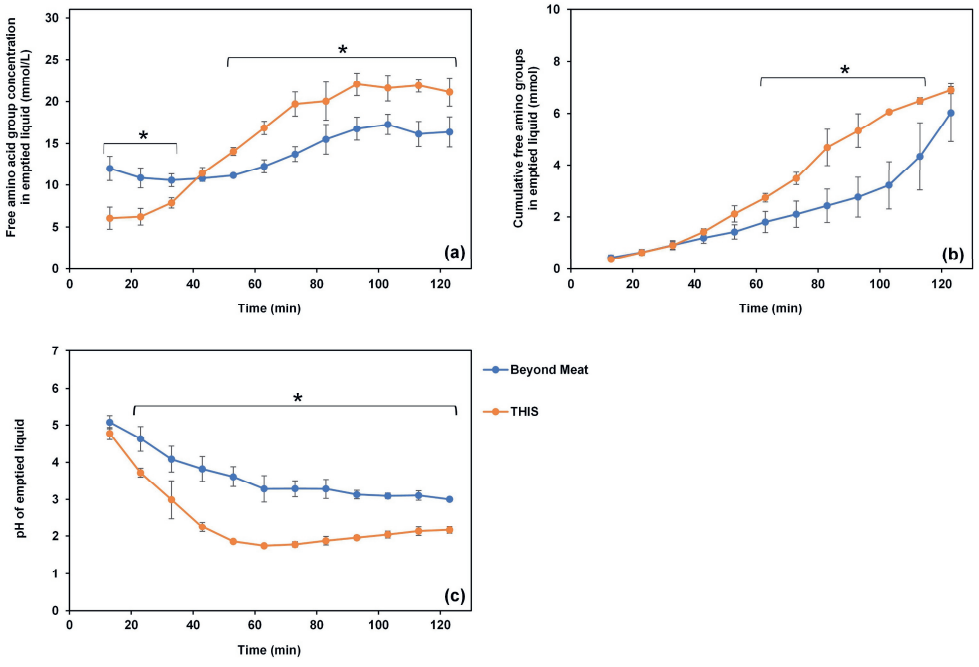

Figure 5.4. *Free amino group concentration (a), cumulative free amino groups (b) and pH (c) of emptied liquid during dynamic in vitro gastric protein digestion of two commercial plant-based meat analogue patties (Beyond Meat: blue; THIS: orange) after in vivo mastication. Error bars denote standard deviations (n = 3). Main effect of interactions between treatment and time was found for all measurements ($p < 0.001$). The * above the line denotes significant differences ($p<0.05$) between the two patties at each time point covered by the line.*

5.3.2 Static and dynamic in vitro gastric protein digestion of model PBMA patties made from TVPs differing in particle size

5.3.2.1 Properties of rehydrated TVPs and model PBMA patties

The mean particle size of large TVPs was twice that of small TVPs (Table 5.3). The particle size distribution shows that compared to rehydrated small TVPs, rehydrated large TVPs had more particles larger than 80 mm^2 and fewer particles smaller than 20 mm^2 (Supplementary Figure 5.2a). The number of particles per gram of large TVPs was approximately half that of small TVPs (Table 5.3). The total bolus surface area per gram of large TVPs was significantly smaller than that of small TVPs ($p < 0.001$). The particle properties of rehydrated powder TVPs was only measured once to give approximate values because rehydrated powder particles stick together and formed larger particles which could not be separated manually. Therefore, the reported particle size of powder TVPs in Table 5.3 was considerably overestimated while the number of particle per gram and total surface area per gram were considerably underestimated. When additional water was added to rehydrated powder TVP particles, the particles dispersed very well and the apparent size was reduced considerably as shown in the second photo in the column of powder TVPs in Table 5.3. However, these tiny particles were too small to be properly analyzed by image analysis.

Table 5.3. *Particle properties of rehydrated textured yellow pea proteins (TVPs). P values denote significant differences between large TVP and small TVPs. The preparation of large, small and powder TVPs is shown in Figure 5.1.*

		Large TVP	Small TVP	Powder TVP [a]
Mean particle size (mm^2)	Mean ± SD	16 ± 5	8 ± 1	2
	p value	0.02		
Number of particles (-/g)	Mean ± SD	54 ± 17	131 ± 16	489
	p value	<0.001		
Total surface area (mm^2/g)	Mean ± SD	780 ± 40	1040 ± 50	1070
	p value	<0.001		
Appearance[b] (1.5 g)		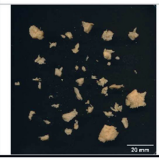	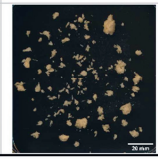	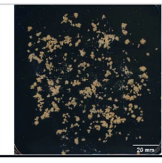 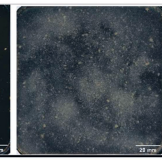

[a] A single measurement was performed for rehydrated powder TVPs shown in the first image under the column of powder TVP. [b] The second image under the column of powder TVPs shows the appearance of 1.5 g rehydrated powder TVPs in additional water.

The Young's moduli of PBMA patties prepared with large, small and powder TVPs were similar and ranged from 19-24 kPa (Table 5.4). These values are close to the Young's moduli reported by van Esbroeck et al. (2024) who made PBMA patties from the same intact (16 kPa) and ground TVPs (18 kPa). After mastication, the bolus of L and S patties did not show significant differences in particle size ($p = 0.17$) (Table 5.4). The bolus particle size distribution of L and S patties was similar, while for the S patties, there were slightly fewer particles with a smaller size and more particles with a larger size (Supplementary Figure 5.2b). These results may not strongly support the first part of our hypothesis (c) that smaller particle size of rehydrated TVP leads to smaller bolus particle size of PBMA patties after mastication. However, the bolus particle number per gram of bolus for L patties was significantly smaller than that for S patties ($p = 0.03$) (Table 5.4). This suggests the presence of a few large particles with high weight in the bolus of L patties as shown in Table 5.3. The particle size distribution reported in this study is based on the particle number and the area of each particle analyzed from 2-D images. A few particles with large area may constitute a small proportion of the total particle number but a large proportion of the total bolus particle mass. The image-analysis-based particle size distribution shown in Supplementary Figure 5.2 is based on number of particles. This overestimates the proportion of small particles (of which there are many in a bolus) in size distribution and underestimates the proportion of large particles (of which there are few in a bolus) compared to weight-based particle size analysis (i.e. sieving and weighing). L patties also exhibited significantly smaller total surface area per gram of bolus compared to S patties ($p = 0.02$) (Table 5.4). These results indicate that the bolus of L patties consisted of fewer and larger particles than the bolus of S patties, but the difference might be modest. The reported value of bolus particle size for powder patties was overestimated because it was difficult to separate individual powder particles. For image analysis, powder particles close to each other tended to be recognized as one larger particle. Nevertheless, the results suggest that the mean particle size of powder particles was below 0.18 mm^2, considerably smaller than that of L and S patty.

Table 5.4. *Young's modulus and bolus particle properties after in vivo mastication of model PBMA patties. P values denote the differences between L and S patties. The preparation of L, S and powder patties is shown in Figure 5.1.*

		L patty	S patty	Powder patty
Young's modulus of patties (kPa)[b]	Mean ± SD	19 ± 5	22 ± 3	24 ± 3
Bolus particle size (mm^2)	Mean ± SD p value	0.68 ± 0.13 0.17	0.59 ± 0.08	0.18 [a]
Number of bolus particles (-/g)	Mean ± SD p value	2700 ± 1700 0.03	4800 ± 1100	28400 [a]
Total bolus surface area (mm^2/g)	Mean ± SD p value	1660 ± 810 0.02	2720 ± 320	5120 [a]
Appearance[c] (0.35 g)		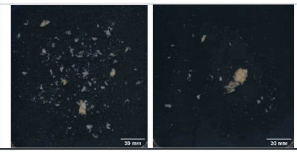	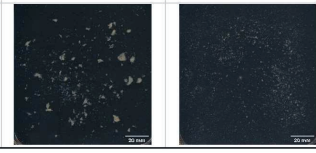	

[a] *A single measurement was performed for powder patty.* [b] *Young's modulus did not differ significantly between patties (p = 0.11).* [c]*The second photo of 0.35 g bolus of L patty after mastication shows one large bolus particle and several small particles.*

5.3.2.2 Static in vitro gastric protein digestion of model PBMA patties differing in TVP size

There was no significant difference in free amino group concentrations in gastric juice during static digestion of L patties, S patties and powder patties (p = 0.06) (Figure 5.5a). For all patties, the pH of gastric juice rapidly increased to approximately 4.5 after 10 min due to the buffering effect of bolus particles. During 0-10 min, powder patties showed a higher pH than the other two patties. This could be due to the stronger buffering effect caused by the larger surface area of the powder particles. These results suggest that differences in bolus particle properties and a 39% smaller total bolus surface area per gram bolus of L patties did not cause differences in protein hydrolysis during static *in vitro* gastric digestion compared to S patties. There was no significant enhancement in protein hydrolysis for powder patties, despite the small particle size and larger total bolus surface area. These results are similar to those of Ribes et al. (2023) who studied the static *in vitro* gastric protein digestion of turkey and cheese after *in vivo* mastication. They found similar free amino group content in the gastric juice after digestion of boli consisting of small and large particles, although they attributed this result to the particle size reduction during static digestion instead of unchanged initial mechanical properties (Ribes et al., 2023). Decreasing bolus particle size by prolonged chewing significantly increased the static *in vitro* gastric protein hydrolysis of chicken, vegetarian chicken and black beans (Alpos et al., 2021; Chen et al., 2021). Compared to these

studies, the difference in bolus particle size between L and S patties in our study was modest, which may also contribute to their similar free amino group concentration during static digestion.

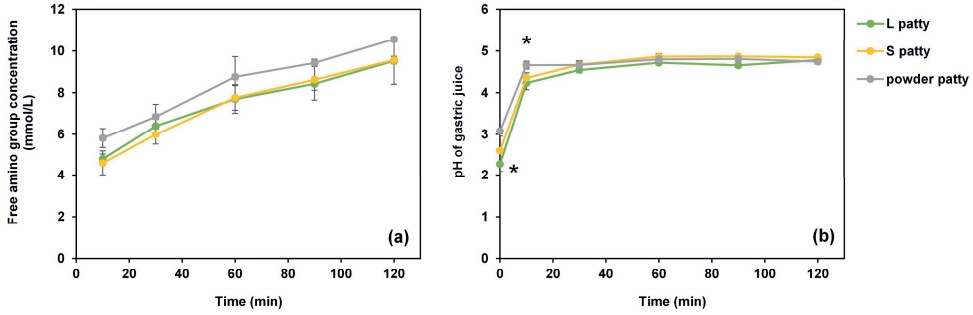

Figure 5.5. *Free amino group concentration (a) and pH (b) of gastric juice during static in vitro gastric protein digestion of model PBMA patties after in vivo mastication. The preparation of L, S and powder patties is shown in Figure 5.1. Error bars denote standard deviations (n = 3), but some bars are too small to be visible. For free amino group concentration, digestion time showed significant effect ($p < 0.001$) and the treatment showed insignificant effect ($p = 0.06$) with no interaction between them ($p = 1.0$). For pH, there was a significant effect of interaction between time and treatment ($p < 0.001$). The * denotes significant differences between the three patties at given time points ($p < 0.05$).*

The results indicate that during static *in vitro* gastric digestion of PBMA patties, Young's modulus dominated protein hydrolysis rather than bolus particle size or total surface area. This finding supports the results for the commercial patties (section 5.3.1.2). The lower free amino group concentration of THIS patties with smaller bolus particles than Beyond Meat patties with larger bolus particles during static digestion might be attributed to the higher Young's modulus of THIS patties. This is also in accordance with our previous study in which we found greater contribution of Young's modulus to protein hydrolysis compared to total surface area during static *in vitro* gastric protein digestion of whey protein gels (Chapter 2). Decreasing the Young's modulus of whey protein gels by 32% increased the digestion rate by a factor of 4.5, while increasing the total surface area of whey protein gels by 260% only increased the digestion rate by a factor of 2.4 (Chapter 2).

5.3.2.3 Dynamic in vitro gastric digestion of PBMA patties differing in TVP size

PBMA patties prepared from powder TVPs (powder patties) showed remarkably faster gastric emptying during dynamic *in vitro* gastric protein digestion compared to patties prepared from large (L patties) and small TVPs (S patties) (Figure 5.6). Half of the total

gastric content and the solid gastric content of powder patties was emptied during the first opening of the pylorus valve (13 min). This was because the powder particles were well dispersed in the gastric juice, passing through the pylorus with no hindrance. After 13 min, approximately 200 g of gastric content was retained at the bottom of the J-shaped silicon stomach and remained there until the end of the digestion (120 min). For S patties, a quarter of the total gastric content along with half of the gastric solid content were emptied after 63 min, while for L patties, it was after 73 min (Figure 5.6). This indicates that S patties emptied faster than L patties. After 83 min, the emptying for both patties stopped due to gravity.

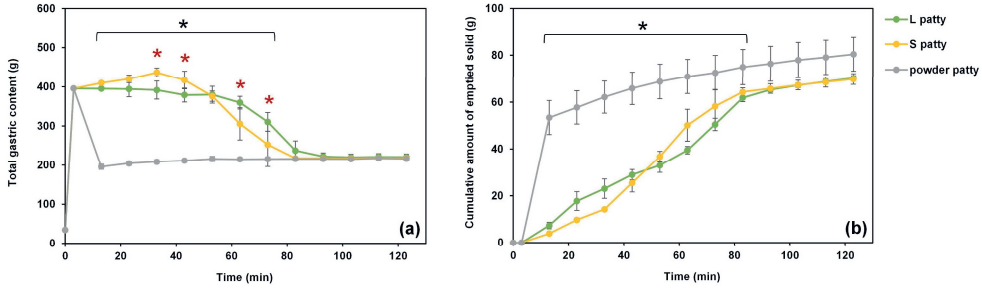

Figure 5.6. *Total gastric content (a) and cumulative amount of emptied solid (b) during dynamic in vitro gastric protein digestion of model PBMA patties after mastication. The preparation of L, S and powder patties is shown in Figure 5.1. Error bars denote standard deviations (n = 3), but some bars are too small to be visible. The interaction between treatment and time showed significant effect on the total gastric content and cumulative amount of emptied solid ($p < 0.001$). The black * above the line denotes significant differences ($p<0.05$) between powder patties and the other two patties at each time point covered by the line. The red * denotes significant differences between L patties and S patties at given time points ($p < 0.05$).*

These results demonstrate that compared to L and S patties, the very small particle size (powders) of powder patties led to faster gastric emptying. The smaller bolus particle size of S patties also resulted in faster gastric emptying compared to L patties. These results corroborate the findings of many studies that suggested a positive correlation between intragastric particle size and gastric emptying rate during dynamic *in vitro* gastric digestion (Guo et al., 2015; Mennah-Govela & Bornhorst, 2021) and are consistent with *in vivo* studies (Holt et al., 1982; Hornby et al., 2021). Sun et al. (2023) reported higher *in vitro* gastric emptying rate in purees made from fine chickpea particles compared to purees made from coarse chickpea particles. Tagle-Freire et al. (2022) reported faster *in vitro* gastric emptying of quinoa after simulated mastication by mincing, compared to only mixing the quinoa with simulated saliva. Our results and these studies support our suggestion in section 5.3.1.3 that

the faster gastric emptying of THIS patties compared to Beyond Meat patties can be attributed to their smaller bolus particles, although the former were stiffer than the latter.

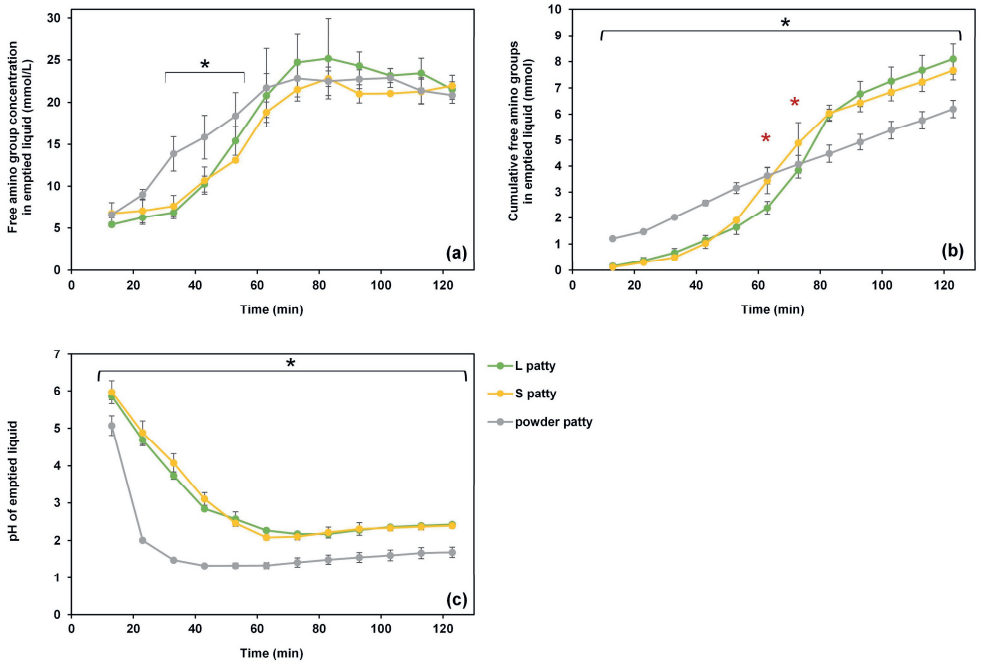

Figure 5.7. *Free amino group concentration (a), cumulative free amino groups (b) and pH (c) of the emptied liquid during dynamic in vitro gastric protein digestion of model PBMA patties. The preparation of L, S and powder patties is shown in Figure 5.1. Error bars denote standard deviations (n = 3), but some bars are too small to be visible. The interaction between treatment and time showed significant effect on all measurements (p < 0.001). The black * above the line denotes significant differences (p < 0.05) between powder patties and the other two patties at each time point covered by the line. The red * denotes significant differences between L and S patties at given time points (p < 0.05).*

For all patties, the free amino group concentration in the emptied liquid increased from 13 to 73 min of digestion time and then levelled off after 73 min at around 20-25 mmol/L until the end of digestion time (Figure 5.7a). This trend aligns with the pH in the emptied liquid (Figure 5.7c), which could reflect the intragastric pH. During 33-53 min of dynamic digestion, powder patties displayed significantly higher free amino group concentration in the emptied liquid than L and S patties (Figure 5.7a), even though the hydrolytic substrate (gastric solid content) for powder patties was remarkably less after 23 min (Figure 5.6). This is due to the rapid emptying of half of the total gastric content for powder patties after 13 min while 0.5 M HCl and acid SGF continued to be secreted, which could lead to a rapid decrease in

intragastric pH. The pH of emptied liquid for powder patties decreased to 2 after only 23 min and levelled off at around 1.5, remaining lower than that of L and S patties throughout the entire digestion period (Figure 5.7c). This result suggests a higher pepsin activity during dynamic digestion of powder patties compared to L and S patties, which explained the higher free amino group concentration and the larger amount of cumulative free amino groups in emptied liquid of powder patties during the first hour of dynamic digestion (Figure 5.7b). At 63 and 73 min, the cumulative free amino groups in the emptied liquid of powder patties was exceeded by that of S and L patties, respectively (Figure 5.7b). This indicates that the protein hydrolysis was eventually limited by the smaller gastric content of powder patties compared to L and S patties. At 63 and 73 min, S patties exhibited a significantly larger amount of cumulative free amino groups than L patties. This was mainly due to the more gastric emptying (less gastric content) for S patties as shown in Figure 5.6a.

These results show that for PBMA patties with similar Young's modulus, very small bolus particle size (powder patties) facilitated protein hydrolysis at the early stage of dynamic digestion. The slightly smaller bolus particle size of S patties compared to L patties also resulted in more free amino groups in emptied liquid due to faster gastric emptying. These findings confirm the second part of our hypothesis (c) that smaller bolus particle size of PBMA patties after mastication accelerates gastric emptying and facilitates protein hydrolysis during dynamic *in vitro* gastric protein digestion. This also supports our assumption in section 5.3.1.4 that the smaller bolus particle size of THIS patties was responsible for the faster gastric emptying and greater protein hydrolysis during dynamic digestion compared to Beyond Meat patties. Consistent with this outcome, previous studies suggested a greater contribution of particle size than textural or mechanical properties to dynamic *in vitro* gastric protein digestion (Chen et al., 2024a; Lou et al., 2022; Sun et al., 2023). A study on tofu reported higher total amino acid content during the first 60 min of dynamic *in vitro* gastric digestion for harder tofu with smaller bolus particles compared to softer tofu with larger bolus particles, although after 120 min of digestion, harder tofu showed less total amino acids than softer tofu (Lou et al., 2022). For plant-based food ingredients, textured soy proteins (TSPs) with a harder texture but smaller particle size after mastication-mimicking grinding exhibited faster dynamic *in vitro* gastric digestion than softer TSPs with a larger particle size (Chen et al., 2024a).

The impact of bolus particle size on protein hydrolysis is more pronounced during dynamic than static *in vitro* gastric digestion. This was attributed to the different mechanisms by which bolus particle size influences protein hydrolysis. In static models, decreasing bolus particle size promotes protein hydrolysis depending on the extent of increase in total surface area. After *in vivo* mastication, it is possible that the total surface area of bolus remains similar despite significant differences in bolus particle size (as seen in the boli of commercial patties in this study). Consequently, other factors that affect protein hydrolysis, such as Young's modulus, may dominate and exert a greater influence on proteolysis during static digestion. In contrast, while using dynamic models that mimic gastric emptying, decreasing bolus particle size enhances protein hydrolysis by accelerating gastric emptying, which directly affects the intragastric pH and the retention time of foods in the stomach. Due to the high sensitivity of gastric emptying to particle size and proteolysis to intragastric pH, changes in bolus particle size and distribution have a primary effect on protein hydrolysis during dynamic digestion, regardless of variations in total bolus surface area or mechanical properties.

5.4. Conclusions

This study demonstrated that the impact of Young's modulus on protein hydrolysis was more pronounced during static than dynamic *in vitro* gastric digestion of PBMA patties after *in vivo* mastication. In contrast, the impact of bolus particle size was more pronounced during dynamic than static *in vitro* gastric digestion. In the advanced dynamic model that mimics gastric motility (NERDT), the smaller bolus particle size led to enhanced protein hydrolysis, surpassing the influence of Young's modulus which hindered protein hydrolysis during static digestion (INFOGEST). This suggests that using static digestion models to study *in vitro* gastric protein digestibility of foods may overestimate certain effects, such as those of the mechanical properties of foods. It is noted that using dynamic *in vitro* models like NERDT, which lack metabolic regulation of gastric fluid secretion, duodenal motility and intestinal signaling, may overestimate the effects of gastric emptying and the impact of bolus particle properties on gastric protein digestion. These outcomes suggest that future studies on *in vitro* protein digestion apply dynamic gastric-motility-mimicking models when investigating factors sensitive to gastric emptying, such as viscosity for semi-solid foods and particle size for solid foods. Regardless of the applied digestion model, results from *in vitro* digestion

studies should be interpreted with care considering the omission of gastrointestinal motility and/or metabolic regulation.

This study emphasizes the importance of oral macrostructural breakdown for gastric protein digestion. Oral macrostructural breakdown is influenced by food texture, leading to variations in bolus properties that can significantly impact gastric protein digestibility by modulating gastric emptying. This effect has likely been underestimated due to the common use of static *in vitro* digestion models. Therefore, we propose to include mastication of foods by humans followed by characterization of bolus properties as a first step in *in vitro* digestion studies.

5.5 Supplementary material

Supplementary Table 5.1. *Macronutrient compositions of two commercial patties (Beyond Meat Plant-based burger, Beyond Meat EU BV, and This Plant-based burger, THIS). The information is provided by the manufacturer.*

	Beyond Meat (per 100 g)	THIS (per 100 g)
Energy (kcal)	196	224
Fat (g)	12	15.5
Carbohydrates (g)	5.6	2.1
Dietary fiber (g)	1.2	3
Proteins (g)	16	14.3

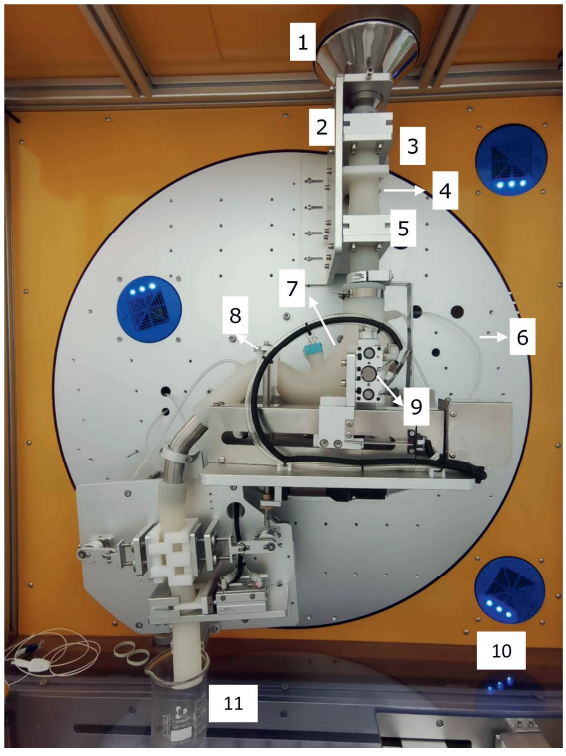

1: Funnel for sample loading
2: upper clamp of esophagus
3: esophagus vibrator
4: silicone esophagus model
5: lower clamp of the esophagus
6: gastric secretion tube
7: silicone stomach model
8: pyloric valve
9: stomach rolling-extrusion device
10: heating lamp
11: digesta collection beaker

Supplementary Figure 5.1. *The near-real dynamic gastric digestion model (Near Real Digestive Track, NERDT, Xiao Dong Pro-health Instrumentation Co. Ltd., Suzhou, China).*

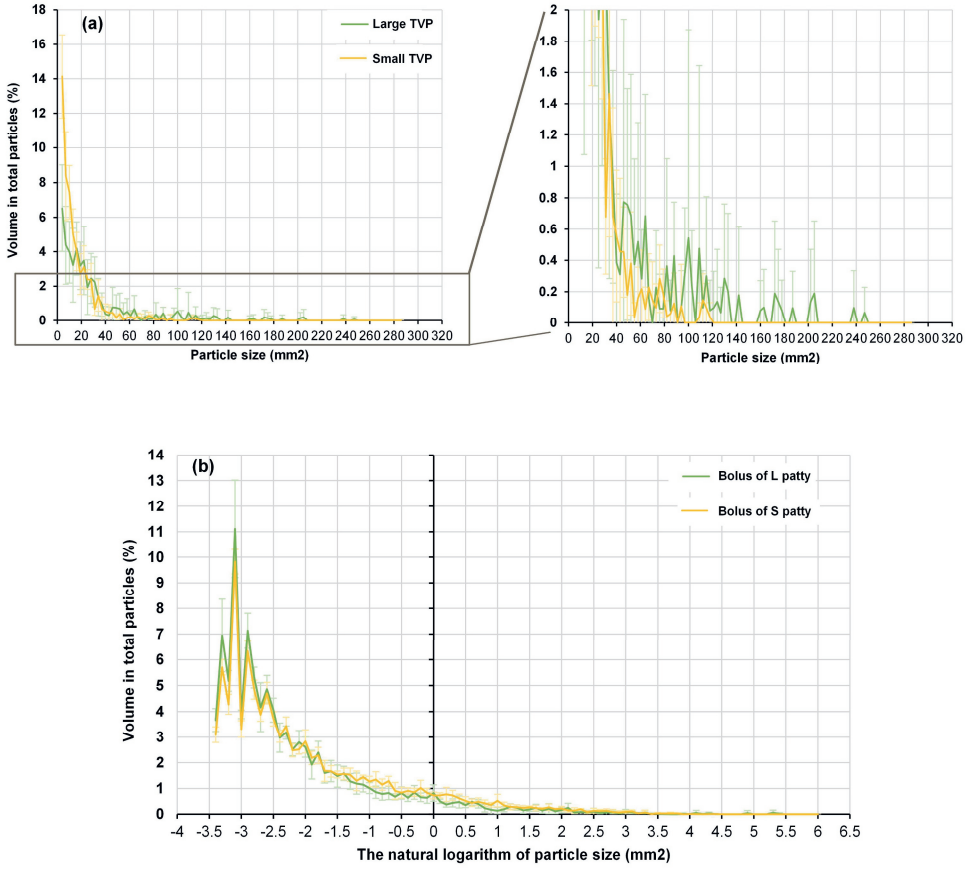

Supplementary Figure 5.2. *The particle size distribution of (a) rehydrated TVPs and (b) the bolus of plant-based meat analogue patties made from large (L patty) and small TVPs (S patty).*

Chapter 6

General discussion

6.1 Main findings

This thesis aimed to untangle the interplay between food microstructure, mechanical properties, oral macrostructural breakdown and *in vitro* gastric protein digestion of model foods and commercially available foods using static and dynamic models.

Figure 6.1 summarizes the key results of this thesis. For whey protein/polysaccharide mixed gels with similar mechanical properties, gels with homogeneous microstructure showed the highest degree of protein hydrolysis during static *in vitro* gastric digestion, followed by protein continuous, coarse stranded and bi-continuous gels **(Chapter 2)**. Increasing the Young's modulus (representing stiffness) of homogenous gels hindered protein hydrolysis whereas Young's modulus did not impact protein hydrolysis of protein continuous gels **(Chapter 2)**. Bi-continuous gels displayed the largest increase in protein hydrolysis after standard macrostructural breakdown caused by manually cutting a gel into several small cubes **(Chapter 2)**. After *in vivo* mastication, the increase in *in vitro* gastric protein digestion was not proportional to the degree of macrostructural breakdown during mastication and depended on gel microstructure. Bi-continuous gels exhibited the largest increase **(Chapter 3)**. The impact of microstructure on *in vitro* gastric protein digestion was also observed for textured vegetable proteins (TVPs) which are commonly used as the main ingredient in the production of plant-based meat analogues **(Chapter 4)**. For TVPs with a porous structure, pore size was positively correlated with protein hydrolysis during static *in vitro* gastric digestion. In contrast, wall density was negatively correlated with protein hydrolysis when the porous structure of the TVPs was removed. These correlations persisted for patties prepared from the TVPs highlighting the impact of microstructure on protein digestion in commonly consumed foods **(Chapter 4)**. In **Chapter 5**, two commercial plant-based meat analogue patties differing in mechanical properties (Young's modulus) and bolus properties after *in vivo* mastication exhibited opposite results in *in vitro* gastric protein digestion when using static or dynamic models. Smaller bolus particles facilitated protein hydrolysis, primarily impacting dynamic *in vitro* gastric digestion, whereas a higher Young's modulus hindered protein hydrolysis, primarily impacting static *in vitro* gastric digestion.

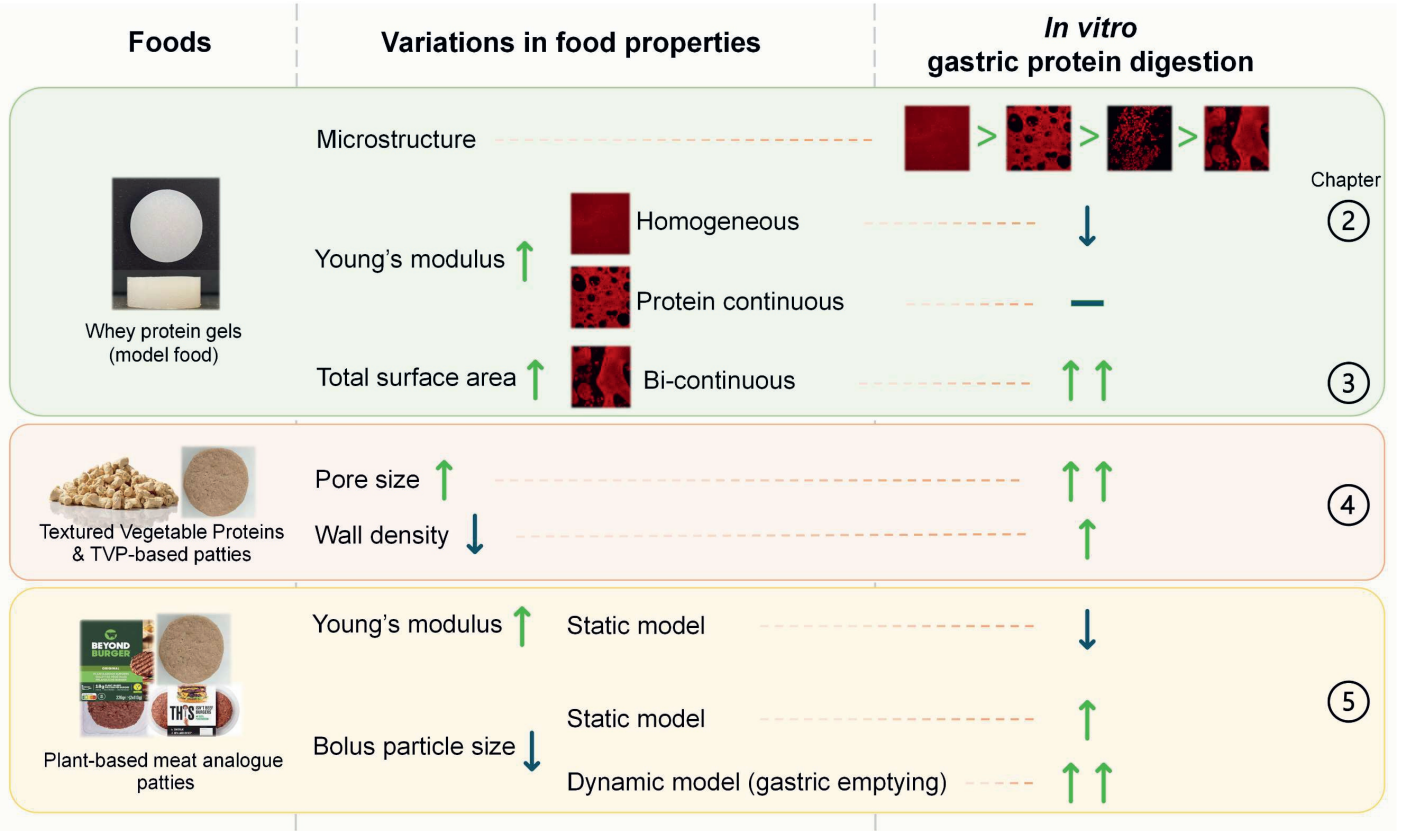

Figure 6.1. *Overview of the main findings of this thesis. Upward arrows indicate an increase in a property, downward arrows indicate a decrease. Straight lines indicate no change in a property; double arrows indicate a large change.*

In the following sections, these findings are discussed in relation to digestion methodologies accompanied by suggestions for future *in vitro* digestion studies. A preliminary concept of food structure design to optimize protein digestion is provided along with the challenges and future directions.

6.2 The interplay between food microstructure, mechanical properties, macrostructural breakdown and in vitro gastric protein digestion models

Figure 6.2 illustrates the proposed mechanisms through which food microstructure, mechanical properties and macrostructural breakdown influence gastric protein digestion along with the features of the *in vitro* digestion models used in this thesis.

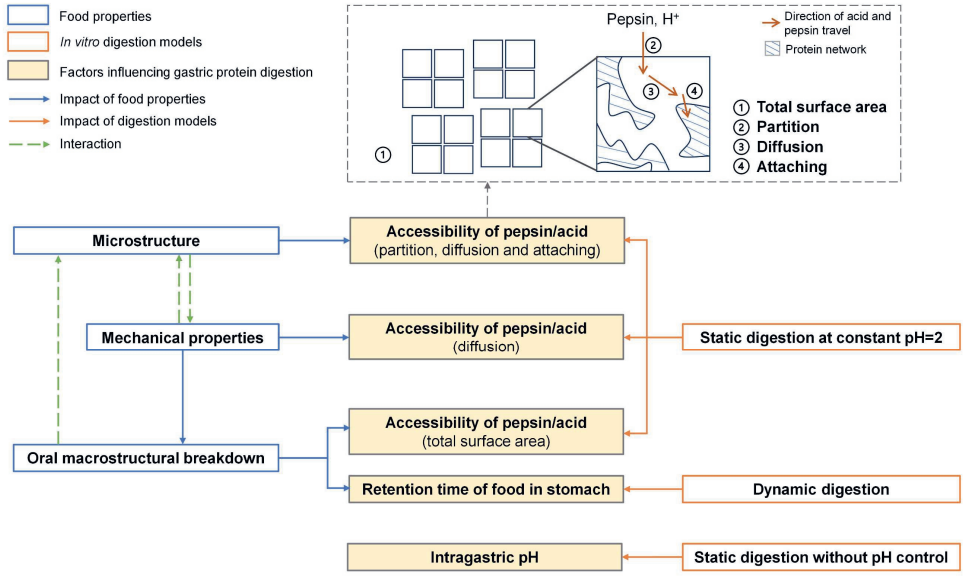

Figure 6.2. *Proposed mechanisms underlying the interplay between food microstructure, mechanical properties and macrostructural breakdown and in vitro gastric protein digestion determined using static and dynamic models.*

Proposed mechanisms by which food microstructure, mechanical properties and macrostructure breakdown impact gastric protein digestion:

- Food microstructure influences gastric protein digestion mainly by modulating the accessibility of acid and pepsin to protein molecules. This includes acid/pepsin

partitioning at the food-gastric fluid interface (Chapter 3), acid/pepsin diffusion in the food particle (Thévenot et al., 2017) and pepsin attachment to proteins (Singh et al., 2014) (see inlet figure 6.2).

- Food mechanical properties influence gastric protein digestion by two ways: First, mechanical properties influence the extent of macrostructural breakdown during oral processing, which affects the size and total surface area of bolus particles (Chapter 2 and 5). Second, mechanical properties affect the swelling/shrinking behavior of food and bolus particles, which may alter the microstructure and thereby the accessibility of acid and pepsin to proteins (Deng et al., 2020).

- Macrostructural breakdown influences gastric protein digestion by increasing the total surface area through which acid and pepsin diffuse into food particles during static *in vitro* digestion (Chapter 2). During dynamic *in vitro* digestion, macrostructural breakdown affects gastric protein digestion by modulating particle-size-dependent gastric emptying, which strongly affects the retention time of foods in the stomach and consequently its protein digestion (Chapter 5).

The features of the in vitro digestion models used in this thesis:

- Static digestion without pH control: This method is adapted from the static INFOGEST 2.0 protocol. During digestion, the pepsin concentration and gastric content remain nearly unchanged, but the intragastric pH can be remarkably altered due to the buffering effect of digested foods. This model provides an efficient and straightforward setup to investigate gastric protein hydrolysis. However, the increased pH during digestion may affect pepsin activity and consequently protein hydrolysis.

- Static digestion at constant pH=2: This method is adapted from the INFOGEST 2.0 protocol. During digestion, the intragastric pH is kept at 2 via a titration set-up. The pepsin concentration and gastric content remain nearly constant. This model creates optimal conditions for protein hydrolysis by maintaining the ideal pH during digestion. Therefore, the ability of foods to absorb acid and pepsin becomes the most dominant factor affecting gastric protein digestion.

- For the dynamic *in vitro* digestion, the NEar Real Digestive Track (NERDT) model was used. During dynamic *in vitro* digestion, the secretion of acid and gastric fluid containing pepsin is programmed, guiding the kinetic changes over time. Gastric contractions are simulated three times per minute. Gastric emptying occurs spontaneously as digestion progresses by opening the pylorus to 4 mm once per minute. Consequently, intragastric pH, the amount of food in the stomach, and pepsin concentration differ spatially within the simulated stomach and change as digestion continues, affecting the gastric protein digestion kinetics. This model provides realistic gastric motility. However, the setup requires time and effort to optimize operation settings for specific foods.

Food microstructure, mechanical properties, macrostructural breakdown impact gastric protein digestion through different mechanisms which occur simultaneously. *In vitro* digestion models place varying emphasis on simulating gastric digestion conditions. The static digestion model with constant pH=2 emphasizes the ability of foods to absorb acid and pepsin. The digestion using the static model without pH control can be limited by increased pH in the vessel. Dynamic digestion strongly depends on the kinetic changes in the retention time of foods in the stomach. All these variations affect the gastric protein digestion of foods differing in structure. The following section discusses the interplay between food structure and gastric protein digestion under varying conditions.

6.2.1 Oral macrostructural breakdown alters the impact of microstructure on static in vitro gastric protein digestion

In Chapter 2, we reported higher protein digestion rates during static *in vitro* gastric digestion for whey protein gels with homogeneous microstructure compared to gels with heterogeneous microstructure, including bi-continuous gels. We proposed four explanations including the differences in pepsin partition at gel-liquid interface caused by microstructure. However, in Chapter 3, it was reported that bi-continuous gels that displayed the lowest digestion rate (Chapter 2) had the highest partition coefficient of simulated pepsin at gel-liquid interface (i.e., there was higher pepsin concentration inside the surface of bi-continuous gels compared to other gels). This finding contrasts the proposed third

explanation in Chapter 2, which suggested that homogeneous gels might have higher pepsin concentration inside the gel surface, promoting their protein digestion. Therefore, in Chapter 2, the lower protein digestion rate of bi-continuous gels compared to homogeneous gels can be attributed to their denser protein aggregates in the protein-rich phase. This seemed to have hindered the attachment of pepsins to protein molecules. In other words, for bi-continuous gels, denser protein aggregates limited pepsin attachment to proteins, affecting hydrolysis more than the increased pepsin partitioning at the gel surface due to high phase connectivity.

Interestingly, this outcome is observed only in intact gels before macrostructural breakdown is induced by mastication. In Chapter 3, after oral macrostructural breakdown, we found higher protein digestion rates for bi-continuous gels than for homogeneous gels despite both gels showing similar total bolus surface area and Young's modulus. It is assumed that the large increase in total surface area by 3.4-fold after mastication enhanced the effect of pepsin partition at the gel-liquid interface on protein hydrolysis by reducing the time needed to reach the maximum pepsin concentration in the gel matrix. The combined results of Chapter 2 and 3 suggest that oral macrostructural breakdown can alter the mechanism by which microstructure influences protein hydrolysis. This finding highlights the importance of including a realistic oral phase in *in vitro* digestion studies. The omission of oral phase may potentially alter the conclusions when studying the impact of microstructure on gastric protein digestion.

In Chapter 4, we concluded that for textured vegetable proteins (TVPs) with porous structure, increasing pore size contributes more to enhancing protein hydrolysis during static *in vitro* gastric digestion of TVPs and TVP-based patties than decreasing wall density. However, as discussed above, macrostructural breakdown during mastication interacts with microstructure, which may affect the outcome. For the TVPs studied in Chapter 4, the porous structure varies at the micro to millimeter scale. After mastication, the bolus particle size of TVP-based patties ranged from 0.50-1.05 mm^2 (Chapter 5). It is speculated that oral macrostructural breakdown of TVPs could decrease pore size of the TVPs, diminishing the impact of pore size while increasing the impact of wall density.

6.2.2 Comparing the relative impact of food properties on dynamic in vitro gastric digestion: Macrostructural breakdown > mechanical properties > microstructure

In Chapter 5, we demonstrated that dynamic gastric emptying increases the impact of oral macrostructural breakdown on gastric protein digestion due to its sensitivity to particle size. It has been discussed in Chapter 5 that bolus particle size can exhibit a more pronounced impact on dynamic gastric protein digestion of plant-based meat analogue patties than Young's modulus. Dynamic *in vitro* gastric protein digestion primarily depends on gastric emptying, as it modifies the retention time of foods in the stomach, as well as intragastric pH and pepsin concentration. Therefore, food microstructure, which has minimal influence on gastric emptying, is less likely to influence dynamic *in vitro* gastric protein digestion. It can be speculated that the size and distribution of bolus particles, which have primary impact on gastric emptying, dominate the dynamic gastric protein digestion of foods differing in microstructure.

As for the relative impact of microstructure and mechanical properties on dynamic gastric protein digestion, it is hypothesized that mechanical properties may exhibit a greater impact on dynamic gastric protein digestion than microstructure. This is because mechanical properties are closely related to bolus particle disintegration (Guo et al., 2015; Kong & Singh, 2008a). Decreasing the hardness of carrots by cooking accelerated the *in vitro* gastric disintegration of carrots (Kong & Singh, 2008a). Both initial hardness and softening rate in gastric juice were recommended to be considered to classify the food breakdown behavior during gastric digestion (Bornhorst et al., 2015). Therefore, food mechanical properties could to some extent influence gastric emptying by affecting particle disintegration during gastric digestion. This impact may not be as strong as the impact of initial size and distribution of bolus particles after mastication, it may act more as a modification of the impact of bolus particle properties on gastric emptying. Nevertheless, compared to microstructure which barely affects gastric emptying, foods with mechanical properties that benefit gastric particle disintegration (such as brittle foods) may have a stronger impact on dynamic gastric protein digestion.

It is important to note that the magnitude of structural modifications needs to be carefully considered when comparing the relative contributions of different food properties to gastric

protein digestion. For example, a 10-fold increase in the Young's modulus of protein gels may have less impact on dynamic *in vitro* gastric protein digestion than a 0.5-fold decrease in bolus particle size. However, a 50-fold increase in Young's modulus could likely result in a smaller degree of protein digestion by significantly increasing the resistance of bolus particles to proteolysis, even with the smaller particle size.

6.2.3 The impact of macrostructural breakdown on in vivo gastric emptying

Although dynamic digestion models mimic gastric motility, bringing them closer to real physiological conditions, they lack some simulations that can considerably impact gastric digestion, such as hormonal feedback regulations (Mackie, 2023; Singh, 2024). Therefore, the outcomes of *in vitro* digestion studies should be validated *in vivo*. In Chapter 5, we reported that during dynamic *in vitro* gastric protein digestion using the NERDT, PBMA patties with small bolus particles showed faster gastric emptying than PBMA patties with large bolus particles. To validate this result (Chapter 5), a preliminary *in vivo* study was performed. Three volunteers were asked to consume the patties following a fixed chewing protocol, and their gastric volumes were monitored for 90 min after ingestion using magnetic resonance imaging (MRI) (Figure 6.3).

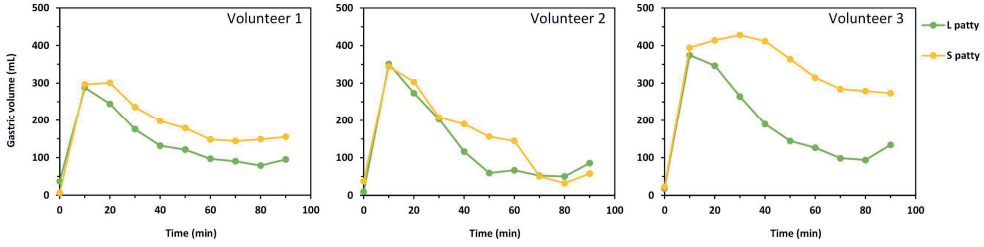

Figure 6.3. *In vivo human gastric volumes after consumption of PBMA patties prepared from large (16 mm^2, L patty) and small TVPs (8 mm^2, S patty). TVP: textured yellow pea protein.*

Gastric volumes of three volunteers decreased after ingestion of patties. However, it is unexpected that, during *in vivo* digestion, the patties prepared from small TVPs consistently exhibited slower gastric emptying than the patties prepared from large TVPs. Patties prepared from small TVPs displayed larger gastric volumes over time, although the differences between the two patties varied among the three participants (Figure 6.3). This preliminary result is contrary to the results described in Chapter 5, indicating that *in vivo* gastric emptying

of PBMA patties is affected by other factors that were not mimicked in the dynamic *in vitro* digestion model. We speculate that the slower gastric emptying of S patties may be due to the hormonal regulation resulting from faster nutrient exposure in the small intestine (Akhavan et al., 2014; Karamanlis et al., 2007). Although the model patties in this study had the same protein content (14 w/w%), the smaller TVP particle size may have promoted the digestion of other nutrients, such as carbohydrates and lipids. The faster exposure of these nutrients in the small intestine could stimulate the release of glucagon-like peptide-1 (GLP-1) which slows down gastric emptying and gastric acid secretion (Frost et al., 2003; Layer et al., 1995). The bottom line is that while the NERDT has done an excellent job mimicking the morphological and mechanical conditions of gastric environment, *in vitro* gastric emptying might still differ considerably compared to *in vivo gastric* emptying due to its omission of hormonal regulations. It should be noted that these *in vivo* observations come from an explorative pilot study. A larger sample size would be needed to draw firm conclusions. Further studies on the impact of bolus particle size on *in vivo* gastric emptying and gastric protein digestion of PBMA patties are needed.

6.3 Suggestions for oral-to-intestinal in vitro digestion studies

6.3.1 Methods for performing standardized mastication

This thesis emphasizes the importance of realistic oral macrostructural breakdown in digestion studies, highlighting the necessity of including the oral phase in *in vitro* digestion studies and improving the relevant methods. *In vivo* mastication and expectoration of food boli are easy to perform and being integrated with *in vitro* gastrointestinal digestion. However, significant inter-individual variation in oral structural breakdown due to differences in mastication behavior and oral physiology can introduce variability in bolus properties, consequently adding variability to the outcomes of the *in vitro* digestion studies. Therefore, for studies focusing on the impact of food properties on *in vitro* digestion, rather than on the impact of mastication behavior, it is essential to standardize mastication to minimize inter-individual variation. Available methods for performing standardized mastication are summarized in Figure 6.4.

	***Standardized in vivo* mastication** (following an instructed chewing protocol)		**Standardized *in vitro* mastication simulation** (following a fixed protocol)	
	By a group of participants	**By a single person**	**By mincing**	**Using a mastication simulator**
Bolus sample	Sampling from pooled boli	Complete real bolus	Complete artificial bolus	Complete artificial bolus
Example	Chapter 3	Chapter 5	Guo et al., 2015	Peyron et al., 2021
Advantages	*In vivo* mastication Reduced inter-individual variation	*In vivo* mastication and complete boli	Convenient, efficient	Objective, reproducible
Disadvantages	Properties of sampled boli may differ from complete boli	Bolus properties depend on the person's oral physiology	Less realistic bolus properties	Require relevant facilities

Figure 6.4. *Summary of methods for performing standardized mastication.*

Standardized *in vivo* mastication can be achieved by following an instructed chewing protocol that define bite size, chewing frequency and number of chews. These parameters regarding chewing behavior need to be determined based on natural *in vivo* mastication. Standardized *in vivo* mastication can be performed either by a group of participants (Chapter 3) or by one person (Chapter 5). The boli collected form instructed *in vivo* mastication by a group of participants are pooled. Bolus samples for subsequent *in vitro* digestion are taken from the pooled boli. This method reduces inter-individual differences, but the properties (e.g., particle size distribution) of bolus particles sampled from pooled boli may differ from those of complete boli expectorated after *in vivo* mastication. Standardized *in vivo* mastication performed by a single person allows for studying the digestion of complete expectorated boli. However, the bolus properties would depend on the oral physiology of the person who chews the samples.

The alternative of standardized *in vivo* mastication is standardized *in vitro* oral phase simulation following a fixed protocol. A easy way to simulate mastication is mincing foods while mixing with simulated saliva fluid, as described in the INFOGEST 2.0 protocol (Brodkorb et al., 2019). Some studies applying this method to produce artificial boli that had similar bolus particle size as real boli collected from *in vivo* mastication on the same samples (Guo et al., 2015, 2016). Most *in vitro* digestion studies simply mince their samples without using real bolus properties as guidance (Bayrak et al., 2021; Hiolle et al., 2020; Homer et al., 2021; Xie et al., 2022; Zhang et al., 2023b). Consequently, the boli produced through this method might exhibit significantly different properties from real boli formed by *in vivo* mastication. For instance, simulating mastication by blending roasted peanut produced boli with higher moisture content and larger mean particle size compared to real boli formed

through *in vivo* mastication (Xu et al., 2024). Simulating mastication using advanced mastication simulators that closely mimic oral physiology could help producing boli with more realistic bolus properties (Xu et al., 2024). Multiple mastication simulators such as the artificial masticatory advanced machine (AM^2) (Peyron et al., 2019), the bite master II (Meullenet & Gandhapuneni, 2006), the chewing robot (Wang et al., 2015) and the *in vitro* bio-inspired oral mastication simulator (iBOMS-III) (Xu et al., 2024) have been developed over the past decades. These models are developed to study the kinetics of food oral processing including oral breakdown and the release of flavor compounds (Guo et al., 2024). AM^2 has been applied in several *in vitro* digestion studies (Blanquet-Diot et al., 2021; Peyron et al., 2021; Ribes et al., 2024). These studies applied the number of chews during *in vivo* mastication to set the operation parameters of AM^2 to obtain artificial boli. Standardizing the design of these simulators and developing relevant operational protocols for different food categories according to *in vivo* oral processing could provide a reproducible and objective method for collecting boli for *in vitro* digestion studies.

To sum up, multiple methods are available for performing standardized mastication. The strengths and limitations along with other aspects need to be considered when selecting methods. For instance, instructed *in vivo* mastication for elderly individuals or patients can be challenging, whereas simulating mastication using advanced mastication simulators may be unfeasible due to a lack of facilities. Regardless of the method used, information on natural *in vivo* mastication, such as bite size, number of chews, chewing frequency, and bolus properties, is required to provide guidance for standardizing mastication.

6.3.2 In vitro gastrointestinal digestion studies

The applied *in vitro* digestion model remarkably influences the *in vitro* digestion outcomes as shown in Chapter 5 and a few other studies (Homer et al., 2021; Mella et al., 2021). Therefore, *in vitro* digestion studies need to carefully consider the choice of *in vitro* models which vary from simple static models to near-real dynamic models. Additionally, other aspects need to be considered alongside digestion models, including study samples (ranging from simplified model foods to full meals), whether the study focuses on digestion kinetics or endpoints, and the targeted populations (general healthy adults or specific groups such as infants or elderly) (Duijsens et al., 2022). For studies aiming to understand the interactions

between food properties and macronutrient digestibility, the author suggests to start by investigating the digestion kinetics using simplified model foods and simple static models. These simple static models allow to manipulate variables easily and the interpretation of outcomes are usually straightforward. One of the advantages of *in vitro* digestion studies compared to *in vivo* studies is the great flexibility to control digestive conditions. Starting directly with complex methodologies could introduce unnecessary difficulties in interpreting results. After identifying relevant properties and gaining mechanistic insights through simplified methodologies, the complexity can be gradually increased to investigate more detailed interactions. Finally, advanced dynamic digestion models that closely mimic digestive physiology can be applied to explore the digestion of complex food or meals. The added complexity would help to bridge the gap between *in vitro* studies and *in vivo* reality, while the outcomes influenced by multiple variations can be properly explained by the underlaying mechanisms learned from simple models.

It is crucial to keep in mind that all *in vitro* models have specific features that can introduce bias. For example, static models usually overemphasize the accessibility of enzymes to substrates, thereby overestimating the impact of food properties that directly affect enzyme accessibility, such as microstructure. In contrast, gastric-emptying-mimicking models could overestimate the impact of food properties that directly affect gastric emptying, such as particle size, due to their lack of metabolic regulation. Interpretating *in vitro* results with awareness of the features and limitations of the applied models can avoid misinterpretations caused by shortcomings of the simulated digestive conditions.

The strengths and limitations of various *in vitro* digestion models have been reviewed along with suggestions for improvements (Bohn et al., 2018; Duijsens et al., 2022; Dupont et al., 2019; Li et al., 2020; Mackie et al., 2020). These reviews give constructive advice including standardizing dynamic digestion models and integrating current *in vitro* gastrointestinal digestion models with *in vitro* absorption systems that involve intestinal digestion and absorption via brush border membranes (Mackie et al., 2020). However, efforts to improve *in vitro* digestion systems are often focused on the gastrointestinal tract, with less attention given to the oral phase. Integrating *in vivo* mastication or realistic *in vitro* oral phase simulation in *in vitro* gastrointestinal digestion methods is highly recommended. Developing

and standardizing oral-to-intentional *in vitro* digestion protocol could significantly benefit studies on the role of oral processing in food digestion.

6.4 Designing food structures to modify protein digestibility

Food structure design refers to the concept of controlling the release of dietary lipids and carbohydrates or delivering bioactive components in the gastrointestinal tract (McClements et al., 2008, 2009; Pellegrini et al., 2020). A systematic concept of food structure design focusing on modifying protein digestibility is missing. Here, we propose a preliminary concept of food structure design to optimize protein digestion based on the outcomes of this thesis and previous studies.

6.4.1 Proposed guideline: from molecular to macroscopic scale

The following aspects need to be considered when designing food structures with the aim to maximize gastric protein digestibility (Bornhorst et al., 2016). Examples of structures at difference length scales are given in Figure 6.5.

a) **Molecular / nanometer scale (< 1 µm):**
First, the molecular protein composition, i.e., the amino acid composition, can be improved by mixing various proteins (Gorissen et al., 2018). Proteins differ significantly in their amino acid profiles and combinations of various proteins aid in balancing the essential amino acids, enhancing protein quality (Adhikari et al., 2022; Jiménez-Munoz et al., 2021; Sá et al., 2020b). Secondly, it has been shown that pepsin tends to cleave the peptide bonds involving hydrophobic aromatic amino acids which are often directed toward the interior of the protein structure (Gajdos et al., 1963). Therefore, at molecular scale, the key to improve protein digestibility is to expose these peptide bonds as much as possible to pepsin by unfolding the protein structure. Increasing the fraction of disordered structure such as random coil while decreasing the ordered structure such as β-sheet can aid in protein hydrolysis of legume proteins (Sun et al., 2020; Yang et al., 2016). These modification on the secondary structure can be achieved by processing (e.g., microwave or heating) or

changing the protein sources. Modifications on proteins (i.e., denaturation) that can open the tertiary or quaternary structure can also help proteolysis. It should be noted that processes such as severe heating result in formation of protein aggregates which increases the number of disulfide bonds and inhibits proteolysis (Duodu et al., 2002).

b) Microscopic scale (1 µm - 1 mm):

At the micrometer scale, micro-phase separation can occur due to interactions between components or protein aggregations (Chapter 2; Singh et al., 2014). Generally, for heterogeneous microstructures, porous structures and less compact protein networks are preferred. For instance, soy protein gels with porous protein network with pores of approximately 10 µm diameter showed higher protein hydrolysis than gels with compact, thin, layer-like protein networks (Zhao et al., 2020). In contrast, at larger scales, around 100-200 µm, a homogeneous structure is preferred instead of microphase separation (Chapter 2). This is because at larger scale, a heterogeneous structure often indicates a dense protein network in a protein-rich phase (Singh et al., 2014). Specially, at this length scale, spatial barriers such as cell walls should be avoided (Zahir et al., 2018). These findings are based on model systems as study subjects. Modifying the microstructure of foods is possible by adjusting the formulation and processing conditions. The translation of these findings from model systems to commercially available foods should be explored in future studies.

c) Macroscopic scale (> 1 mm):

At the macroscopic scale, the impact of structure on digestion could be associated with multiple factors. For individual food particles, an open structure, such as the large pores in TVPs, could facilitate protein hydrolysis. Additionally, increasing macroscopic surface area enhances static *in vitro* gastric protein digestion (Chapter 4). Furthermore, solid foods are often broken down into food fragments ranging from millimeters to centimeters during oral mastication. Increasing the fraction of small fragments (i.e., decreasing the mean particle size) tended to enhance protein hydrolysis during *in vitro* dynamic gastric digestion (Chapter 5), although *in vivo* studies are needed to validate this finding. Food structures at the millimeter scale can be modified by food processing, such as altering TVP structure by adjusting

extrusion conditions. Control of macroscopic surface area or particle size of food boli could be achieved by modifying food texture, for example, brittle foods tend to form more and smaller food particles, thereby increasing total surface area. These associations enable food designers to modify food structure and texture through processing techniques to optimize protein digestibility.

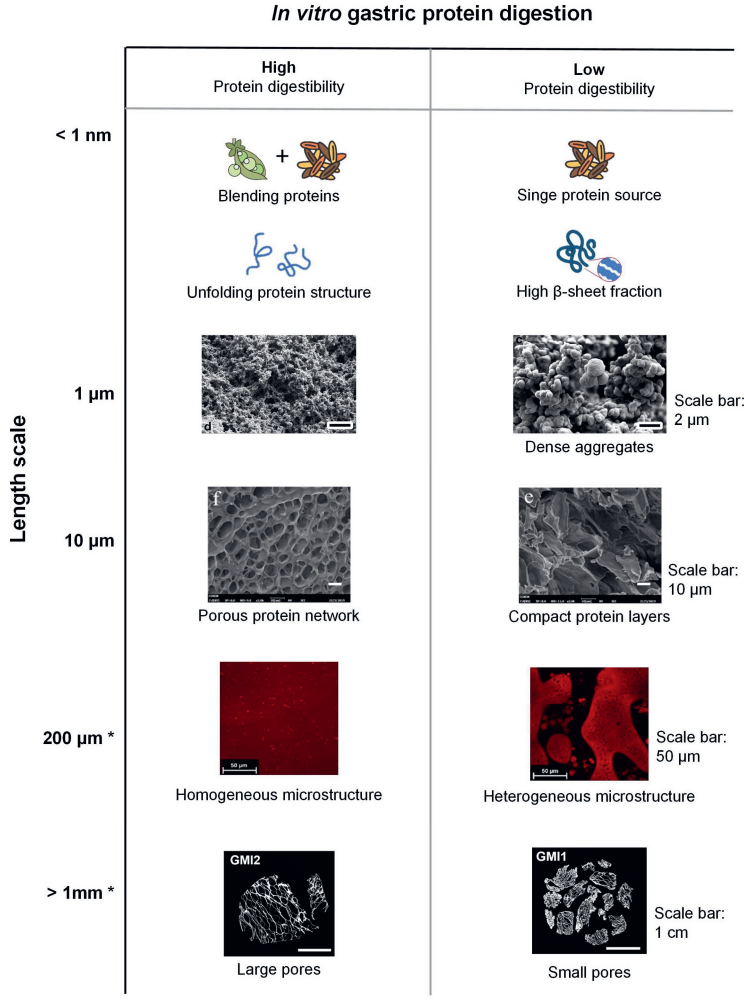

* Oral macrostructural breakdown may affect the impact of these structures on *in vitro* protein digestibility.

Figure 6.5. *Examples of food structure at different length scales and their influence on in vitro gastric protein digestion. Images are reproduced from Chapter 2, Chapter 4, Zhao et al. (2020) and MacIerzanka et al. (2012).*

6.4.2 Challenges and future directions

Modifying protein digestibility by altering food structure as described in section 6.4.1 is challenging for various reasons. The first is the inevitable associations between sensory perception and food structure. Food structure at different length scales is known to impact sensory properties of foods, so it is important to quantify the sensory properties of the structurally modified foods together with the protein digestibility. Additionally, reverse engineering of food structure tailored to a specific digestion of macronutrients requires deep understanding of the structure formation mechanisms during food processing. Furthermore, the complex interactions between food structures and digestion as shown in this thesis require compromises. Non-structural properties, such as pH, temperature of foods and the combination of different food items into meals, may show a greater impact on protein digestion than structure of individual food items.

Future studies should explore sensory perception, oral behavior, breakdown of foods differing in structure and macronutrient bioavailability. Fundamental understanding of the formation of food structure at different length scales in the context of complex formulas and processing techniques could aid in the implementation of structural design. Moreover, the interactions between food structure and special digestive conditions of specific populations such as elderly and gastrointestinal disease patients need further investigation. Development of *in vitro* digestion systems tailored to these specific groups could facilitate the relevant studies.

6.5 Concluding remarks

In this chapter, the interplay between food structure and *in vitro* digestion models is discussed, followed by suggestions for *in vitro* digestion studies. Including real or realistic mastication as a standardized step before *in vitro* gastrointestinal digestion is recommended. For studies investigating the impact of food properties on macronutrients digestion, simple static *in vitro* models can be a good starting point. Increasing the complexity of *in vitro* models helps to better understand potential interactions during digestion. Interpreting *in vitro* digestion results with awareness of the strengths and limitations of applied models is crucial to avoid misinterpretation caused by simulated digestive conditions. Furthermore, designing food

structures to optimize protein digestibility requires collaboration across fields including food physics, food engineering, sensory and nutrition science. Although there is a long way to go, tailoring food structure to meet specific nutritional needs could offer a promising solution to address global challenges related to malnutrition and obesity.

Summary

Due to increasing global population, limited resources, and environmental challenges, it is crucial to establish a more efficient and sustainable food system. Enhancing the digestibility of proteins, which are essential for growth and metabolism, is a key focus. The shift away from animal-based proteins, due to their resource intensity and greenhouse gas emissions, has led to the rise of plant-based meat alternatives. However, these alternatives often have low protein digestibility due to the unbalanced amino acid composition and the presence of anti-nutritional factors. Nevertheless, new protein sources and technologies present opportunities to improve food texture and structure, enhancing protein digestibility and thereby improving the nutritional value of meat analogues. A thorough understanding of the interactions between food structure and the protein digestion is essential for developing nutritious foods. This thesis aimed to untangle the interplay between food microstructure, mechanical properties, macrostructural breakdown caused by oral processing, and gastric protein digestion using *in vitro* digestion models.

We started with model foods (whey protein gels) and static *in vitro* digestion models to explore the interplay between microstructure, mechanical properties, macrostructural breakdown and *in vitro* gastric protein digestion (**Chapter 2**). Whey protein isolate/polysaccharide mixed gels were developed to obtain gels with distinct microstructures (homogeneous, coarse stranded, bi-continuous and protein continuous) but similar mechanical properties (Young's modulus). During static *in vitro* gastric protein digestion, homogeneous gels displayed the highest digestion rate followed by protein continuous, coarse stranded and bi-continuous gels. Increasing Young's modulus led to decrease in protein digestion rate for homogeneous gels, while it did not influence the protein digestion for protein continuous gels. Increasing the total surface area by a factor of 2.6 enhanced protein digestion rate to different extents depending on gel microstructure. We concluded that microstructure has independent impact on *in vitro* gastric protein and this impact interacts with mechanical properties and macrostructural breakdown.

In **Chapter 3**, the whey protein isolate/polysaccharide mixed gels differing in microstructure were chewed by a group of people following a standard chewing behaviour. Both intact gels and expectorated boli were subjected to static *in vitro* gastric protein digestion to investigate the impact of microstructure on protein digestion after *in vivo* mastication. The results show that the increase in *in vitro* gastric protein digestion was not proportional to the degree of

macrostructural breakdown during mastication and depended on gel microstructure. Bi-continuous gels exhibited the largest increase which might be attributed to their highest partition coefficient of pepsin at the gel-gastric juice interface. We concluded that the impact of microstructure on *in vitro* gastric protein digestion is sustained after great macrostructural breakdown induced by *in vivo* mastication.

Chapter 4 moved from model gels to textured vegetable proteins (TVPs) which are the main ingredients in plant-based meat analogues (PMBAs). This study aimed to investigate the impact of structural properties of TVPs on *in vitro* gastric protein digestion of TVPs and TVP-based meat analogue patties in a quantitative way. Eight TVPs differing in structural properties, such as surface area, porosity, pore size and wall density, were used to prepare TVP-based meat analogue patties. Both TVPs and TVP-based patties were subjected to static *in vitro* gastric protein digestion. Additionally, these TVPs were ground into powders to remove the porous structure as a control group. The results show that macroscopic surface area and pore size were positively correlated with protein hydrolysis, while wall density was negatively correlated with protein hydrolysis when porous structure was removed. We concluded that in addition to macroscopic surface area, pore-related, rather than wall-related properties were primary structural properties influencing *in vitro* gastric protein digestion of TVPs and TVP-based patties.

In **Chapter 5**, a dynamic gastric-motility-mimicking model (NERDT) was used for studying *in vitro* gastric protein digestion of PBMAs in addition to a static digestion model (INFOGEST). This study aimed to explore the impact of mechanical and bolus properties on *in vitro* gastric protein digestion of PBMA patties using static and dynamic models. Two commercial patties (Beyond Meat and THIS) differing in Young's modulus and bolus particle size were subjected to static and dynamic digestion. THIS patties had higher Young's modulus and were broken down into more and smaller particles during *in vivo* mastication compared to Beyond Meat patties. During static digestion, THIS patties showed lower free amino group concentrations in gastric juice compared to Beyond Meat patties, which was likely due to their stiffer texture. In contrast, during dynamic digestion, THIS patties displayed faster gastric emptying and higher free amino group concentrations in the emptied liquid compared to Beyond Meat patties. These results suggest that bolus particle size had a primary impact on dynamic *in vitro* gastric protein digestion of PMBA patties. To further

investigate the impact of bolus properties, three model PBMA patties were prepared from textured yellow pea proteins differing only in particle size. The patties with bolus particles smaller than 0.18 mm^2 exhibited faster gastric emptying and higher free amino group concentrations in the emptied liquid at the early stage of dynamic digestion as compared to patties with larger bolus particles (0.59-0.68 mm^2). We concluded that bolus particle size, rather than mechanical properties, primarily impact dynamic gastric protein digestion. Specifically, smaller bolus particles facilitate dynamic *in vitro* gastric protein digestion by accelerating gastric emptying and modulating intragastric pH.

Chapter 6 discussed the main results of chapter 2-5 and provided suggestions for *in vitro* digestion studies. For *in vitro* digestion studies, static models can be a reliable starting point and follow-up experiments using advanced dynamic models can help to bridge the gap between *in vitro* simulation and *in vivo* reality. *In vivo* mastication or realistic oral phase simulation should be integrated with *in vitro* digestion methods. Moreover, a preliminary concept of designing food structure at different length scales to optimize protein digestibility is provided along with challenges and future directions, suggesting the potential of modifying protein digestibility by manipulating food structure.

In conclusion, this thesis demonstrated the interactions between microstructure, mechanical properties, (oral) macrostructural breakdown and *in vitro* gastric protein digestion of model foods and complex foods using static and dynamic models. The main findings indicate the potential to optimize protein digestibility by modulate food structures at both the micro- and macroscopic levels. The importance of *in vivo* mastication or realistic mastication simulation prior to *in vitro* gastrointestinal digestion is highlighted in this thesis. The conclusions drawn in this thesis are based on optimal oral-to-intestinal conditions which are typically shown in healthy adults. Further studies are needed to transfer these conclusions to specific populations such as infants and elderly.

References

Abrahamse, E., Thomassen, G. G. M., Renes, I. B., Wierenga, P. A., & Hettinga, K. A. (2022). Gastrointestinal Protein Hydrolysis Kinetics: Opportunities for Further Infant Formula Improvement. *Nutrients*, *14*(7). https://doi.org/10.3390/nu14071512

Acevedo-Fani, A., Roy, D., Do, D. T., & Singh, H. (2022). Understanding food structure modifications during digestion and their implications in nutrient release. *Food Structure Engineering and Design for Improved Nutrition, Health and Well-being* (pp. 277–314). Elsevier. https://doi.org/10.1016/B978-0-323-85513-6.00010-4

Adhikari, S., Schop, M., de Boer, I. J. M., & Huppertz, T. (2022). Protein Quality in Perspective: A Review of Protein Quality Metrics and Their Applications. *Nutrients*, *14*(5). https://doi.org/10.3390/nu14050947

Aguayo-Mendoza, M. G., Ketel, E. C., van der Linden, E., Forde, C. G., Piqueras-Fiszman, B., & Stieger, M. (2019). Oral processing behavior of drinkable, spoonable and chewable foods is primarily determined by rheological and mechanical food properties. *Food Quality and Preference*, *71*, 87–95. https://doi.org/10.1016/j.foodqual.2018.06.006

Aiking, H., & de Boer, J. (2020). The next protein transition. *Trends in Food Science and Technology*, *105*, 515–522. https://doi.org/10.1016/j.tifs.2018.07.008

Akhavan, T., Luhovyy, B. L., Panahi, S., Kubant, R., Brown, P. H., & Anderson, G. H. (2014). Mechanism of action of pre-meal consumption of whey protein on glycemic control in young adults. *Journal of Nutritional Biochemistry*, *25*(1), 36–43. https://doi.org/10.1016/j.jnutbio.2013.08.012

Alpos, M., Leong, S. Y., Liesaputra, V., Martin, C. E., & Oey, I. (2021). Understanding in vivo mastication behaviour and in vitro starch and protein digestibility of pulsed electric field-treated black beans after cooking. *Foods*, *10*(11). https://doi.org/10.3390/foods10112540

Azzollini, D., Derossi, A., Fogliano, V., Lakemond, C. M. M., & Severini, C. (2018). Effects of formulation and process conditions on microstructure, texture and digestibility of extruded insect-riched snacks. *Innovative Food Science and Emerging Technologies*, *45*, 344–353. https://doi.org/10.1016/j.ifset.2017.11.017

Barbé, F., Ménard, O., Le Gouar, Y., Buffière, C., Famelart, M. H., Laroche, B., Le Feunteun, S., Dupont, D., & Rémond, D. (2013). The heat treatment and the gelation are strong determinants of the kinetics of milk proteins digestion and of the peripheral availability

of amino acids. *Food Chemistry*, *136*(3–4), 1203–1212. https://doi.org/10.1016/J.FOODCHEM.2012.09.022

Baune, M. C., Terjung, N., Tülbek, M. Ç., & Boukid, F. (2022). Textured vegetable proteins (TVP): Future foods standing on their merits as meat alternatives. *Future Foods*, *6*. https://doi.org/10.1016/j.fufo.2022.100181

Bayrak, M., Mata, J., Raynes, J. K., Greaves, M., White, J., Conn, C. E., Floury, J., & Logan, A. (2021). Investigating casein gel structure during gastric digestion using ultra-small and small-angle neutron scattering. *Journal of Colloid and Interface Science*, *594*, 561–574. https://doi.org/10.1016/j.jcis.2021.03.087

Blanquet, S., Meunier, J. P., Minekus, M., Marol-Bonnin, S., & Alric, M. (2003). Recombinant Saccharomyces cerevisiae expressing P450 in artificial digestive systems: A model for biodetoxication in the human digestive environment. *Applied and Environmental Microbiology*, *69*(5), 2884–2892. https://doi.org/10.1128/AEM.69.5.2884-2892.2003

Blanquet-Diot, S., François, O., Denis, S., Hennequin, M., & Peyron, M. A. (2021). Importance of oral phase in in vitro starch digestibility related to wholegrain versus refined pastas and mastication impairment. *Food Hydrocolloids*, *112*. https://doi.org/10.1016/j.foodhyd.2020.106277

Bohn, T., Carriere, F., Day, L., Deglaire, A., Egger, L., Freitas, D., Golding, M., Le Feunteun, S., Macierzanka, A., Menard, O., Miralles, B., Moscovici, A., Portmann, R., Recio, I., Rémond, D., Santé-Lhoutelier, V., Wooster, T. J., Lesmes, U., Mackie, A. R., & Dupont, D. (2018). Correlation between in vitro and in vivo data on food digestion. What can we predict with static in vitro digestion models? *Critical Reviews in Food Science and Nutrition*, *58*(13), 2239–2261. https://doi.org/10.1080/10408398.2017.1315362

Bornhorst, G. M., & Singh, R. P. (2012). Bolus Formation and Disintegration during Digestion of Food Carbohydrates. *Comprehensive Reviews in Food Science and Food Safety*, *11*(2), 101–118. https://doi.org/10.1111/j.1541-4337.2011.00172.x

Bornhorst, G. M., Ferrua, M. J., & Singh, R. P. (2015). A Proposed Food Breakdown Classification System to Predict Food Behavior during Gastric Digestion. *Journal of Food Science*, *80*(5), R924–R934. https://doi.org/10.1111/1750-3841.12846

Bornhorst, G. M., Gouseti, O., Wickham, M. S. J., & Bakalis, S. (2016). Engineering Digestion: Multiscale Processes of Food Digestion. *Journal of Food Science*, *81*(3), R534–R543. https://doi.org/10.1111/1750-3841.13216

Borreani, J., Llorca, E., Larrea, V., & Hernando, I. (2016). Adding neutral or anionic hydrocolloids to dairy proteins under in vitro gastric digestion conditions. *Food Hydrocolloids*, *57*, 169–177. https://doi.org/10.1016/j.foodhyd.2016.01.030

Brishti, F. H., Chay, S. Y., Muhammad, K., Ismail-Fitry, M. R., Zarei, M., & Saari, N. (2021). Texturized mung bean protein as a sustainable food source: Effects of extrusion on its physical, textural and protein quality. *Innovative Food Science and Emerging Technologies*, *67*. https://doi.org/10.1016/j.ifset.2020.102591

Brodkorb, A., Egger, L., Alminger, M., Alvito, P., Assunção, R., Ballance, S., Bohn, T., Bourlieu-Lacanal, C., Boutrou, R., Carrière, F., Clemente, A., Corredig, M., Dupont, D., Dufour, C., Edwards, C., Golding, M., Karakaya, S., Kirkhus, B., Le Feunteun, S., … Recio, I. (2019). INFOGEST static in vitro simulation of gastrointestinal food digestion. *Nature Protocols*, *14*(4), 991–1014. https://doi.org/10.1038/s41596-018-0119-1

Çakir, E., & Foegeding, E. A. (2011). Combining protein micro-phase separation and protein-polysaccharide segregative phase separation to produce gel structures. *Food Hydrocolloids*, *25*(6), 1538–1546. https://doi.org/10.1016/j.foodhyd.2011.02.002

Çakir, E., Vinyard, C. J., Essick, G., Daubert, C. R., Drake, M. A., & Foegeding, E. A. (2012). Interrelations among physical characteristics, sensory perception and oral processing of protein-based soft-solid structures. *Food Hydrocolloids*, *29*(1), 234–245. https://doi.org/10.1016/j.foodhyd.2012.02.006

Camps, G., Mars, M., De Graaf, C., & Smeets, P. A. M. (2016). Empty calories and phantom fullness: A randomized trial studying the relative effects of energy density and viscosity on gastric emptying determined by MRI and satiety. *American Journal of Clinical Nutrition*, *104*(1), 73–80. https://doi.org/10.3945/ajcn.115.129064

Camps, G., Mars, M., de Graaf, C., & Smeets, P. A. M. (2017). A tale of gastric layering and sieving: Gastric emptying of a liquid meal with water blended in or consumed separately. *Physiology and Behavior*, *176*, 26–30. https://doi.org/10.1016/j.physbeh.2017.03.029

Capuano, E., & Janssen, A. E. M. (2021). Food Matrix and Macronutrient Digestion. *Annual Review of Food Science and Technology*, *12*, 193–212. https://doi.org/10.1146/annurev-food-032519

Chen, J. (2009). Food oral processing-A review. *Food Hydrocolloids*, *23*(1), 1–25. https://doi.org/10.1016/j.foodhyd.2007.11.013

Chen, J., & Rosenthal, A. (2015). Food texture and structure. In *Modifying Food Texture: Novel Ingredients and Processing Techniques* (pp. 3–24). Elsevier. https://doi.org/10.1016/B978-1-78242-333-1.00001-2

Chen, J., Khandelwal, N., Liu, Z., & Funami, T. (2013). Influences of food hardness on the particle size distribution of food boluses. *Archives of Oral Biology*, *58*(3), 293–298. https://doi.org/10.1016/j.archoralbio.2012.10.014

Chen, J., Wu, K., Guo, W., Guo, J., Wang, J., & Yang, X. (2024a). Digestion behavior of plant-based meat analogs with anisotropic fibrous structure in a semi-dynamic gastric digestion system. *Food Research International*, *190*, 114631. https://doi.org/10.1016/j.foodres.2024.114631

Chen, L., Xu, Y., Fan, T., Liao, Z., Wu, P., Wu, X., & Chen, X. D. (2016). Gastric emptying and morphology of a "near real" in vitro human stomach model (RD-IV-HSM). *Journal of Food Engineering*, *183*, 1–8. https://doi.org/10.1016/j.jfoodeng.2016.02.025

Chen, Y., Capuano, E., & Stieger, M. (2021). Chew on it: Influence of oral processing behaviour on in vitro protein digestion of chicken and soya-based vegetarian chicken. *British Journal of Nutrition*, *126*(9), 1408–1419. https://doi.org/10.1017/S0007114520005176

Chen, Y., Capuano, E., & Stieger, M. (2024b). The effects of carrot shape and oral processing behaviour on bolus properties and β-carotene bioaccessibility of raw carrots. *Food Research International*, *179*. https://doi.org/10.1016/j.foodres.2024.114051

Choy, J. Y. M., Goh, A. T., Chatonidi, G., Ponnalagu, S., Wee, S. M. M., Stieger, M., & Forde, C. G. (2021). Impact of food texture modifications on oral processing behaviour, bolus properties and postprandial glucose responses. *Current Research in Food Science*, *4*, 891–899. https://doi.org/10.1016/j.crfs.2021.11.018

Croguennoc, P., Nicolai, T., Durand, D., & Clark, A. (2001). *Phase Separation and Association of Globular Protein Aggregates in the Presence of Polysaccharides: 2. Heated Mixtures of Native-Lactoglobulin and K-Carrageenan*. https://doi.org/10.1021/la001675i

Cutroneo, S., Prandi, B., Faccini, A., Pellegrini, N., Sforza, S., & Tedeschi, T. (2023). Comparison of protein quality and digestibility between plant-based and meat-based burgers. *Food Research International*, *172*. https://doi.org/10.1016/j.foodres.2023.113183

Day, L., & Golding, M. (2018). Food structure, rheology, and texture. In *Encyclopedia of Food Chemistry* (pp. 125–129). Elsevier. https://doi.org/10.1016/B978-0-08-100596-5.03412-0

De Groot, L. C. P. G. M. (2016). Nutritional issues for older adults: Addressing degenerative ageing with long-term studies. *Proceedings of the Nutrition Society*, *75*(2), 169–173. https://doi.org/10.1017/S0029665116000033

De Jong, S., & Van De Velde, F. (2007). Charge density of polysaccharide controls microstructure and large deformation properties of mixed gels. *FOOD HYDROCOLLOIDS*, *21*, 1172–1187. https://doi.org/10.1016/j.foodhyd.2006.09.004

Del Rio, A. R., Boom, R. M., & Janssen, A. E. M. (2022). Effect of Fractionation and Processing Conditions on the Digestibility of Plant Proteins as Food Ingredients. In *Foods* (Vol. 11, Issue 6). MDPI. https://doi.org/10.3390/foods11060870

Deng, R., Mars, M., Van Der Sman, R. G. M., Smeets, P. A. M., & Janssen, A. E. M. (2020). The importance of swelling for in vitro gastric digestion of whey protein gels. *Food Chemistry*, *330*, 127182. https://doi.org/10.1016/j.foodchem.2020.127182

Devezeaux De Lavergne, M., Van De Velde, F., & Stieger, M. (2017). Bolus matters: the influence of food oral breakdown on dynamic texture perception. *Food & Function*, *8*, 464–480. https://doi.org/10.1039/c6fo01005a

Dong, X., Wu, P., Cong, H., & Chen, X. D. (2022). Mechanistic study on in vitro disintegration and proteolysis of whey protein isolate gels: Effect of the strength of sodium ions. *Food Hydrocolloids*, *132*. https://doi.org/10.1016/j.foodhyd.2022.107862

Drechsler, K. C., & Ferrua, M. J. (2016). Modelling the breakdown mechanics of solid foods during gastric digestion. *Food Research International*, *88*, 181–190. https://doi.org/10.1016/j.foodres.2016.02.019

Duijsens, D., Pälchen, K., Guevara-Zambrano, J. M., Verkempinck, S. H. E., Infantes-Garcia, M. R., Hendrickx, M. E., Van Loey, A. M., & Grauwet, T. (2022). Strategic choices for in vitro food digestion methodologies enabling food digestion design. *Trends in Food Science and Technology*, *126*, 61–72. https://doi.org/10.1016/j.tifs.2022.06.017

Duodu, K. G., Nunes, A., Delgadillo, I., Parker, M. L., Mills, E. N. C., Belton, P. S., & Taylor, J. R. N. (2002). Effect of grain structure and cooking on sorghum and maize in vitro protein digestibility. *Journal of Cereal Science*, *35*(2), 161–174. https://doi.org/10.1006/jcrs.2001.0411

Dupont, D., Alric, M., Blanquet-Diot, S., Bornhorst, G., Cueva, C., Deglaire, A., Denis, S., Ferrua, M., Havenaar, R., Lelieveld, J., Mackie, A. R., Marzorati, M., Menard, O., Minekus, M., Miralles, B., Recio, I., & Van den Abbeele, P. (2019). Can dynamic in vitro digestion systems mimic the physiological reality? *Critical Reviews in Food Science and Nutrition*, *59*(10), 1546–1562. https://doi.org/10.1080/10408398.2017.1421900

Fang, X., Rioux, L. E., Labrie, S., & Turgeon, S. L. (2016). Commercial cheeses with different texture have different disintegration and protein/peptide release rates during simulated in vitro digestion. *International Dairy Journal*, *56*, 169–178. https://doi.org/10.1016/j.idairyj.2016.01.023

Flory, J., & Alavi, S. (2024). Use of hydration properties of proteins to understand their functionality and tailor texture of extruded plant-based meat analogues. *Journal of Food Science*, *89*(1), 245–258. https://doi.org/10.1111/1750-3841.16804

Foegeding, E. A., Stieger, M., & van de Velde, F. (2017). Moving from molecules, to structure, to texture perception. *Food Hydrocolloids*, *68*, 31–42. https://doi.org/10.1016/J.FOODHYD.2016.11.009

Frost, G. S., Brynes, A. E., Dhillo, W. S., Bloom, S. R., & Mcburney, M. I. (2003). The effects of fiber enrichment of pasta and fat content on gastric emptying, GLP-1, glucose, and insulin responses to a meal. *European Journal of Clinical Nutrition*, *57*, 293–298. https://doi.org/10.1038=sj.ejcn.1601520

Fundo, J. F., & Silva, C. L. M. (2017). Microstructure, composition and their relationship with molecular mobility, food quality and stability. In *Food Microstructure and Its Relationship with Quality and Stability* (pp. 29–41). Elsevier. https://doi.org/10.1016/B978-0-08-100764-8.00002-2

Gajdos, A., Gajdos-Tiiriik, M., Gajdos, C. R., Gajdos-Tiirok, A., Danieli, M., Gajdos, G., Gajdos-Tiiriik, A., Cohen-Bazire, C. R., Slstrom, G., & Stanier, W. R. (1963). Specificity of Pepsin and its Dependence on a Possible “Hydrophobic Binding Site.” *Ciba Found. Symp. Cm Porphyrin Biosynthesis and Metabolism*, *199*(1), 25.

Goh, A. T., Chatonidi, G., Choy, M., Ponnalagu, S., Stieger, M., & Forde, C. G. (2021). Impact of Individual Differences in Eating Rate on Oral Processing, Bolus Properties and Post-Meal Glucose Responses. *Physiology & Behavior*, *238*, 113495. https://doi.org/10.1016/J.PHYSBEH.2021.113495

Gonzalez-Estanol, K., Libardi, M., Biasioli, F., & Stieger, M. (2022). Oral processing behaviours of liquid, solid and composite foods are primarily driven by texture, mechanical and lubrication properties rather than by taste intensity. *Food and Function*. https://doi.org/10.1039/d2fo00300g

Gorissen, S. H. M., Crombag, J. J. R., Senden, J. M. G., Waterval, W. A. H., Bierau, J., Verdijk, L. B., & van Loon, L. J. C. (2018). Protein content and amino acid composition of commercially available plant-based protein isolates. *Amino Acids*, *50*(12), 1685–1695. https://doi.org/10.1007/s00726-018-2640-5

Guo, Q. (2021). Understanding the oral processing of solid foods: Insights from food structure. *Comprehensive Reviews in Food Science and Food Safety*, *20*(3), 2941–2967. https://doi.org/10.1111/1541-4337.12745

Guo, Q., Ye, A., Bellissimo, N., Singh, H., & Rousseau, D. (2017). Modulating fat digestion through food structure design. *Progress in Lipid Research*, *68*, 109–118. https://doi.org/10.1016/j.plipres.2017.10.001

Guo, Q., Ye, A., Lad, M., Dalgleish, D., & Singh, H. (2014). *Effect of gel structure on the gastric digestion of whey protein emulsion gels †*. https://doi.org/10.1039/c3sm52758a

Guo, Q., Ye, A., Lad, M., Dalgleish, D., & Singh, H. (2016). Impact of colloidal structure of gastric digesta on in-vitro intestinal digestion of whey protein emulsion gels. *Food Hydrocolloids*, *54*, 255–265. https://doi.org/10.1016/j.foodhyd.2015.10.006

Guo, Q., Ye, A., Lad, M., Ferrua, M., Dalgleish, D., & Singh, H. (2015). Disintegration kinetics of food gels during gastric digestion and its role on gastric emptying: an in vitro analysis. *Food & Function*, *6*, 756. https://doi.org/10.1039/c4fo00700j

Guo, Q., Ye, A., Singh, H., & Rousseau, D. (2020). Destructuring and restructuring of foods during gastric digestion. *COMPREHENSIVE REVIEWS IN FOOD SCIENCE AND FOOD SAFETY*, *19*(4), 1658–1679. https://doi.org/10.1111/1541-4337.12558

Guo, Y., Zhao, Q., Li, T., & Mao, Q. (2024). Masticatory simulators based on oral physiology in food research: A systematic review. *Journal of Texture Studies*, *55*(5). https://doi.org/10.1111/jtxs.12864

Hellström, P. M., Grybäck, P., & Jacobsson, H. (2006). The physiology of gastric emptying. *Best Practice and Research: Clinical Anaesthesiology*, *20*(3), 397–407. https://doi.org/10.1016/j.bpa.2006.02.002

Heuven, L. A. J., de Graaf, K., Forde, C. G., & Bolhuis, D. P. (2023). Al dente or well done? How the eating rate of a pasta dish can be predicted by the eating rate of its components. *Food Quality and Preference*, *108*. https://doi.org/10.1016/j.foodqual.2023.104883

Hiolle, M., Lechevalier, V., Floury, J., Boulier-Monthéan, N., Prioul, C., Dupont, D., & Nau, F. (2020). In vitro digestion of complex foods: How microstructure influences food disintegration and micronutrient bioaccessibility. *Food Research International*, *128*, 108817. https://doi.org/10.1016/J.FOODRES.2019.108817

Holt, S., Reid, J., Taylor, T. V., Tothill, P., & Heading, R. C. (1982). Gastric emptying of solids in man. *Gut*, *23*(4), 292–296. https://doi.org/10.1136/gut.23.4.292

Homer, S., Williams, R., Williams, A., & Logan, A. (2021). *WPI Gel Microstructure and Mechanical Behaviour and Their Influence on the Rate of In Vitro Digestion*. https://doi.org/10.3390/foods10051066

Hong, S., Shen, Y., & Li, Y. (2022). Physicochemical and Functional Properties of Texturized Vegetable Proteins and Cooked Patty Textures: Comprehensive Characterization and Correlation Analysis. *Foods*, *11*(17). https://doi.org/10.3390/foods11172619

Hornby, H., Collado-González, M., Zhang, X., Abrehart, N., Alshammari, M., Bakalis, S., Mackie, A., & Marciani, L. (2021). Size and number of food boluses in the stomach after eating different meals: Magnetic resonance imaging insights in healthy humans. *Nutrients*, *13*(10). https://doi.org/10.3390/nu13103626

How, M. S., Jones, J. R., Morgenstern, M. P., Gray-Stuart, E., Bronlund, J. E., Saint-Eve, A., Trelea, I. C., & Souchon, I. (2021). Modelling the role of oral processing on in vivo aroma release of white rice: Conceptual model and experimental validation. *LWT*, *141*, 110918. https://doi.org/10.1016/j.lwt.2021.110918

Imran, M., & Liyan, Z. (2023). Production of plant-based meat: functionality, limitations and future prospects. *European Food Research and Technology*, *249*(9), 2189–2213. https://doi.org/10.1007/s00217-023-04287-w

Ishaq, A., Irfan, S., Sameen, A., & Khalid, N. (2022). Plant-based meat analogs: A review with reference to formulation and gastrointestinal fate. In *Current Research in Food Science* (Vol. 5, pp. 973–983). Elsevier B.V. https://doi.org/10.1016/j.crfs.2022.06.001

Jalabert-Malbos, M. L., Mishellany-Dutour, A., Woda, A., & Peyron, M. A. (2007). Particle size distribution in the food bolus after mastication of natural foods. *Food Quality and Preference*, *18*(5), 803–812. https://doi.org/10.1016/j.foodqual.2007.01.010

Jeon, Y. H., Gu, B. J., & Ryu, G. H. (2023). Investigating the Potential of Full-Fat Soy as an Alternative Ingredient in the Manufacture of Low- and High-Moisture Meat Analogs. *Foods*, *12*(5). https://doi.org/10.3390/foods12051011

Jha, U. C., Nayyar, H., Parida, S. K., Deshmukh, R., von Wettberg, E. J. B., & Siddique, K. H. M. (2022). Ensuring Global Food Security by Improving Protein Content in Major Grain Legumes Using Breeding and 'Omics' Tools. *International Journal of Molecular Sciences*, *23*(14). https://doi.org/10.3390/ijms23147710

Jiménez-Munoz, L. M., Tavares, G. M., & Corredig, M. (2021). Design future foods using plant protein blends for best nutritional and technological functionality. *Trends in Food Science and Technology*, *113*, 139–150. https://doi.org/10.1016/j.tifs.2021.04.049

Karamanlis, A., Chaikomin, R., Doran, S., Bellon, M., Bartholomeusz, D., Wishart, J. M., Jones, K. L., Horowitz, M., & Rayner, C. K. (2007). Effects of protein on glycemic and incretin responses and gastric emptying after oral glucose in healthy subjects 1-3. *Am J Clin Nutr*, *86*, 1364–1372.

Kaur, L., Mao, B., Beniwal, A. S., Abhilasha, Kaur, R., Chian, F. M., & Singh, J. (2022). Alternative proteins vs animal proteins: The influence of structure and processing on their gastro-small intestinal digestion. *Trends in Food Science and Technology*, *122*, 275–286. https://doi.org/10.1016/j.tifs.2022.02.021

Ketel, E. C., Aguayo-Mendoza, M. G., de Wijk, R. A., de Graaf, C., Piqueras-Fiszman, B., & Stieger, M. (2019). Age, gender, ethnicity and eating capability influence oral processing behaviour of liquid, semi-solid and solid foods differently. *Food Research International*, *119*, 143–151. https://doi.org/10.1016/j.foodres.2019.01.048

Kong, F., & Singh, R. P. (2008a). A model stomach system to investigate disintegration kinetics of solid foods during gastric digestion. *Journal of Food Science*, *73*(5). https://doi.org/10.1111/j.1750-3841.2008.00745.x

Kong, F., & Singh, R. P. (2008b). Disintegration of Solid Foods in Human Stomach. *Journal Of Food Science*, *73*(5), R67–R80. https://doi.org/10.1111/j.1750-3841.2008.00766.x

Kong, F., & Singh, R. P. (2010). A Human Gastric Simulator (HGS) to Study Food Digestion in Human Stomach. *Journal of Food Science*, *75*(9). https://doi.org/10.1111/j.1750-3841.2010.01856.x

Kortman, G. A. M., Dutilh, B. E., Maathuis, A. J. H., Engelke, U. F., Boekhorst, J., Keegan, K. P., Nielsen, F. G. G., Betley, J., Weir, J. C., Kingsbury, Z., Kluijtmans, L. A. J., Swinkels, D. W., Venema, K., & Tjalsma, H. (2016). Microbial metabolism shifts

towards an adverse profile with supplementary iron in the TIM-2 in vitro model of the human colon. *Frontiers in Microbiology*, *6*(JAN). https://doi.org/10.3389/fmicb.2015.01481

Kraak, V. I., & Aschemann-Witzel, J. (2024). *The Future of Plant-Based Diets: Aligning Healthy Marketplace Choices with Equitable, Resilient, and Sustainable Food Systems*. *12*, 16. https://doi.org/10.1146/annurev-publhealth

Lasschuijt, M. P., Mars, M., Stieger, M., Miquel-Kergoat, S., de Graaf, C., & Smeets, P. A. M. (2017). Comparison of oro-sensory exposure duration and intensity manipulations on satiation. *Physiology and Behavior*, *176*, 76–83. https://doi.org/10.1016/j.physbeh.2017.02.003

Layer, P., Holst, J. J., Grandt, D., & Goebell, H. (1995). Ileal Release of Glucagon-Like Peptide-1 (GLP-1) Association with Inhibition of Gastric Acid Secretion in Humans. *Digestive Diseases and Sciences*, *40*(5), 1074–1082.

Lee, S., Jo, K., Jeong, H. G., Choi, Y. S., Yong, H. I., & Jung, S. (2023). Understanding protein digestion in infants and the elderly: Current in vitro digestion models. *Critical Reviews in Food Science and Nutrition*, *63*(7), 975–992. https://doi.org/10.1080/10408398.2021.1957765

Li, C., Yu, W., Wu, P., & Chen, X. D. (2020). Current in vitro digestion systems for understanding food digestion in human upper gastrointestinal tract. *Trends in Food Science and Technology*, *96*, 114–126. https://doi.org/10.1016/j.tifs.2019.12.015

Li, H., Chen, X. D., & Mercadé-Prieto, R. (2017). Elastic modulus and equilibrium swelling of stranded and particulate protein hydrogels at acid pH. *Food Hydrocolloids*, *71*, 168–175. https://doi.org/10.1016/j.foodhyd.2017.05.008

Lin, Q., Pan, L., Deng, N., Sang, M., Cai, K., Chen, C., Han, J., & Ye, A. (2022). Protein digestibility of textured-wheat-protein (TWP) -based meat analogues: (I) Effects of fibrous structure. *Food Hydrocolloids*, *130*. https://doi.org/10.1016/j.foodhyd.2022.107694

Lin, Q., Sang, M., Jin, H., Huang, D., Zhang, Y., Han, J., & Ye, A. (2023). Protein digestibility of textured wheat protein (TWP)-based meat analogs: (II) Effects of sodium tripolyphosphate. *Food Research International*, *173*. https://doi.org/10.1016/j.foodres.2023.113280

Liu, D., Deng, Y., Sha, L., Abul Hashem, M., & Gai, S. (2017). Impact of oral processing on texture attributes and taste perception. In *Journal of Food Science and Technology* (Vol.

54, Issue 8, pp. 2585–2593). Springer India. https://doi.org/10.1007/s13197-017-2661-1

Liu, D., Janssen, A. E. M., Smeets, P. A. M., & Stieger, M. (2024). Interplay between microstructure, mechanical properties, macrostructure breakdown and in vitro gastric digestion of whey protein gels. *Food Hydrocolloids*, *147*, 109352. https://doi.org/10.1016/j.foodhyd.2023.109352 (Chapter 2 in this thesis)

Liu, D., Janssen, A. E. M., Smeets, P. A. M., & Stieger, M. (2025). Impact of microstructure of whey protein gels on in vitro gastric protein digestion is sustained after oral structural breakdown by mastication. *Food Hydrocolloids*, *159*, 110619. https://doi.org/10.1016/j.foodhyd.2024.110619 (Chapter 3 in this thesis)

Lou, M., Ritzoulis, C., Liu, J., Zhang, X., Han, J., & Liu, W. (2022). In vitro digestion of tofu with different textures using an artificial gastric digestive system. *Food Research International*, *157*, 111458. https://doi.org/10.1016/J.FOODRES.2022.111458

Luo, N., Ye, A., Wolber, F. M., & Singh, H. (2020). In-mouth breakdown behaviour and sensory perception of emulsion gels containing active or inactive filler particles loaded with capsaicinoids. *Food Hydrocolloids*, *108*. https://doi.org/10.1016/j.foodhyd.2020.106076

Luo, N., Ye, A., Wolber, F. M., & Singh, H. (2021). Effect of gel structure on the in vitro gastrointestinal digestion behaviour of whey protein emulsion gels and the bioaccessibility of capsaicinoids. *Molecules*, *26*(5). https://doi.org/10.3390/molecules26051379

Luo, Q., Boom, R. M., & Janssen, A. E. M. (2015). Digestion of protein and protein gels in simulated gastric environment. *LWT - Food Science and Technology*, *63*(1), 161–168. https://doi.org/10.1016/J.LWT.2015.03.087

Luo, Q., Borst, J. W., Westphal, A. H., Boom, R. M., & Janssen, A. E. M. (2017). Pepsin diffusivity in whey protein gels and its effect on gastric digestion. *Food Hydrocolloids*, *66*, 318–325. https://doi.org/10.1016/j.foodhyd.2016.11.046

Luo, Q., Sewalt, E., Borst, J. W., Westphal, A. H., Boom, R. M., & Janssen, A. E. M. (2019). Analysis and modeling of enhanced green fluorescent protein diffusivity in whey protein gels. *Food Research International*, *120*, 449–455. https://doi.org/10.1016/j.foodres.2018.10.087

Luo, Q., Zhan, W., Boom, R. M., & Janssen, A. E. M. (2018). Interactions between acid and proteins under in vitro gastric condition-a theoretical and experimental quantification. *Food and Function*, *9*(10), 5283–5289. https://doi.org/10.1039/C8FO01033A

Lv, Y., Zhang, M., He, X., Du, F., Xiao, Y., Wang, J., Xin, Y., & Yang, Y. (2024). Impact of konjac glucomannan with varied deacetylation degrees on plant-based meat analogue: Study on the gel properties, digestibility, and microstructure. *International Journal of Biological Macromolecules*, *277*. https://doi.org/10.1016/j.ijbiomac.2024.134377

MacIerzanka, A., Böttger, F., Lansonneur, L., Groizard, R., Jean, A. S., Rigby, N. M., Cross, K., Wellner, N., & MacKie, A. R. (2012). The effect of gel structure on the kinetics of simulated gastrointestinal digestion of bovine β-lactoglobulin. *Food Chemistry*, *134*(4), 2156–2163. https://doi.org/10.1016/J.FOODCHEM.2012.04.018

Mackie, A. (2023). The role of food structure in gastric emptying rate, absorption and metabolism. *Proceedings of the Nutrition Society*. https://doi.org/10.1017/S0029665123003609

Mackie, A., Mulet-Cabero, A. I., & Torcello-Gomez, A. (2020). Simulating human digestion: Developing our knowledge to create healthier and more sustainable foods. *Food and Function*, *11*(11), 9397–9431. https://doi.org/10.1039/d0fo01981j

Maningat, C. C., Jeradechachai, T., & Buttshaw, M. R. (2022). Textured wheat and pea proteins for meat alternative applications. *Cereal Chemistry*, *99*(1), 37–66. https://doi.org/10.1002/cche.10503

Markussen, J. Ø., Madsen, F., Young, J. F., & Corredig, M. (2021). A semi dynamic in vitro digestion study of milk protein concentrate dispersions structured with different polysaccharides. *Current Research in Food Science*, *4*, 250–261. https://doi.org/10.1016/J.CRFS.2021.03.012

McClements, D. J., Decker, E. A., Park, Y., & Weiss, J. (2008). Designing food structure to control stability, digestion, release and absorption of lipophilic food components. *Food Biophysics*, *3*(2), 219–228. https://doi.org/10.1007/s11483-008-9070-y

McClements, D. J., Decker, E. A., Park, Y., & Weiss, J. (2009). Structural design principles for delivery of bioactive components in nutraceuticals and functional foods. *Critical Reviews in Food Science and Nutrition*, *49*(6), 577–606. https://doi.org/10.1080/10408390902841529

Mella, C., Quilaqueo, M., Zúñiga, R. N., & Troncoso, E. (2021). *Impact of the Simulated Gastric Digestion Methodology on the In Vitro Intestinal Proteolysis and Lipolysis of Emulsion Gels*. https://doi.org/10.3390/foods10020321

Ménard, O., Famelart, M. H., Deglaire, A., Le Gouar, Y., Guérin, S., Malbert, C. H., & Dupont, D. (2018). Gastric emptying and dynamic in vitro digestion of drinkable yogurts: Effect of viscosity and composition. *Nutrients*, *10*(9). https://doi.org/10.3390/nu10091308

Mennah-Govela, Y. A., & Bornhorst, G. M. (2021). Breakdown mechanisms of whey protein gels during dynamic in vitro gastric digestion. *Food and Function*, *12*(5), 2112–2125. https://doi.org/10.1039/d0fo03325a

Mennah-Govela, Y. A., Cai, H., Chu, J., Kim, K., Maborang, M. K., Sun, W., & Bornhorst, G. M. (2020a). Buffering capacity of commercially available foods is influenced by composition and initial properties in the context of gastric digestion. *Food and Function*, *11*(3), 2255–2267. https://doi.org/10.1039/c9fo03033f

Mennah-Govela, Y. A., Keppler, S., Januzzi-Guerreiro, F., Follador-Lemos, C., Vilpont, K., & Bornhorst, G. M. (2020b). Acid and Moisture Uptake into Red Beets during in Vitro Gastric Digestion as Influenced by Gastric pH. *Food Biophysics*, *15*(2), 261–272. https://doi.org/10.1007/s11483-019-09623-w

Mennah-Govela, Y. A., Singh, R. P., & Bornhorst, G. M. (2019). Buffering capacity of protein-based model food systems in the context of gastric digestion. *Food and Function*, *10*(9), 6074–6087. https://doi.org/10.1039/c9fo01160a

Meullenet, J. F., & Gandhapuneni, R. K. (2006). Development of the BITE Master II and its application to the study of cheese hardness. *Physiology and Behavior*, *89*(1), 39–43. https://doi.org/10.1016/j.physbeh.2006.05.012

Minekus, M., Alminger, M., Alvito, P., Ballance, S., Bohn, T., Bourlieu, C., Carrì, F., Boutrou, R., Corredig, M., Dupont, D., Dufour, C., Egger, L., Golding, M., Karakaya, L. S., Kirkhus, B., Le Feunteun, S., Lesmes, U., Macierzanka, A., Mackie, A., … Jorge, I. P. (2014). A standardised static in vitro digestion method suitable for food – an international consensus. *Food & Function*, *5*, 1113–1124. https://doi.org/10.1039/c3fo60702j

Moughan, P. J. (2021). Population protein intakes and food sustainability indices: The metrics matter. *Global Food Security*, *29*. https://doi.org/10.1016/j.gfs.2021.100548

Mulet-Cabero, A.-I., Egger, L., Portmann, R., Ménard, O., Marze, S., Minekus, M., Le Feunteun, S., Sarkar, A., M-L Grundy, M., Carrière, F., Golding, M., Dupont, D., Recio, I., Brodkorb, A., & Mackie, A. (2020a). A standardised semi-dynamic in vitro digestion method suitable for food – an international consensus. *Food & Function*, *11*(2), 1702–1720. https://doi.org/10.1039/c9fo01293a

Mulet-Cabero, A.-I., Mackie, A. R., Brodkorb, A., & Wilde, P. J. (2020b). Dairy structures and physiological responses: a matter of gastric digestion. *Critical Reviews in Food Science and Nutrition*, *60*(22), 3737–3752. https://doi.org/10.1080/10408398.2019.1707159

Nath, P. C., Debnath, S., Sridhar, K., Inbaraj, B. S., Nayak, P. K., & Sharma, M. (2023). A Comprehensive Review of Food Hydrogels: Principles, Formation Mechanisms, Microstructure, and Its Applications. *Gels*, *9*(1). https://doi.org/10.3390/gels9010001

Nielsen, P. M., Petersen, D., & Dambmann, C. (2001). Improved method for determining food protein degree of hydrolysis. *Journal of Food Science*, *66*(5), 642–646. https://doi.org/10.1111/j.1365-2621.2001.tb04614.x

Norton, J. E., Gonzalez Espinosa, Y., Watson, R. L., Spyropoulos, F., & Norton, I. T. (2015). Functional food microstructures for macronutrient release and delivery. *Food and Function*, *6*(3), 663–678. https://doi.org/10.1039/c4fo00965g

Nyemb, K., Guérin-Dubiard, C., Pézennec, S., Jardin, J., Briard-Bion, V., Cauty, C., Rutherfurd, S. M., Dupont, D., & Nau, F. (2016). The structural properties of egg white gels impact the extent of in vitro protein digestion and the nature of peptides generated. *Food Hydrocolloids*, *54*, 315–327. https://doi.org/10.1016/j.foodhyd.2015.10.011

Oppen, D., Grossmann, L., & Weiss, J. (2024). Insights into characterizing and producing anisotropic food structures. *Critical Reviews in Food Science and Nutrition*, *64*(4), 1158–1176. https://doi.org/10.1080/10408398.2022.2113365

Peh, F. Z. W., Zhao, L., Chia, Y. Y., Ng, C. K. Z., & Du, J. (2024). Texture improvement and in vitro digestion modulation of plant-based fish cake analogue by incorporating hydrocolloid blends. *Current Research in Food Science*, *8*. https://doi.org/10.1016/j.crfs.2024.100775

Pellegrini, N., Vittadini, E., & Fogliano, V. (2020). Designing food structure to slow down digestion in starch-rich products. *Current Opinion in Food Science*, *32*, 50–57. https://doi.org/10.1016/j.cofs.2020.01.010

Pematilleke, N., Kaur, M., Adhikari, B., & Torley, P. (2020). Influence of meat texture on oral processing and bolus formation. *Journal of Food Engineering*, *283*, 110038. https://doi.org/10.1016/j.jfoodeng.2020.110038

Peng, Z., Wu, P., Wang, J., Dupont, D., Menard, O., Jeantet, R., & Chen, X. D. (2021). Achieving realistic gastric emptying curve in an advanced dynamic: In vitro human digestion system: Experiences with cheese - A difficult to empty material. *Food and Function*, *12*(9), 3965–3977. https://doi.org/10.1039/d0fo03364b

Pentikäinen, S., Sozer, N., Närväinen, J., Ylätalo, S., Teppola, P., Jurvelin, J., Holopainen-Mantila, U., Törrönen, R., Aura, A. M., & Poutanen, K. (2014). Effects of wheat and rye bread structure on mastication process and bolus properties. *Food Research International*, *66*, 356–364. https://doi.org/10.1016/j.foodres.2014.09.034

Peyron, M. A., Santé-Lhoutellier, V., Dardevet, D., Hennequin, M., Rémond, D., François, O., & Woda, A. (2019). Addressing various challenges related to food bolus and nutrition with the AM2 mastication simulator. *Food Hydrocolloids*, *97*. https://doi.org/10.1016/j.foodhyd.2019.105229

Peyron, M. A., Sayd, T., Sicard, J., Mirade, P. S., Pinguet, J., Chambon, C., & Santé-Lhoutellier, V. (2021). Deciphering the protein digestion of meat products for the elderly by: In vitro food oral processing and gastric dynamic digestion, peptidome analysis and modeling. *Food and Function*, *12*(16), 7283–7297. https://doi.org/10.1039/d1fo00969a

Qasrawi, R., Sgahir, S., Nemer, M., Halaikah, M., Badrasawi, M., Amro, M., Vicuna Polo, S., Abu Al-Halawa, D., Mujahed, D., Nasreddine, L., Elmadfa, I., Atari, S., & Al-Jawaldeh, A. (2024). Investigating the Association between Nutrient Intake and Food Insecurity among Children and Adolescents in Palestine Using Machine Learning Techniques. *Children*, *11*(6). https://doi.org/10.3390/children11060625

Ribes, S., Arnal, M., & Talens, P. (2023). Influence of food oral processing, bolus characteristics, and digestive conditions on the protein digestibility of turkey cold meat and fresh cheese. *Food Research International*, *173*. https://doi.org/10.1016/j.foodres.2023.113297

Ribes, S., Aubry, L., Kristiawan, M., Jebalia, I., Dupont, D., Guillevic, M., Germain, A., Chesneau, G., Sayd, T., Talens, P., Peyron, M.-A., & Santé-Lhoutellier, V. (2024). Fava bean (Vicia faba L.) protein concentrate added to beef burgers improves the bioaccessibility of some free essential amino acids after in vitro oral and

gastrointestinal digestion. *Food Research International*, *177*, 113916. https://doi.org/10.1016/j.foodres.2023.113916

Roelofs, J. J. M., van Eijnatten, E. J. M., Prathumars, P., de Jong, J., Wehrens, R., Esser, D., Janssen, A. E. M., & Smeets, P. A. M. (2024). Gastric emptying and nutrient absorption of pea protein products differing in heat treatment and texture: A randomized in vivo crossover trial and in vitro digestion study. *Food Hydrocolloids*, *149*. https://doi.org/10.1016/j.foodhyd.2023.109596

Sá, A. G. A., Moreno, Y. M. F., & Carciofi, B. A. M. (2020a). Food processing for the improvement of plant proteins digestibility. *Critical Reviews in Food Science and Nutrition*, *60*(20), 3367–3386. https://doi.org/10.1080/10408398.2019.1688249

Sá, A. G. A., Moreno, Y. M. F., & Carciofi, B. A. M. (2020b). Plant proteins as high-quality nutritional source for human diet. *Trends in Food Science and Technology*, *97*, 170–184. https://doi.org/10.1016/j.tifs.2020.01.011

Saeed, F., Afzaal, M., Khalid, A., Shah, Y. A., Ateeq, H., Islam, F., Akram, N., Ejaz, A., Nayik, G. A., & Shah, M. A. (2023). Role of mycoprotein as a non-meat protein in food security and sustainability: a review. *International Journal of Food Properties*, *26*(1), 683–695. https://doi.org/10.1080/10942912.2023.2178456

Samard, S., Gu, B. Y., & Ryu, G. H. (2019). Effects of extrusion types, screw speed and addition of wheat gluten on physicochemical characteristics and cooking stability of meat analogues. *Journal of the Science of Food and Agriculture*, *99*(11), 4922–4931. https://doi.org/10.1002/jsfa.9722

Samard, S., Maung, T. T., Gu, B. Y., Kim, M. H., & Ryu, G. H. (2021). Influences of extrusion parameters on physicochemical properties of textured vegetable proteins and its meatless burger patty. *Food Science and Biotechnology*, *30*(3), 395–403. https://doi.org/10.1007/s10068-021-00879-y

Sassi, A. P., Shaw, A. J., Han, S. M., Blanch, H. W., & Prausnitz, J. M. (1996). *Partitioning of proteins and small biomolecules in temperature-and pH-sensitive hydrogels* (Vol. 37, Issue 11).

Schreuders, F. K. G., Schlangen, M., Kyriakopoulou, K., Boom, R. M., & van der Goot, A. J. (2021). Texture methods for evaluating meat and meat analogue structures: A review. *Food Control*, *127*. https://doi.org/10.1016/j.foodcont.2021.108103

Sicard, J., Mirade, P. S., Portanguen, S., Clerjon, S., & Kondjoyan, A. (2018). Simulation of the gastric digestion of proteins of meat bolus using a reaction-diffusion model. *Food and Function*, *9*(12), 6455–6469. https://doi.org/10.1039/c8fo01120f

Singh, M., Trivedi, N., Enamala, M. K., Kuppam, C., Parikh, P., Nikolova, M. P., & Chavali, M. (2021). Plant-based meat analogue (PBMA) as a sustainable food: a concise review. *European Food Research and Technology*, *247*(10), 2499–2526. https://doi.org/10.1007/s00217-021-03810-1

Singh, R. P. (2024). Progress and challenges in designing dynamic in vitro gastric models to study food digestion. *Frontiers in Nutrition*, *11*. https://doi.org/10.3389/fnut.2024.1399534

Singh, T. K., Øiseth, S. K., Lundin, L., & Day, L. (2014). Influence of heat and shear induced protein aggregation on the in vitro digestion rate of whey proteins. *Food & Function*, *5*. https://doi.org/10.1039/c4fo00454j

Somaratne, G., Ferrua, M. J., Ye, A., Nau, F., Floury, J., Dupont, D., & Singh, J. (2020a). Food material properties as determining factors in nutrient release during human gastric digestion: a review. *Critical Reviews in Food Science and Nutrition*, *60*(22), 3753–3769. https://doi.org/10.1080/10408398.2019.1707770

Somaratne, G., Nau, F., Ferrua, M. J., Singh, J., Ye, A., Dupont, D., Singh, R. P., & Floury, J. (2020b). In-situ disintegration of egg white gels by pepsin and kinetics of nutrient release followed by time-lapse confocal microscopy. *Food Hydrocolloids*, *98*, 105228. https://doi.org/10.1016/j.foodhyd.2019.105228

Somaratne, G., Ye, A., Nau, F., Ferrua, M. J., Dupont, D., Paul Singh, R., & Singh, J. (2020c). Egg white gel structure determines biochemical digestion with consequences on softening and mechanical disintegration during in vitro gastric digestion. *Food Research International*, *138*. https://doi.org/10.1016/j.foodres.2020.109782

Stieger, M., & Van de Velde, F. (2013). Microstructure, texture and oral processing: New ways to reduce sugar and salt in foods. *Current Opinion in Colloid and Interface Science*, *18*(4), 334–348. https://doi.org/10.1016/j.cocis.2013.04.007

Sun, W., Tribuzi, G., & Bornhorst, G. M. (2023). Particle size and water content impact breakdown and starch digestibility of chickpea snacks during in vitro gastrointestinal digestion. *Food Research International*, *173*. https://doi.org/10.1016/j.foodres.2023.113201

Sun, X., Ohanenye, I. C., Ahmed, T., & Udenigwe, C. C. (2020). Microwave treatment increased protein digestibility of pigeon pea (Cajanus cajan) flour: Elucidation of underlying mechanisms. *Food Chemistry*, *329*. https://doi.org/10.1016/j.foodchem.2020.127196

Svook, J. T. (1973). Protein Digestion Nutritional and Metabolic Considerations. *World Review of Nutrition and Dietetics*, *18*, 121–176. http://karger.com/books/book/chapter-pdf/2013866/000394230.pdf

Tagle-Freire, D., Mennah-Govela, Y., & Bornhorst, G. M. (2022). Starch and protein hydrolysis in cooked quinoa (: Chenopodium quinoa Willd.) during static and dynamic in vitro oral and gastric digestion. *Food and Function*, *13*(2), 920–932. https://doi.org/10.1039/d1fo02685b

Thévenot, J., Cauty, C., Legland, D., Dupont, D., & Floury, J. (2017). Pepsin diffusion in dairy gels depends on casein concentration and microstructure. *Food Chemistry*, *223*, 54–61. https://doi.org/10.1016/j.foodchem.2016.12.014

van den Berg, L., van Vliet, T., van der Linden, E., van Boekel, M. A. J. S., & van de Velde, F. (2007). Breakdown properties and sensory perception of whey proteins/polysaccharide mixed gels as a function of microstructure. *Food Hydrocolloids*, *21*(5–6), 961–976. https://doi.org/10.1016/j.foodhyd.2006.08.017

van der Sman, R. G. M. (2018). Theoretical investigation of the swelling of polysaccharide microgels in sugar solutions. *Food and Function*, *9*(5), 2716–2724. https://doi.org/10.1039/c8fo00452h

van der Sman, R. G. M., Houlder, S., Cornet, S., & Janssen, A. (2020). Physical chemistry of gastric digestion of proteins gels. *Current Research in Food Science*, *2*, 45–60. https://doi.org/10.1016/j.crfs.2019.11.003

van Eck, A., Hardeman, N., Karatza, N., Fogliano, V., Scholten, E., & Stieger, M. (2019). Oral processing behavior and dynamic sensory perception of composite foods: Toppings assist saliva in bolus formation. *Food Quality and Preference*, *71*, 497–509. https://doi.org/10.1016/j.foodqual.2018.05.009

van Esbroeck, T., Sala, G., Stieger, M., & Scholten, E. (2024). Effect of structural characteristics on functional properties of textured vegetable proteins. *Food Hydrocolloids*, *149*. https://doi.org/10.1016/j.foodhyd.2023.109529

Verboven, P., Defraeye, T., & Nicolai, B. (2017). Measurement and visualization of food microstructure. In *Food Microstructure and Its Relationship with Quality and Stability* (pp. 3–28). Elsevier. https://doi.org/10.1016/B978-0-08-100764-8.00001-0

Waldum, H. L., Sørdal, Ø., & Fossmark, R. (2018). Proton pump inhibitors (PPIs) may cause gastric cancer–clinical consequences. *Scandinavian Journal of Gastroenterology*, *53*(6), 639–642. https://doi.org/10.1080/00365521.2018.1450442

Wan, A. C. A., Tai, B. C. U., & Du, C. (2021). Food security and nutrition- a systematic approach. *Trends in Food Science and Technology*, *109*, 738–745. https://doi.org/10.1016/j.tifs.2020.12.024

Wang, G., Cong, M., Xu, W., Wen, H., & Du, J. (2015). A biomimetic chewing robot of redundantly actuated parallel mechanism. *Industrial Robot*, *42*(2), 103–109. https://doi.org/10.1108/IR-11-2014-0416

Wang, J., Wu, P., Liu, M., Liao, Z., Wang, Y., Dong, Z., & Chen, X. D. (2019). An advanced near real dynamic: In vitro human stomach system to study gastric digestion and emptying of beef stew and cooked rice. *Food and Function*, *10*(5), 2914–2925. https://doi.org/10.1039/c8fo02586j

Wang, Y., Zheng, Z., Zhang, C., Wu, C., Tan, C. P., & Liu, Y. (2024). Comparative structural, digestion and absorption characterization of three common extruded plant proteins. *Food Research International*, *177*. https://doi.org/10.1016/j.foodres.2023.113852

Wee, M. S. M., Goh, A. T., Stieger, M., & Forde, C. G. (2018). Correlation of instrumental texture properties from textural profile analysis (TPA) with eating behaviours and macronutrient composition for a wide range of solid foods. *Food and Function*, *9*(10), 5301–5312. https://doi.org/10.1039/c8fo00791h

Wu, G. (2016). Dietary protein intake and human health. *Food and Function*, *7*(3), 1251–1265. https://doi.org/10.1039/c5fo01530h

Xie, Y., Cai, L., Zhao, D., Liu, H., Xu, X., Zhou, G., & Li, C. (2022). Real meat and plant-based meat analogues have different in vitro protein digestibility properties. *Food Chemistry*, *387*. https://doi.org/10.1016/j.foodchem.2022.132917

Xu, Y., Lv, B., Wu, P., & Chen, X. D. (2024). Creating similar food boluses as that in vivo using a novel in vitro bio-inspired oral mastication simulator (iBOMS-III): The cases with cooked rice and roasted peanuts. *Food Research International*, *190*. https://doi.org/10.1016/j.foodres.2024.114630

Yang, Y., Wang, Z., Wang, R., Sui, X., Qi, B., Han, F., Li, Y., & Jiang, L. (2016). Secondary Structure and Subunit Composition of Soy Protein in Vitro Digested by Pepsin and Its Relation with Digestibility. *BioMed Research International*, *2016*. https://doi.org/10.1155/2016/5498639

Young, P. M., Edge, S., Staniforth, J. N., Steele, D. F., & Price, R. (2005). Dynamic Vapor Sorption Properties of Sodium Starch Glycolate Disintegrants. *Pharmaceutical Development and Technology*, *10*(2), 249–259. https://doi.org/10.1081/pdt-54448

Zahir, M., Fogliano, V., & Capuano, E. (2018). Food matrix and processing modulate: In vitro protein digestibility in soybeans. *Food and Function*, *9*(12), 6326–6336. https://doi.org/10.1039/c8fo01385c

Zhang, K., Tian, X., Shen, R., Zhao, K., Wang, Y., Zhang, Y., & Wang, W. (2023a). Delaying In vitro gastric digestion of myofibrillar protein gel using carboxymethylated cellulose nanofibrils: Forming a compact and uniform microstructure. *Food Hydrocolloids*, *140*. https://doi.org/10.1016/j.foodhyd.2023.108661

Zhang, X., Zhang, T., Zhao, Y., Jiang, L., & Sui, X. (2024a). Structural, extraction and safety aspects of novel alternative proteins from different sources. *Food Chemistry*, *436*. https://doi.org/10.1016/j.foodchem.2023.137712

Zhang, Y., Sala, G., Scholten, E., & Stieger, M. (2024b). Role of bolus properties in dynamic texture perception of meat analogue and beef patties: Juiciness is driven by serum release during early stages of mastication. *Food Hydrocolloids,* 157. https://doi.org/10.1016/j.foodhyd.2024.110450

Zhang, Z., Qin, D., Kobata, K., Rao, J., Lu, J., & McClements, D. J. (2023b). An In Vitro Comparison of the Digestibility and Gastrointestinal Fate of Scallops and Plant-Based Scallop Analogs. *Foods*, *12*(15). https://doi.org/10.3390/foods12152928

Zhao, J., Wu, J., Chen, Y., Zhao, M., & Sun, W. (2020). Gel Properties of Soy Protein Isolate Modified by Lipoxygenase-Catalyzed Linoleic Acid Oxidation and Their Influence on Pepsin Diffusion and In Vitro Gastric Digestion. *Cite This: J. Agric. Food Chem*, *68*, 5698. https://doi.org/10.1021/acs.jafc.0c00808

Appendices

Acknowledgement

About the author

List of publications

Overview of completed training activities

Acknowledgement

Over these four years, I have always been surrounded by lovely people. Many of them did not significantly contribute to this thesis, some of them are not even in the Netherlands. But I believe, over these years, every face that smiled at me, every ear that listened to me, supported me through this challenging journey, making it enjoyable and unforgettable.

Dear **Markus**, **Anja,** and **Paul**, thank you so much for being such a perfect supervision team for me. I always tell people that I have the dream supervision team, and I mean every word of it. **Markus**, thank you for your professional, thoughtful, and clear responses to all my questions; thank you for answering my messages filled with confusion, sentence by sentence, at the beginning of my PhD; thank you for all the jokes and chats; and thank you for being the secret Sinterklaas and for the chocolate. I am truly lucky to have you as my promotor.

Anja, perhaps because we are both women, I always feel a special warmth and connection with you. While giving me professional advice, you always cared about my feelings. Every time I saw you in the office, I felt more at ease during my experiments. Your encouragement and support meant a lot to me, especially while I was writing my thesis.

Paul, firstly, thank you for the online meeting in 2020. Without that meeting, I wouldn't have spent the past four years in Wageningen surrounded by such lovely people. Thank you for your advice and critical thinking, which have definitely improved these studies. I enjoyed our lunch meetings, our chats while waiting for the scanning of someone else's stomach, and the wine you gave me for my first publication. I will cherish all these memories, including your dancing at the division party :)

I would also like to express my special thanks to **Kees** and **Ciarán**. **Kees**, you were the first person I met from Wageningen, and our meeting in 2020 is where all these memories began. Thank you for your support afterward. **Ciarán**, thank you for all the chats and encouraging words, even though I understood only about 70% of them most of the time. Haha!

These studies would never be complete if I worked on them alone. First, a big thank you to my co-authors, **Thiemo** and **Elke**. I deeply appreciate your contributions to the third chapter. Secondly, I want to highlight my gratitude to the **FPE technicians**, especially **Jarno, Jos, Maurice**, and **Wouter**. Thank you for being my lifesavers when something went wrong with the experiments. I also won't forget the timely assistance from **Corine** and **Els** during the oral processing sessions at Helix. Thank you for helping me set up everything. I also want to

express my gratitude to **João** for her clear explanations and endless patience whenever I had questions about data analysis. Lastly, thank you to my brilliant students, **Gabriella, Nienke, Rosa**, and **Yichuan**. It was a pleasure working with you, and I learned so much through the supervision process.

To my fantastic office mates, **Lisa**, **Julia**, **Marieke**, **Maria**, **Jacintha**, **Karleen**, and **Frederick**, thank you for all the lunches and chats. Whether it was asking for help, sharing frustrations, or just chatting over coffee, you all made working in the office so much more enjoyable. A special thank you to **Maria**, sharing a room with you during our PhD trip made the trip even more enjoyable. **Danny**, our official 1056er, please keep your promise to come back in one year. **Chrisja**, it was nice meeting you at 1056. Enjoy your PhD here, I'm sure you'll love it.

I want to extend my gratitude to all my friends and colleagues at HNH: **Abisola**, **Arli**, **Birgit**, **Bryan**, **Catoo**, **Charlotte**, **Cong**, **Esther**, **Eva**, **Femke**, **Fenna**, **Gaelle**, **Hanhong**, **Hongyi**, **Ina**, **Inga**, **Jiachun**, **Koen**, **Luc**, **Maria**, **Mashina**, **Max**, **Meirong**, **Michele**, **Naomi**, **Nienke**, **Pari**, **Robby**, **Ruoxuan**, **Rutger**, **Samantha**, **Tesfaye**, **Tsitsi**, **Umi**, **Xinhang**, **Xinmeng**, **Yan Fang**, **Yanyang**, **Zhen**, **Zhiyao**, and **Zoe**. Thank you for all the greetings, chats and for creating such a welcoming environment. To **Julia**, **Morwarid**, **Elise**, **Ruoxuan**, **Xinhang**, and **Louise**, thank you for the small talks during our MRI lunch meetings. A special thanks to **Hanae**, meeting you at the end of my PhD was a wonderful surprise. Thank you for the chats, bubble teas, and, of course, feeding me Korean sushi when I was too busy for a proper lunch. Hopefully, someday I will visit you in Japan.

Even though I did not spend much time at FPE, I always felt welcomed when surrounded by FPEers. To **Hilda**, **Sirinan**, **Nattawan**, **Luc**, **Eric**, **Yafei**, **Julia V.**, **Iris**, **Lingfeng**, **Fathinah**, **Ana**, **Laurens**, and **Anneloes**, thank you for sharing the office with me and for chatting with me in the lab whenever I was at FPE. To **Polly**, **Jiarui**, and **Ting**, thank you for sharing a room with me during our trips or conferences. Also, to everyone who joined the trip to the UK, I truly enjoyed our time together as a group.

Over these years, I have always been accompanied and supported by sweet and lovely people. **Zongyao** and **Keqing**, the first hotpot I had in Wageningen was at your place, thank you for helping me start my life here. **Yao**, **Yifan**, and **Peiheng**, our trip to France was my first one outside NL. It was such a beautiful memory. I will always remember the stars at the Pantheon that night. **Dounia**, you were almost the first friend I made here (technically in Baarlo). Thank

you for asking to sit next to me on the bus back to Wageningen and for all the trips and hangouts afterward.

Dear **Julia** and **Lise**, thank you for always being there when I needed to talk, complain, share, or hang out. I enjoyed our walks, whether to the coffee corner or the small forest. The friendship with you is definitely a highlight and a precious memory of my time in NL. **Lise**, you deserve extra thanks for being my paranymph. Thank you for everything you did for me, many, many thanks!

Dear **Kübra**, thank you for sharing your colorful life with me. I truly enjoyed our picnics, dinners, and hangouts. I wish you all the best in Turkey.

Dear **Baoyous**, **Qing H.**, **Qing R.**, **Xiaofang**, **Yifan**, and **Zekun** (random ranking), meeting you all in the Netherlands has been one of my greatest fortunes over these years. You are my family in NL, thank you for all the hotpot parties and trips. I will miss the times we spent together, laughing, singing, and talking nonsense. Dear **晴姐**, thank you for being my paranymph. When you asked why I chose you, honestly, I don't know, your name just popped into my mind when I thought about it. I guess this means something.

亲爱的**毛毛** (毛晓慧)，**大姐** (庞思琦)，还有**杨寓钦**，感谢你们这些年一如既往的赛博陪伴和支持，你们证明了友情的距离在于心的距离。

Dear **Jianchao**, being with you has been the most beautiful thing that happened to me during these four years. 感谢你的陪伴，让我们一起继续向前吧。

Finally, to my **dad**, **爸爸**，感谢你一直以来做我的山，我的依靠，我的后盾。

It was not easy for me to write this acknowledgment. My mind keeps flashing back to all the moments, it feels like a farewell to my PhD journey. Every person I met has contributed to this thesis and this journey in a special way. It is impossible to write everything down in a few pages, but it will always be written in my mind and heart. I wish you all the best.

THANK YOU.

Dan Liu, 刘丹
31 Dec, 2024, Wageningen

About the author

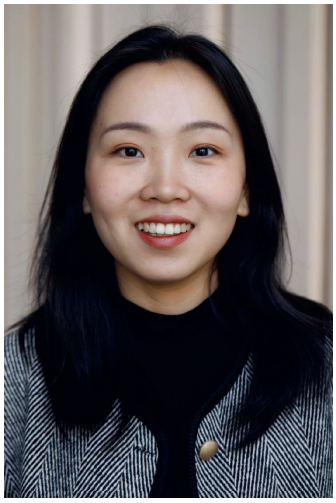

Dan Liu (刘丹) was born on 29th July 1995 in Shanxi, China. She obtained her Bachelor's degree in Bioengineering from Shanxi Agricultural University in 2017. During her Bachelor's studies, she joined the Shanxi Province Higher Education Innovation Training Program with her groupmates to investigate the antioxidant activity of edible fungus powder. This experience inspired her interest in food science and research. In 2020, she completed her Master's degree in food microbiology at Northwest A&F University, where she explored the influence of glutathione-rich inactive dry yeast on the quality attributes of kiwi wine. In March 2021, Dan embarked on her PhD journey at Wageningen University in the Division of Human Nutrition and Health, under the guidance of Prof. Markus Stieger, Dr. Anja Janssen, and Dr. Paul Smeets. Her research delves into the interplay between food microstructure, mechanical properties, macrostructural breakdown and *in vitro* gastric protein digestion. The result of this research is presented in this thesis.

Contact the author: liudan95730@outlook.com

List of publications

This thesis:

Publications in peer reviewed journals:

Liu, D.*, Janssen, A. E. M., Smeets, P. A. M., & Stieger, M. (2024). Interplay between microstructure, mechanical properties, macrostructure breakdown and *in vitro* gastric digestion of whey protein gels. *Food Hydrocolloids*, 147, 109352.

Liu, D.*, Janssen, A. E. M., Smeets, P. A. M., & Stieger, M. (2025). Impact of microstructure of whey protein gels on *in vitro* gastric protein digestion is sustained after oral structural breakdown by mastication. *Food Hydrocolloids*, 159, 110619.

Liu, D.*, van Esbroeck, T., Janssen, A. E. M., Scholten, E., Smeets, P. A. M., & Stieger, M. (2025). Influence of structural properties of textured vegetable proteins on *in vitro* gastric digestion kinetics of plant-based meat analogue patties. *Food Hydrocolloids*, 162, 111011.

Submitted papers:

Liu, D.*, Janssen, A. E. M., Smeets, P. A. M., & Stieger, M. Impact of mechanical and bolus properties on static and dynamic *in vitro* gastric protein digestion of plant-based meat analogues.

Others:

Liu, D., Qi, Y., Zhao, N., Cao, Y., Xu, J., Fan, M.*. (2020). Multivariate analysis reveals effect of glutathione-enriched inactive dry yeast on amino acids and volatile components of kiwi wine. *Food Chemistry*, 329, 127086.

Liu, D., Xu, J., Cao, Y., Qi, Y., Yang, K., Wei, X., Xu, Y. Fan, M*. (2020). Effect of glutathione-enriched inactive dry yeast on color, phenolic compounds, and antioxidant activity of kiwi wine. *Journal of Food Processing and Preservation*, 44, e14347.

Zhao, N., Zhang, Y., **Liu, D.**, Zhang, J., Qi, Y., Xu, J., Wei, X., & Fan, M. (2020). Free and bound volatile compounds in 'Hayward' and 'Hort16A' kiwifruit and their wines. *European Food Research and Technology*, 246(5), 875–890.

Overview of completed training activities

Discipline specific activities

Sensory Perception & Food Preference: into the Future!	VLAG	NL	2021
Healthy and sustainable diets: synergies and trade-offs	VLAG	NL	2021
Protein quality evaluation and application	VLAG	NL	2023

Conferences

Virtual International Conference on Food Digestion	INFOGEST	online	2021
Food Oral Processing Conference	CSIC	online	2021
4th Food Structure and Functionality Forum Symposium	Elsevier	online	2021
36th EFFoST conference (oral presentation)	EFFoST	Ireland	2022
The International Symposium Dietary Protein for Human Health	FAO	NL	2023
8th International Conference on FOOD DIGESTION	INFOGEST	Portugal	2024
3rd NIZO Plant Protein Functionality Conference	NIZO	NL	2024

General courses

VLAG PhD week	VLAG	NL	2021
The Essentials of Scientific Writing & Presenting	WGS	NL	2021
Introduction to R	VLAG	NL	2021
Research Data Management	WUR	NL	2021
Supervising BSc & MSc thesis students	WGS	NL	2021
Scientific Writing	WGS	online	2022
Applied statistics	VLAG	NL	2022
Chemometrics (Multivariate Statistics)	VLAG	NL	2024

Other activities

Preparation of research proposal	HNH	NL	2021
Research group meeting	HNH	NL	2021-2024
Supervising one BSc & three MSc thesis students	SSEB &FPE	NL	2022-2024
International PhD excursions	HNH	Switzerland & Italy	2022
International PhD excursions	FPE	UK	2024

Colophon

This research described in this thesis was carried out at the division of Human Nutrition and Health and the laboratory of Food Process Engineering at Wageningen University.

The research described in this thesis was financially supported by Chinese Scholarship Council.

Financial support from Wageningen University for printing this thesis is gratefully acknowledged.

Cover design by Dan Liu and Our Friday Goldfish Design Studio
Printed by Proefschriftmaken.nl